UNIVERSITY
OF GÄVLE

FACULTY OF ENGINEERING AND SUSTAINABLE DEVELOPMENT
Department of Building, Energy and Environmental Engineering

Investigation of the Performance of a Large PV system

Júlia Solanes Bosch

June 2017

Student thesis, Master degree (one year), 15 HE

Energy Systems

Master Programme in Energy Systems

2016-2017

Supervisor: Björn Karlsson

Examiner: Richard Thygesen

Abstract

One of the main social challenges that society is facing nowadays is the energy crisis. So, head towards renewable energy resources such as solar, hydraulic, wind, geothermal and biomass, could be the best solution. Solar photovoltaic is one of the most promising sources to produce electricity due to its cleanness, noiselessness and sustainability, and the fact that it is inexhaustible. However, the power output of the PV systems varies notably because of the ambient conditions: temperature and solar radiation.

The main aim of this thesis is to study if the PV system installed on the wall of the new football arena Gavlehov in Gävle is providing the amount of power promised before the installation. To achieve reliable results, the first step is to develop and install a monitoring system for recording the real power of the system and the ambient conditions at the same time. After that, an evaluation of the performance of the system during one week will be done, comparing the theoretical power and the real power obtained. The theoretical power will be calculated in two ways: using the data from a pyranometer and on the other hand, from a reference solar cell. This will permit to compare which one matches better with the reality.

Different factors such as the temperature, the irradiance and the angle of incidence are studied to know the real influence that they have on the performance of a PV installation. The results obtained show that the measurement system installed is reliable and that the model used to evaluate the system is correct.

It can be concluded that using a reference solar cell to calculate the theoretical power of the system is easier to align and it has the same angular behaviour as a PV module than employing a pyranometer. Regarding the installation, all the panels work similarly and the system works at nominal power. So, it provides the amount of power promised before the installation.

Key words: Renewable energy, PV system, solar radiation, nominal power, pyranometer, solar cell.

Acknowledgements

First, I would like to express my gratitude to my thesis supervisor Professor Björn Karlsson and my co-supervisor Mattias Gustafsson at Högskolan I Gävle. They have been guiding and encouraging me through all the problems and doubts, helping me to find a solution. They have transmitted me their knowledge about solar energy. I also want to thank them for trusting and proposing me this thesis.

Secondly, I want to acknowledge Mikael Sundberg for dedicating his time building and installing the monitoring system. Without him, the development of the project would not have been possible.

Foremost, I would like to thank my family and friends, for supporting me during these years of university studies and specially, during this year abroad when I was far away from home. I also want to thank my sister for her cooperation and help when I have had doubts.

Last but not least, thanks to all the people I have met in Gävle, specially to the ones that have become my family this year in Sweden. Thank you for making this year one of the greatest experiences of my life.

Table of Contents

List of figures

List of tables

Nomenclature

A	Area
AC	Alternating Current
BOS	Balance of System
CO_2	Carbon Dioxide
DC	Direct Current
E_{out}	Output energy
FF	Fill Factor
G	Solar radiation/Irradiance
G_b	Beam/direct radiation
G_d	Diffuse radiation
G_{sc}	Solar constant radiation
h	Convective heat transfer coefficient
H	Sum of global radiation
I	Current
I_D	Diode current
I_L	PV effect current
I_{mpp}	Maximum power point current
I_O	Saturation current of the diode
I_{SC}	Short-circuit current
K_b	Angle of incidence correction factor
K_d	Incidence modifier for diffuse radiation
L_l	Local longitude
L_{st}	Standard longitude
MPP	Maximum Power Point
MPPT	Maximum Power Point Tracking
n	day number of the year
P	Power
P_{peak}	Peak power
$P_{theoretical}$	Theoretical power
PV	Photovoltaic
SE	South-East
STC	Standard Test Conditions
T	Temperature

$T_{ambient}$	Ambient temperature
T_{module}	Module temperature
V	Voltage
V_{mpp}	Maximum power point voltage
V_{OC}	Open-circuit voltage
V_{pyr}	Pyranometer voltage
α	Temperature coefficient
α_s	Solar height
β	Tilt angle
δ	Declination
γ	Azimuth angle
γ_s	Solar azimuth
η	Efficiency
φ	Correction factor
λ	Latitude
θ	Angle of incidence
θ_z	Zenith angle
ω	Hour angle

1 Introduction

1.1 Motivation

One of the main social challenges that society is facing nowadays is the energy crisis. The energy resources (fossil fuels) we are familiar with to power industrial society are being depleted while the energy demand is constantly growing all around the world due to the population growth, the expansion of industry and the constant increase of the energy consumption per capita. Moreover, global warming and climate change are current concerns for civilization and one of the principal causes are the fossil fuels. Carbon dioxide (CO_2) from the combustion of fossil fuels is the main greenhouse gas and it represents about 80% of global emissions [1].

Despite some doubts that surround the climate change and global warming debate, there exists a wide agreement on the fact that CO_2 and other greenhouse gases emissions must be reduced. Greenhouse gases produce undesirable effects on the climate, such as warmer temperatures, storms and flooding. Society is increasingly concerned about the point that we must change the course and head towards renewable energies such as solar, hydropower, wind, geothermal and biomass [2].

Regarding to solar energy, which is basically divided into solar photovoltaic (PV) and solar thermal, PV energy is one of the most promising sources to produce electricity. A PV system uses the irradiance from the Sun and converts it to direct current (DC) [3]. So, the main advantages are its cleanness, noiselessness and sustainability, and the fact that it is inexhaustible. Also, it is easier to maintain comparing with other renewable technologies. However, the power output of the PV systems varies notably because of the ambient conditions: temperature and solar radiation [4]. Moreover, the power also depends on the current, the voltage and the temperature of the module [5].

Apart from the ambient conditions, the performance of the system is also influenced by the surroundings. Shadowing issue is common and sometimes inevitable since there are some parts of the PV module that receive less amount of sunlight because of the shadows from trees or clouds [3].

The market for PV systems is growing rapidly. During the last 15 years, the growth rate of PV installations was of 41% and it is expected to continue growing in the future [6]. Several strategies have been developed with the aim of increase the amount of electricity generated by renewable energies, especially solar energy. For example, Sweden has applied the RPS (Renewable Portfolio Standard), which implies that part of the energy consumed should proceed from renewable sources [6].

Figure 1 shows the distribution of cumulative PV installations in 2015.

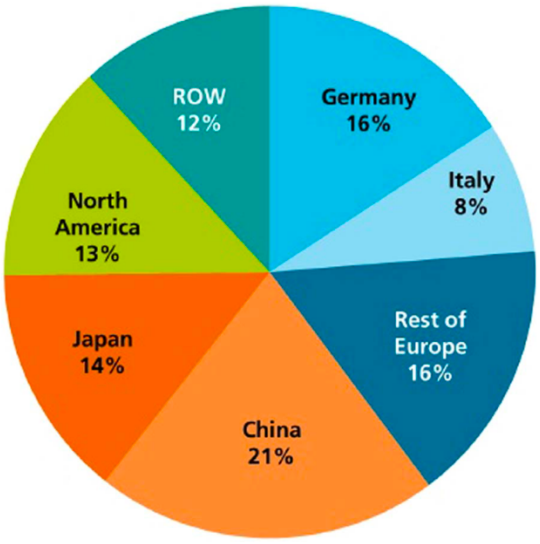

Figure 1. Cumulative global photovoltaic installation by 2015 [6]

1.2 Objectives

This thesis has been proposed by Björn Karlsson and Mattias Gustafsson and it is about a large PV system on the wall of the new football arena Gavlehov in Gävle, which was installed by the housing company Gävle Fastigheter and it is owned by Gävle Energi.

The aim of the study is to know if the system is providing the amount of power promised before the installation. Due to its conditions and orientation, it is thought that the power output may be lower than the expected one. Moreover, another goal to achieve is to know how much the shadows decrease the annual output of the system, because the system studied has severe problems with shadowing of the trees that are in front of the facade where it is installed.

So, evaluating and analysing the impact of shadowing on the performance is an important task to carry out, together with an evaluation of the operation of the system.

The main tasks to accomplish are the following ones:

- Install a measurement system for recording the power of the system, the irradiance and the module and ambient temperatures.
- Monitoring of the performance during a short period.
- Evaluate the performance of the system and the impact of shadowing.

1.3 Limitations

One of the most important limitations is that the study was done with the data of six days of May. So, it does not represent the performance of the system during the whole year. Due to that, it was not possible to evaluate the impact of shadowing on the PV system because it happens when the Sun is lower in the sky.

Another drawback was the time. There were some problems developing the measuring system, so the installation was done later than expected.

Apart from that, the monitoring system is experimental, so the data obtained may not be exact, but it is acceptable for carrying out the study.

2 Theoretical background

2.1 Solar radiation

Solar power resources on Earth are huge, non-polluting and inexhaustible. Additionally, solar energy is the source for other renewable energies such as hydropower, wind, biomass and so on [7]. It is known that the total amount of solar energy that arrives at the Earth exceeds by far the human needs, but nowadays it is not possible to take all the profit out of it [8].

The Sun is a blackbody at a temperature of 5777 K that radiates energy due to its continuous fusion reactions [9]. The intensity of solar radiation that arrives outside the atmosphere of the Earth varies during the year (Figure 2) because of the eccentricity of the Earth's orbit, but it is mainly accepted the average value of G_{SC}=1367 W/m^2 as the solar constant. Solar radiation can be divided into three parts depending on the wave length: ultraviolet radiation (λ<0.38 μm), visible light (0.38<λ<0.78 μm) and infrared radiation (λ>0.78 μm) [7] [9].

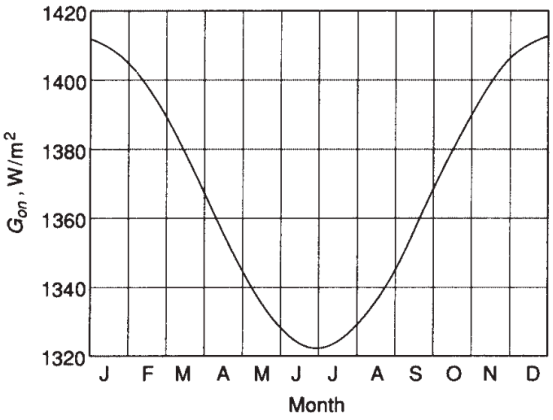

Figure 2. Variation of extraterrestrial solar radiation with time of year [9]

Once the solar radiation passes through the atmosphere the intensity is reduced due to absorption and diffraction in the atmosphere, the weather (clouds or clear sky), the moisture content in the air, and so on [7]. The intensity also depends on the distance that the beam radiation needs to travel through the atmosphere [9]. So, due to some losses, the energy flux that strikes the Earth's surface on a clear day, when the Sun is in its highest position in the sky, is around 900 or 1 000 W/m^2 [7].

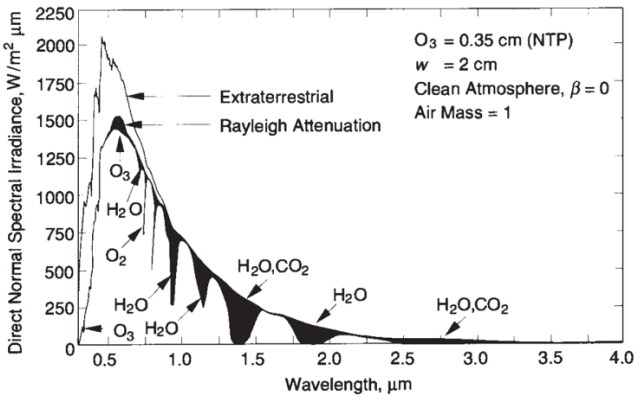

Figure 3. Spectral distribution of direct solar radiation before and after the losses in the atmosphere [9]

The solar radiation received at the Earth's surface can be either direct or diffuse. Direct radiation travels through the atmosphere without any interference or change in its direction. On the other hand, diffuse radiation changes its direction because it scatters in the atmosphere. Depending on how sunlight was diffused, it can reach Earth's surface in many angles. The sum of the direct and diffuse solar radiation is called global radiation [7] [9]. Moreover, apart from beam and diffuse radiation towards a surface, there is also ground reflected radiation. In Figure 4 it is shown the different types of solar radiation transmission.

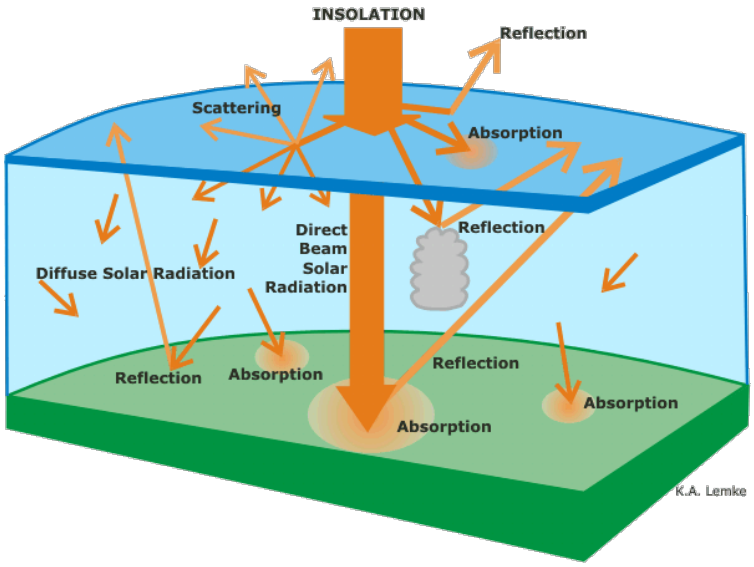

Figure 4. Types of solar radiation transmission [10]

2.1.1 Angle of incidence

The variation of the irradiance reaching the Earth during the year influences the PV system performance and it is important to analyse. The radiation against a surface consists basically of direct and diffuse radiation, but the more direct light the higher the output power generated. Orienting the PV modules towards direct sunlight will optimize the system's efficiency. So, to extract the maximum power, the solar panel should follow Sun's direction. The angle between the normal vector of the surface and the solar beam is called angle of incidence (θ) and it varies during the year and depends on the time of the day [7].

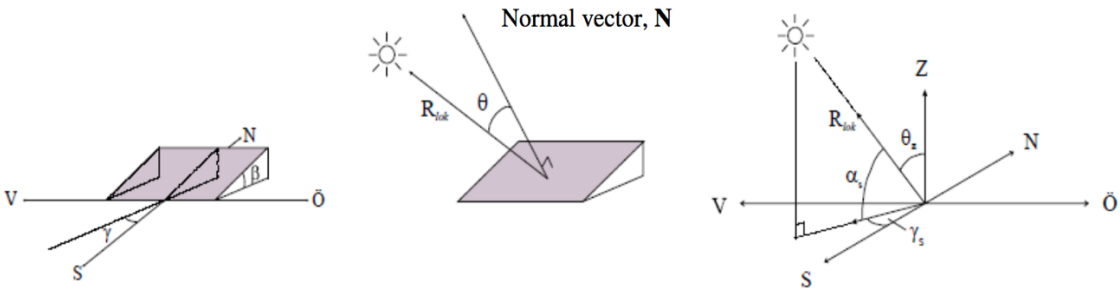

Figure 5. The left figure shows the tilt (β) from the horizontal surface and the azimuth angle (γ). The middle figure shows the normal vector (N) and the angle of incidence (θ) of the solar radiation (R). The right figure shows the solar azimuth (γ_s), the solar height (α_s) and the zenith angle (θ_z) [9].

It is possible to determine the angle of incidence for the solar radiation on a surface by taking the scalar product between the normal of the plane and the solar vector:

$$\begin{aligned}\cos(\theta) = R \cdot N \\ &= \cos(\delta)\sin(\omega)\sin(\beta)\sin(\gamma) \\ &+ \cos(\delta)\cos(\omega)\sin(\lambda)\sin(\beta)\cos(\gamma) \\ &- \sin(\delta)\cos(\lambda)\sin(\beta)\cos(\gamma) + \cos(\delta)\cos(\omega)\cos(\lambda)\cos(\beta) \\ &+ \sin(\delta)\sin(\lambda)\cos(\beta)\end{aligned} \quad (1)$$

Where:

- θ: Angle of incidence [°]
- δ: Declination [°]
- ω: Hour angle [°]
- γ: Azimuth angle [°]
- λ: Latitude [°]
- β: Tilt of the surface [°]

As the distance between the Earth and the Sun varies during the year, also does the angle of incidence. It depends on several variables, called solar angles.

The declination (δ) is the angle between the Sun and the equator plane. Its values are between -23.45° $\leq \delta \leq$ +23.45°, positive when the Sun is north of the equator (after spring equinox and before autumn equinox, in the north hemisphere) and negative the other part of the year. So, in the summer solstice δ=+23.45°, in the equinoxes δ=0° and in the winter solstice δ=-23.45° [9].

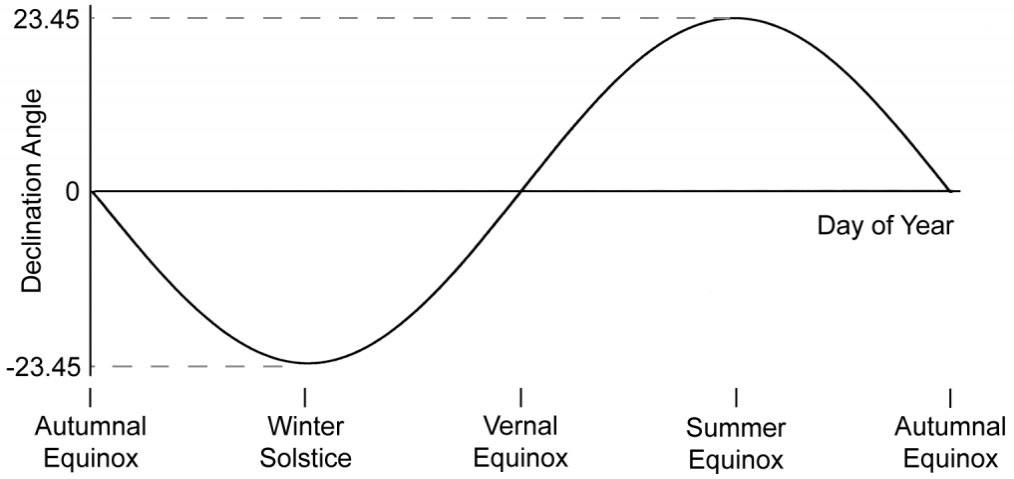

Figure 6. Variation of the declination angle during the year [11]

The declination is different depending on the day number of the year, so it varies between seasons. It can be calculated by the following formula:

$$\delta = 23.45 \cdot \sin\left(360 \cdot \left(\frac{284 + n}{365}\right)\right) \quad (2)$$

Where:

- δ: Declination [°]
- n: Day number of the year

The hour angle (ω) is the angular displacement of the Sun, east or west from the local meridian due to the rotation of the Earth. The rotational speed corresponds to 15° per hour [9]. It can be determined from:

$$\omega = 15 \cdot \left((hh - 12) + \frac{mm}{60} \right) \quad (3)$$

Where:

- ω: Hour angle [°]
- hh: Hour of the solar time
- mm: Minutes of the solar time

As it has been seen, it depends on the solar time which is a way to measure the time based on the apparent movement of the Sun over the horizon of a place. It takes as its origin (ω=0°) the moment when the Sun passes the meridian, which is the highest point in the sky, called noon (12:00). From that moment, the hours are counted at intervals of 24 parts until a complete diurnal cycle [9].

However, the Sun does not have a regular movement throughout the year, so the solar time is divided into two categories:

- Apparent solar time: It is based on the true solar day, which is the interval between two successive returns of the Sun to the local meridian. The solar time can be measured with a sundial.
- Mean solar time (clock time or local time): It is based on a fictitious Sun traveling at a constant speed. The duration of the mean solar day is 24 hours and it is constant the whole year.

These two times do not coincide, so it is necessary to adapt local time to solar time by applying two adjustments. On the one hand, there is a constant that corrects the difference in longitude between the local meridian and the standard meridian. It takes 4 minutes for the Sun to transverse 1° of longitude. On the other hand, the other correction is the equation on time, which takes into account the changes in the Earth's rotation speed and the elliptical shape of the Earth's orbit around the Sun. The following equation provides the difference in minutes between the local time and the solar time [9].

$$Solar\ time - Local\ time = 4 \cdot (L_{st} - L_l) + E \quad (4)$$

Where:

- L_{st}: Longitude of the standard meridian, local time zone (Sweden) [°]
- L_l: Longitude of the local meridian (Gävle) [°]
- E: Equation of time [°]

The equation of time is a function of the time of the year and can be calculated using the following equation:

$$E = 229.2 \cdot (0.000075 + 0.001868 \cdot \cos(B) - 0.032077 \cdot \sin(B) - 0.014615 \cdot \cos(2B) - 0.04089 \cdot \sin(2B)) \quad (5)$$

Where B is obtained from equation 6 and n is the day of the year:

$$B = 360\frac{(n-1)}{365} \tag{6}$$

Finally combining the equations 4 and 5, the precise hour angle is obtained:

$$\omega = 15 \cdot (hh - 12) + \frac{mm + E}{4} + (L_{st} - L_l) \tag{7}$$

A short description of the other angles will be done below [9]:

- Latitude (λ): It indicates the angular position of a place on Earth south or north of the equator (north positive).
- Surface azimuth angle (γ): It is the orientation of the surface towards the south. It is zero due south, east negative and west positive ($-180° \leq \gamma \leq 180°$).
- Tilt (β): It is the angle between the plane of the surface (panels) and the horizontal.

Regarding to the Sun position in the sky:

- Zenith angle (θ_z): It is the angle between the sun beam and the vertical.
- Solar altitude angle (α_s): It is the angle between the sun beam and the horizontal (the complement of the zenith angle).
- Solar azimuth angle (γ_s): It defines the direction of the Sun and it is the angle between the south line and the projection of the beam radiation on the horizontal plane (west positive).

2.2 PV systems

Photovoltaic systems consist of several components like solar cells, electrical and mechanical connections and devices to regulate and modify the electrical output. The amount of electrical power that these systems deliver during a clear day is measured in peak kilowatts [kW_p] [12].

A solar cell is a device that converts the sunlight energy into electricity by the photovoltaic effect. Its electrical characteristics (voltage and current) change when it is exposed to the light. The design of PV cells permits to transfer the energy of the photons that penetrate the panel to electrons that are directed into an external circuit to power an electrical load [7].

A single solar cell generates a voltage of 0.6 V [13], so it is needed to connect more than one (between 50 and 120 cells) [7] to achieve a feasible output power for most applications. A photovoltaic module is obtained connecting multiple solar cells. The connection of the cells can be done in series or in parallel. On the one hand, in the series connection, the output voltage is the sum of the voltage of each cell connected while the current is the same for all of them. On the other hand, when connecting the cells in parallel, the opposite occurs: the current is the sum of the current of all the cells and the voltage is constant. Then, connecting different modules a solar panel is obtained and finally the PV array. In Figure 7 it can be seen the components of a PV array.

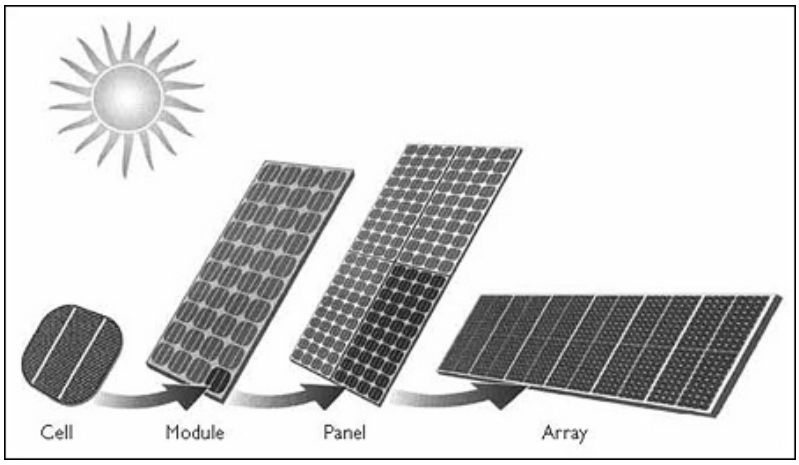

Figure 7. Components of a PV array [14]

2.2.1 Photovoltaic effect

The photovoltaic effect is the direct conversion of solar radiation into electricity. This effect was observed by the first time in 1839 by Becquerel, but until 1954 it was not possible to generate currents [7]. It happens in semiconductor materials, which have two energy bands: valence band, where the presence of electrons is allowed, and conduction band, where there are no electrons [6].

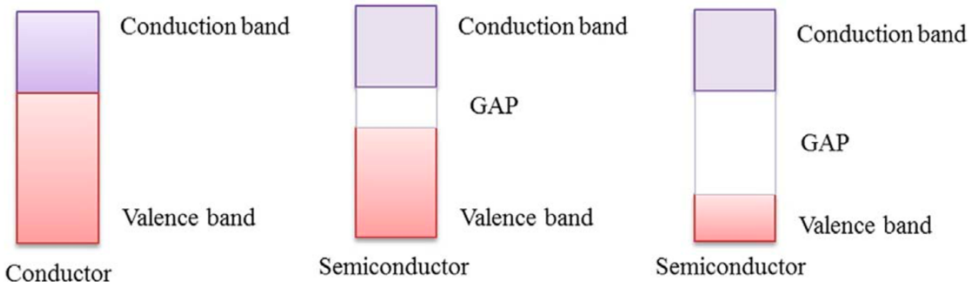

Figure 8. Valence band, band gap and conduction band [6]

The principle of the photovoltaic effect is that the sunlight supplies the necessary amount of energy to the electrons to be able to move from the valence band to the conduction band, generating electricity at the same time. In the case of silicon cells (the most common ones), the electrons need 1.12 eV (electron volts) to surpass the GAP [6].

The main objective of a PV cell is to transform as much of the solar energy incoming as photons as possible into electricity. A solar cell is mainly formed by a semiconductor known as PN junction which consists of two layers, one of N-type material that receives the light and the other of P-type material which is below [6]. The two layers are doped and work in a different way, N-type is expected to produce loose electrons, whereas P-type has lack of free electrons (holes) in the molecular structure where then the electrons can reconnect.

When the light reaches the solar cell, it is absorbed and transfers energy to an electron, liberating it from the atom. Then the electrons excited in the conduction band flow from the P-type layer to the N-type layer, while the holes in the valence band move in the opposite direction [15]. This creates a voltage difference between

the two sides of the cell which makes possible the flow of electrons through the external circuit (load).

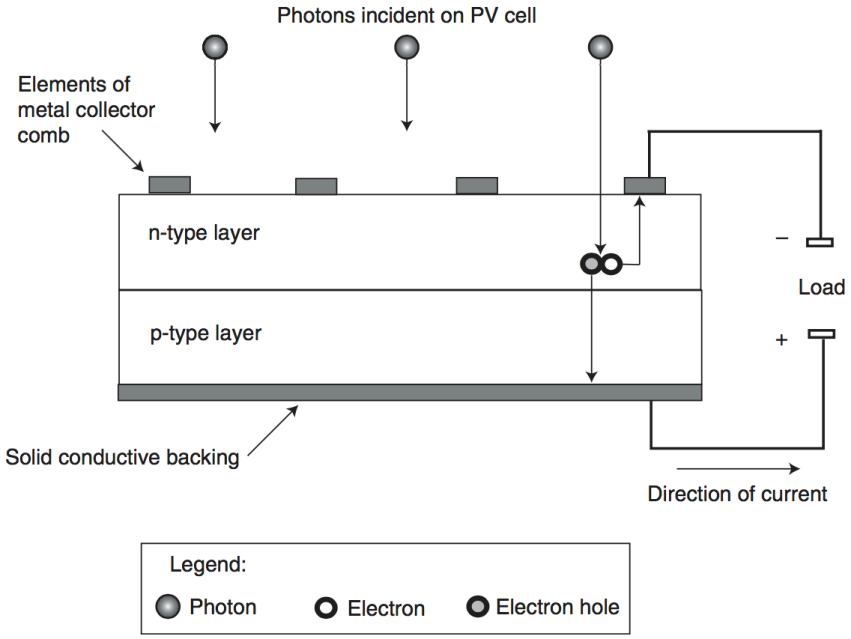

Figure 9. Schema of a solar cell (PN junction) [7]

In Figure 9 it is seen a basic schema of how a solar cell works. In the case of silicon cells, the N-type (upper layer) has an excess of electrons, otherwise, the P-type (lower layer) has extra holes so it can absorb electrons. When a photon hits the PN junction, it breaks an electron within the cell structure. Then the electron travels to the collector and the electron hole moves to the conductive backing, causing current flow to the outside load [7].

Unfortunately, not all the solar energy that arrives to the solar cell is converted to electricity. During the process, there are several losses that reduce the amount of energy. In Figure 10 it is shown the different sources of loss that occur in a solar cell.

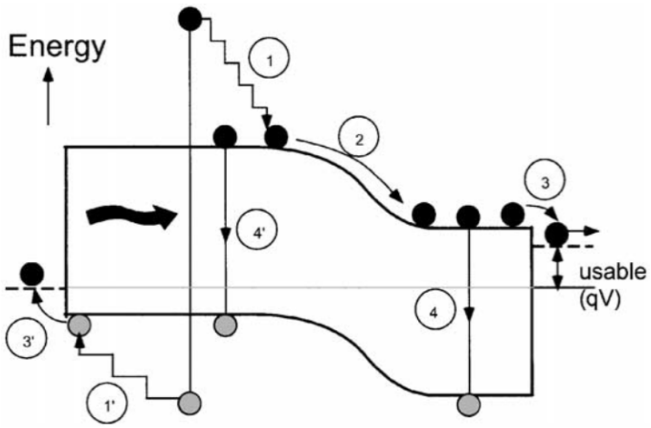

Figure 10. Efficiency loss processes in a PN junction solar cell: (1) thermalisation loss; (2) junction loss; (3) contact loss; (4) recombination loss [15]

2.2.2 Type of solar cells

All solar cells need a light absorbing material which is used to build the structure of the cell to absorb the incoming photons and generate electrons by the photovoltaic effect. Nowadays, there is an extensive diversity of photovoltaic cell technologies that use different types of materials. To consider a solar cell material as ideal, some requirements must be accomplished: a bandgap between 1.1 and 1.7 eV, to facilitate the flow of electrons from one band to the other; non-toxic materials; good efficiency; easy fabrication and long-term stability [6].

At the present time, the most used material for producing PV modules is the silicon wafer, accounting around the 90% of the photovoltaic cell market [6], which is possible to manufacture in two forms: crystalline silicon (monocrystalline and polycrystalline) and amorphous silicon. Crystalline silicon cells have an excellent efficiency (14-19%) [12] rising up lately to 25%, however, monocrystalline cells have high manufacturing costs and require pure materials for its production. Polycrystalline cells appeared later, their production cost is lower because they are easier to manufacture, but they are also less efficient than monocrystalline cells [6].

On the other hand, searching for cost reduction, amorphous (uncrystallised) silicon cells appeared. They are based on thin film technologies which use much less material (99% less than crystalline solar cells [6]) in order to absorb the same amount of light. Their service life time is longer (25 years) and their installation easier. However, the conversion efficiency is lower (5-10%) [12]. Apart from amorphous silicon cells, thin film technologies include other materials such as cadmium telluride, copper indium selenide, titanium dioxide and so on.

Recently, new technologies are arising, like organic photovoltaic cells which offer the potential of achieving the aim of a PV technology economically viable and simple to manufacture [6].

As it can be seen in Figure 11, the use of monocrystalline cells has decreased during the years due to their cost, while polycrystalline has increased. Thin film technologies do not have a high percentage, but it is expected to rise with some improvements in their efficiency.

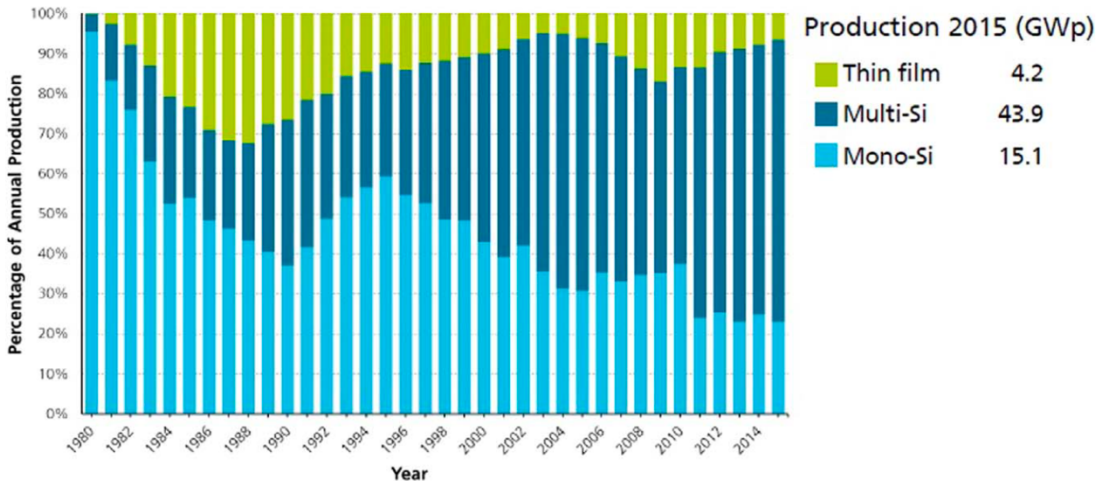

Figure 11. Evolution of the percentage of annual production of the main photovoltaic technologies [6]

2.3 Performance of a PV system

There exist several methods to evaluate the performance of a photovoltaic system, but it is usually tested at Standard Test Conditions (STC) [8] when the solar irradiation (G) incident in the plane of the modules is 1 000 W/m^2, the temperature of the modules (T_{module}) is 25°C and the angle of incidence (θ) is 0°, when the Sun is at zenith and the sun beam travels the minimum distance.

The advantage of using these conditions is that neither the knowledge of the module area nor the PV conversion efficiency are needed.

2.3.1 Efficiency of a PV module

The efficiency (η) of a solar cell with an area A is defined as:

$$\eta = \frac{P}{G \cdot A} \tag{8}$$

Where:

- P: Power [W]
- A: Area [m^2]
- G: Irradiance [W/m^2]

The power P of a module, which is also the maximum power P_{peak} [W_p], is measured at STC. The peak power for a module with an area A and efficiency η is given by:

$$\begin{aligned} P_{peak}(W_p) &= \eta \cdot A \cdot 1000 \\ P_{peak}(kW_p) &= \eta \cdot A \cdot 1 \end{aligned} \tag{9}$$

This means that the efficiency can be calculated as:

$$\eta = \frac{P_{peak}}{A} \tag{10}$$

The efficiency of a solar cell depends on the solar irradiance, temperature (ambient and module) and dust. A high temperature can affect cell performance considerably and many studies have focused on reducing the module's temperature by extracting the heat and utilizing it for other purposes. Regarding the irradiance, lower solar radiation results in decreased efficiency, as fewer photons reach the cell surface. Dust is an easy problem to solve. PV panels need to be cleaned frequently to avoid the accumulation of dust that can block the sunlight on the PV modules [6]. In the following section, the effect of irradiance and temperature will be explained in detail.

2.3.2 Output of a PV module

The output power depends on the module temperature, irradiance and angle of incidence of the solar beams. Knowing the peak power (nominal) of a solar cell, it is possible to know the theoretical output power.

$$P_{peak}(T_{module} = 25°C, \theta = 0°) = \eta(25,0) \cdot A \cdot 1000 \tag{11}$$

The theoretical output power of a PV module is not the same as the peak power since the irradiance reaching the module is different than the one used in STC. So, the theoretical power is proportional to the irradiance received.

$$P_{theoretical} = P_{peak} \cdot \frac{G}{1000} \tag{12}$$

As it was said, the output power is mainly influenced by the irradiance received, but it also depends on the angle of incidence and the temperature of the modules. Subsequently, to calculate the theoretical power all these factors need to be taken into account.

$$P_{theoretical}(T, \theta) = P_{peak}(25,0) \cdot \frac{[K_b(\theta) \cdot G_b + K_d \cdot G_d] \cdot [1 + (T_m - 25) \cdot \alpha]}{1000} \tag{13}$$

Where:

- $P_{theoretical}$: Theoretical power given by the module [W]
- P_{peak}: Peak power of the modules at T_{module}=25°C and θ=0° [W]
- K_b: Angle of incidence correction factor [%]

$$K_b = 1 - b_0 \cdot \left(\frac{1}{\cos\theta} - 1\right) \tag{14}$$

- G_b: Direct (beam) radiation [W/m^2]
- K_d: Incidence modifier for diffuse radiation [%]
- G_d: Diffuse radiation [W/m^2]
- T_{me}: Temperature of the solar module [°C]
- α: Temperature coefficient [α=-0.47%/°C]

The angle of incidence correction factor (K_b) indicates how much is lost because of the incidence of the Sun radiation. Moreover, equation 13 also considers the part of the radiation that does not reach the module directly. K_d indicates the fraction of diffuse radiation.

Regarding the temperature effect, it indicates how the PV system output power depends on the cell surface temperature. The output power decreases as the temperature increases, so this is why it is a negative number.

The aim of a PV system is to provide energy. So, the final output E_{out} [kWh] generated from a PV system is calculated using the following equation [8]:

$$E_{out} = \varphi \cdot \eta \cdot A \cdot H = \varphi \cdot P_{peak} \cdot H \tag{15}$$

Where:

- E_{out}: Output energy of the PV system [kWh]
- φ: Correction factor or system performance ratio [%]
- P_{peak}: Peak power of the modules [kW]
- H: Sum of global irradiation [kWh/m^2]

For a system operating constantly at STC efficiency, the correction factor would be 1. However, in practice, the output of a PV system is lower than the peak power because the operating temperature is usually higher than 25°C and the angle of incidence larger than 0°. A typical correction factor value is between 0.85 and 0.90.

2.3.3 IV curve

The characteristic curve of a photovoltaic panel, also called current-voltage curve (IV curve), represents the values of voltage and current, experimentally measured, of a photovoltaic panel subject to certain constant conditions of irradiance and temperature.

By varying the external resistance from zero to infinity, several values of current and voltage can be measured and interpolating them, the characteristic curve is formed.

In the Figure 12 it is shown the typical I-V and P-V curves. The P-V curve is obtained from the previous measured I-V curve.

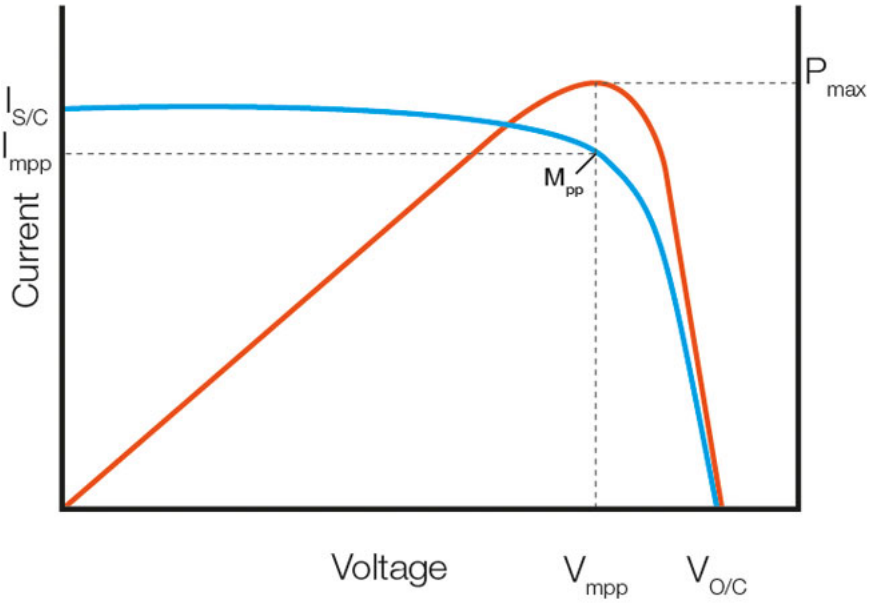

Figure 12. I-V and P-V curves of a solar cell [16]

The equation of the I-V curve [17] can be expressed as:

$$I = I_L - I_D = I_L - I_0 \cdot \left[e^{\frac{qV}{nkT}} - 1 \right] \quad (16)$$

Where:

- I: Current [A]
- V: Voltage [V]
- I_L: Current generated by the photovoltaic effect [A]
- I_D: Diode current [A]
- I_0: Saturation current of the diode [A]
- q: Charge of an electron [C]
- n: Diode ideality factor
- K: Boltzmann's constant [J/K]
- T: Cell temperature [K]

When the voltage is 0 V (impedance is low), the amount of current through the solar cell is called short circuit current (I_{sc}) and it is the maximum current value. In an ideal cell, the short-circuit current would be equal to the current produced in the solar cell because of the photovoltaic effect (I_L) [18].

On the other hand, when there is no current passing through the cell (I = 0 A) the open-circuit voltage (V_{oc}) takes place. It is the maximum voltage difference across the cell [18].

The power produced in a solar cell can be calculated along the I-V curve by the following equation:

$$P = I \cdot V \tag{17}$$

The open-circuit voltage and short-circuit current are the maximum voltage and current respectively from a solar cell. However, at these points, the output power of the solar cell is zero. So, to determine the maximum power from a solar cell, the fill factor (FF) is used together with the I_{sc} and V_{oc}. The FF is a measure of the quality of the cell and it can be defined as:

$$FF = \frac{I_{mpp} \cdot V_{mpp}}{I_{sc} \cdot V_{oc}} \tag{18}$$

The point of the maximum power is called maximum power point (MPP) and at this point the current and voltage are denoted as I_{mpp} and V_{mpp} respectively.

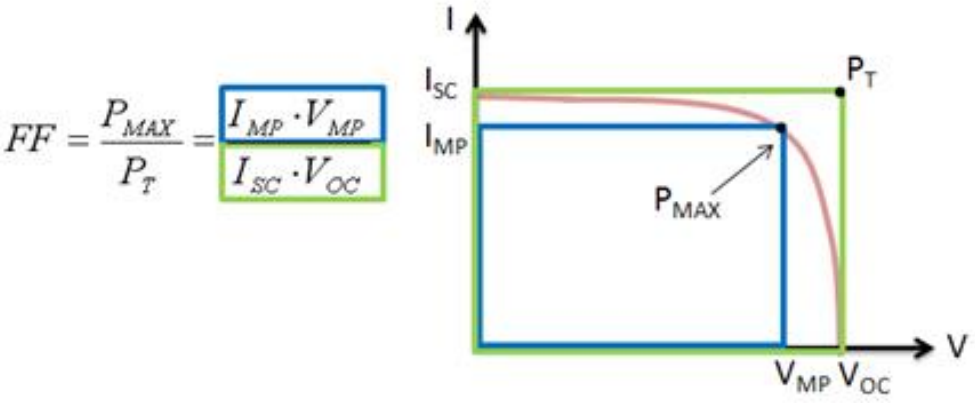

Figure 13. Fill factor from the I-V sweep [19]

2.4 Effect of irradiance and temperature

A solar cell rarely operates at STC. The operating conditions are constantly fluctuating, being able to vary in a range of 0 to 1 000 W/m^2 in the case of the irradiance and the temperature of the cell up to 50°C, higher than the ambient temperature.

The voltage and current generated in a solar cell depend directly on the received illumination. It mainly affects the short-circuit current (I_{sc}) of the cell, which is directly proportional to the irradiance as shown in Figure 14 decreasing while the irradiance diminishes. The open-circuit voltage (V_{oc}) also decreases but its variation is insignificant [20].

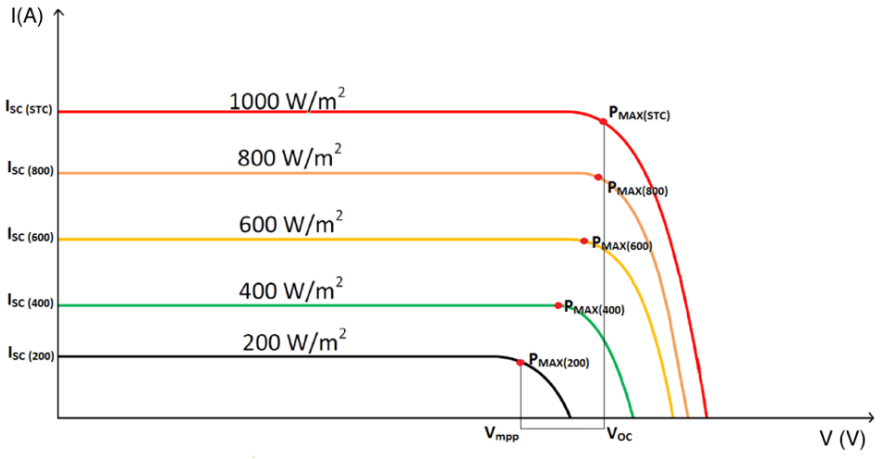

Figure 14. Variation of the I-V curve due to irradiation [21]

The operating temperature of a solar cell depends on the ambient air temperature, the characteristics of the module and the solar irradiance reaching the PV module [17].

A solar cell is a diode, so a change in the temperature will affect the electrical efficiency, and consequently the performance of the PV module. When the light hits the solar cell, the energy of the photons is used to generate electric power, but some heat is retained, which increases the temperature of the solar cell [22].

Solar cell temperature effect is mostly noticeable in the voltage. When the temperature rises, the open-circuit voltage (V_{oc}) drops considerably because the bandgap energy decreases. In contrast, the short-circuit current (I_{sc}) increases a bit due to a lower resistance [23]. It can be seen in Figure 15.

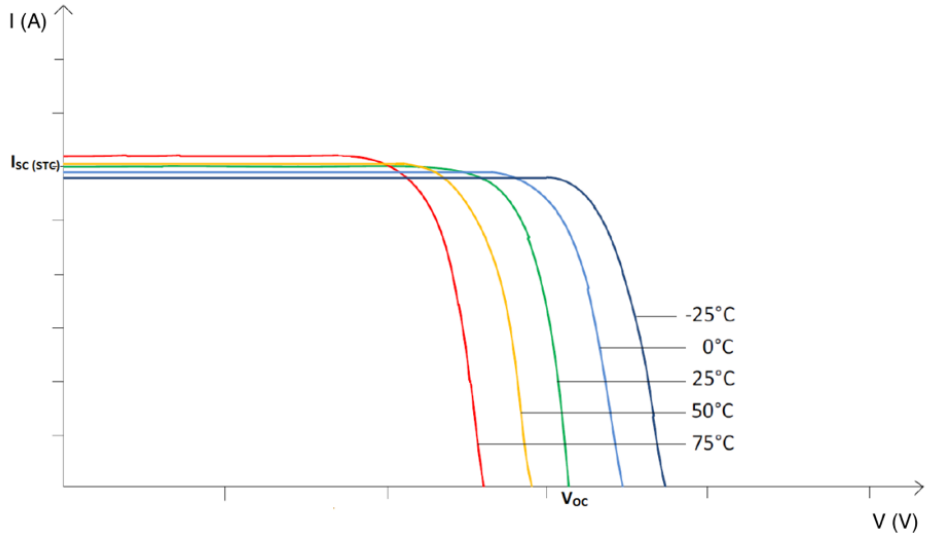

Figure 15. Influence of the temperature in the I-V curve [21]

So, considering all these parameters, the output power will be reduced when the ambient temperature increases (the decrease of voltage is higher than the increase of current) and the solar irradiance decreases.

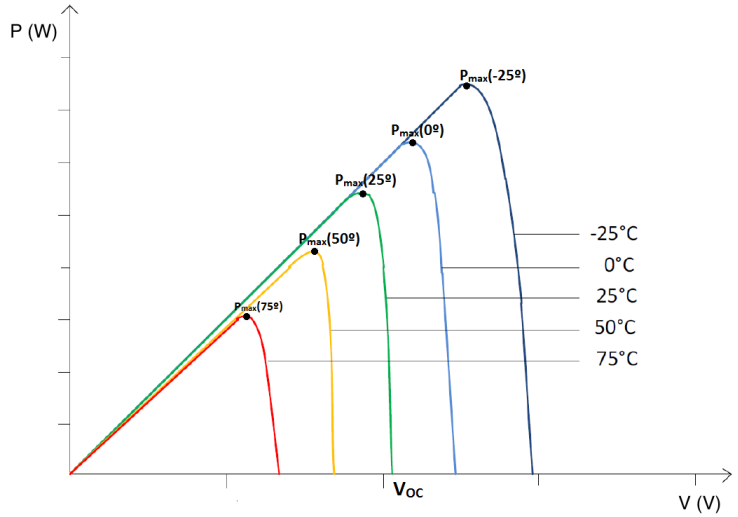

Figure 16. Variation of the maximum power due to changes in the temperature [21]

2.5 Effect of shadows

As it is known, PV modules electricity generation depends on the sunlight that they receive. Sometimes shadows due to clouds, trees or surrounding buildings negatively affect the performance of the PV panels [24]. Usually, the PV cells are connected in series and this means that the cell which produces less current will restrict the current of the string. Consequently, a shadow on one cell will influence the performance of the whole system. The main problem is the reduction of output power, because as the insolation decreases also does the current [25].

When the level of shading is important, thermal stress can appear. This means that some cells can work in reverse bias, operating as resistive loads instead of power generators. When the breakdown voltage is exceeded, the cell can be completely damaged. The losses in the cell can rise the cell temperature severely and overheat it, which might result in hot spots, causing irreversible damage [26].

In order to solve the problems, it is possible to connect in parallel by-pass diodes to several solar cells. Under normal conditions, without shadows, the diodes are blocked. But when shading appears, the by-pass diodes will conduct the current delivered by the other cells [25].

Figure 17 shows the schema of two PV cells connected in series with different irradiance intensities due to shadowing.

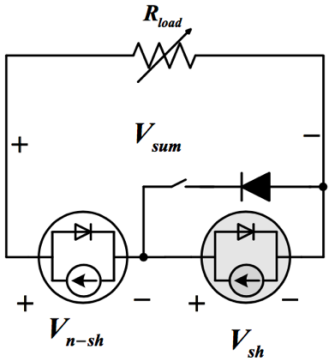

Figure 17. Two PV cells with different irradiance intensities connected in series (with and without bypass diode in parallel with shaded cell) [27]

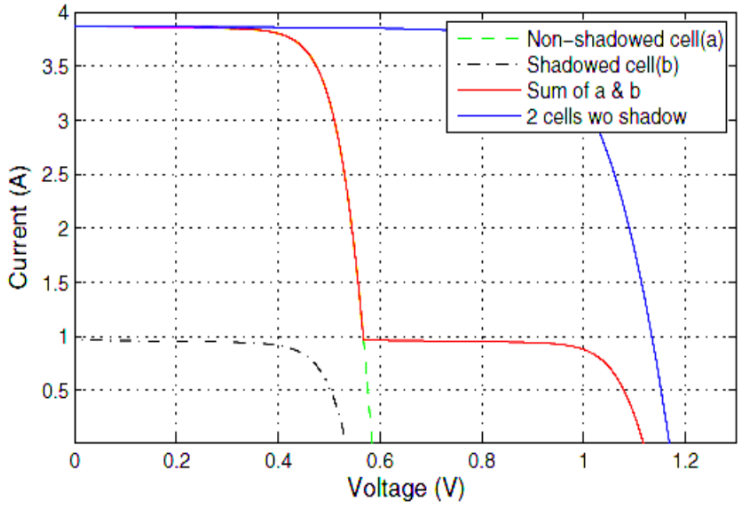

Figure 18. I-V characteristic curve of two PV cells in series with different solar irradiance intensities [27]

In Figure 18 it is shown the I-V characteristic curve of the PV cells in Figure 17 in different conditions.

Another example is the Figure 19 where it can be seen a PV array under different shadow conditions. The modules receive an irradiance of 300 W/m^2, 700 W/m^2 and 1000 W/m^2 respectively [28]. The current of the unshaded modules flows through the by-pass diodes and some maximum points appear.

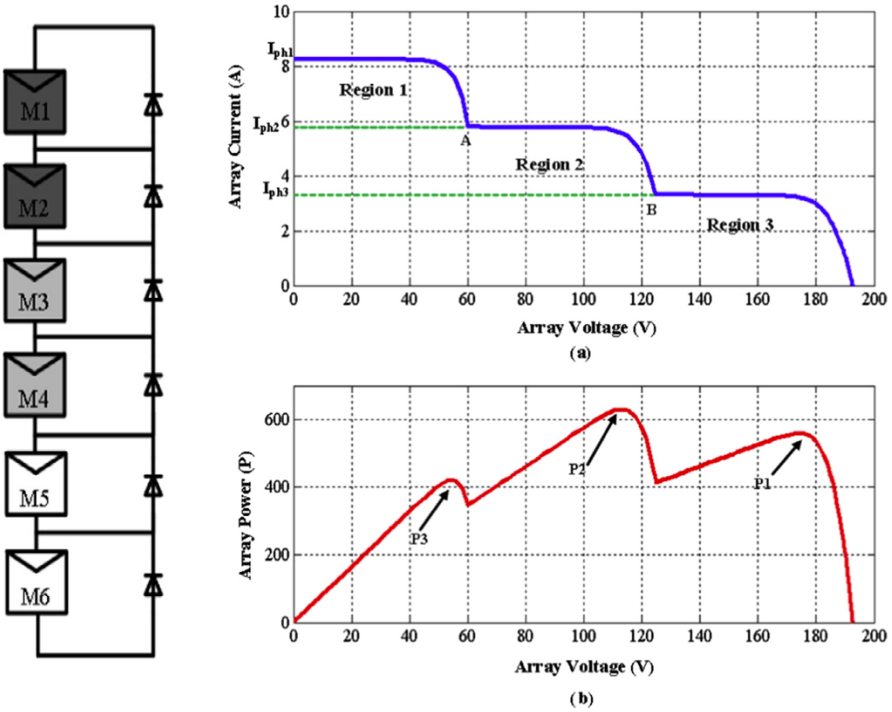

Figure 19. Characteristic curves of the array with shading conditions: (a) I-V curve, (b) P-V curve [28]

By-pass diodes practically solve the problem of damaging the PV modules, but the output power continues being lower. Moreover, there are some disadvantages of installing by-pass diodes such as the higher cost production of the modules, losses in the by-pass diodes and matching problems between the photovoltaic generator and the solar inverter because they operate on different voltage levels [25].

3 Method

This section explains the methodology followed to carry out the study, after doing a deep research about PV systems. First of all, the location and the specifications of the PV system have been studied. Then, some measurements with the appropriate devices have been done and finally the calculations and analysis of the results.

3.1 Location and orientation

The PV system analysed is located in the city of Gävle in Sweden, situated at a latitude of 60°40'28'' N, a longitude of 17°08'30'' E and 3 meters above the sea level [29].

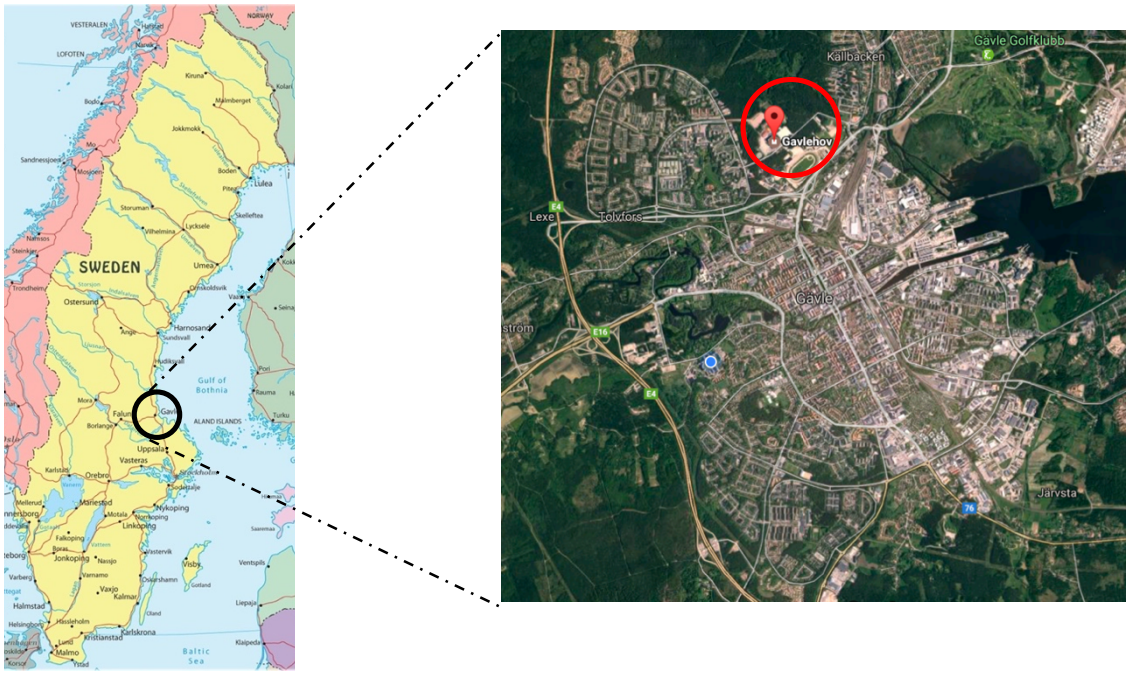

Figure 20. Location of the PV system

Concretely, the PV system was installed on the south-east facade of the new football arena Gavlehof. The orientation of the modules, measured with a compass, is 135°SE, so it means that the azimuth angle (γ) is -45°.

Figure 21. Orientation of the PV modules

3.2 PV installation

The PV installation is connected to the grid, so when there is no electricity demand in the building, the energy produced by the solar panels is sold. The system consists of PV modules and the balance of system (BOS). The BOS comprises several components: mounting systems, the junction box, the inverter, cables that connect the array with the junction box and wires from the junction box to the inverter, protection switches and alternating current wiring from the inverter.

Furthermore, in this case, to carry out the study and be able to collect the data a logger and some sensors were installed and connected to the system.

In Figure 22 a schema of the components of the installation is showed.

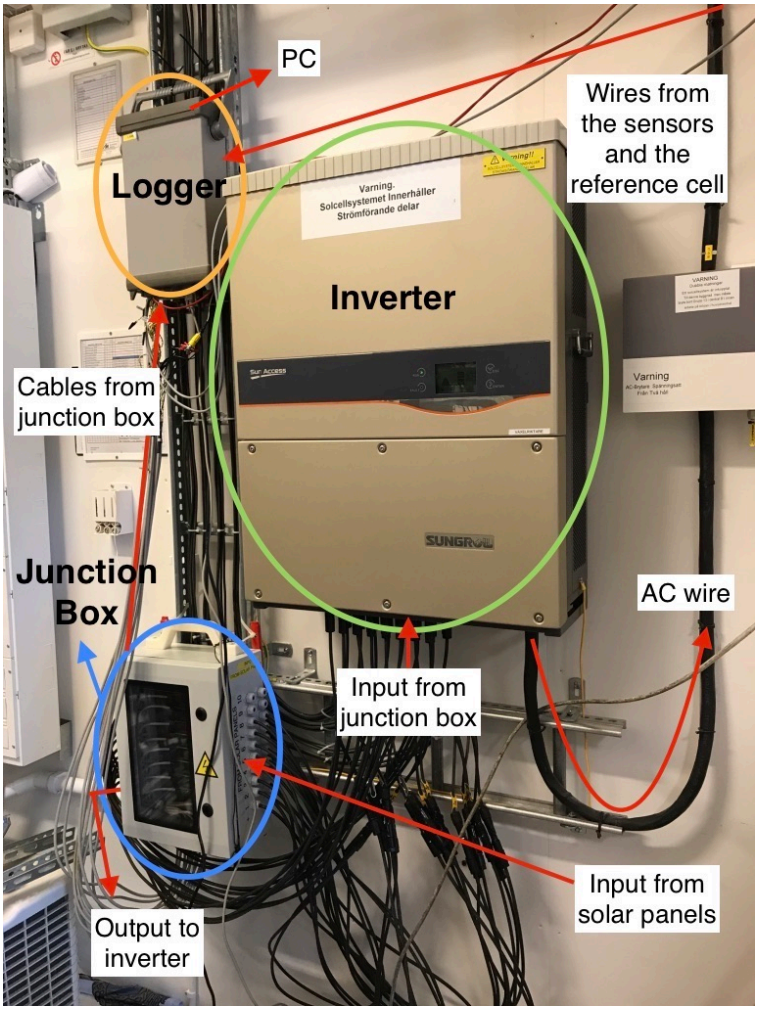

Figure 22. Schema of the connections between the components of the installation

3.2.1 PV system

The PV array consists of eight panels placed vertically on the south-east facade of the building. Seven panels contain 18 modules each one, and the first panel has 17 modules connected in series. So, in total there are 143 PV modules. Mounting PV modules vertically is not the best option because the angle of incidence is not the optimum. Some studies state that the yearly loss of installing the PV modules in vertical instead of at optimum angle in Southern Sweden is smaller than 28% and in the Northern Sweden is below 20% [8].

Figure 23. PV array formed by eight panels

The material of the modules of the system is polycrystalline silicon and the model is ET-P660250WW. One module contains 60 cells connected in series with the dimensions of 156mm x 156mm. The PV array contains 8 580 solar cells. Table 1 shows the electrical specifications of the modules.

Table 1. Electrical specifications of the PV modules [30]

Model Type	**ET- P660250WW**
Peak Power (P_{peak})	250 W_p
Module Efficiency	15.37%
Maximum Power Voltage (V_{mpp})	30.34 V
Maximum Power Current (I_{mpp})	8.24 A
Open Circuit Voltage (V_{oc})	37.47 V
Short Circuit Current (I_{sc})	8.76 A
Power Tolerance	0 to +5 W
Maximum System Voltage	DC 600 V/1000 V
Nominal Operating Cell Temperature	45.3±2°C
Series Fuse Rating (A)	15 A

Another important factor to consider is the temperature coefficient of the solar cells. In Table 2 the different temperature coefficients are shown.

Table 2. Temperature coefficients [30]

Temp. Coeff. of I_{sc} (TK I_{sc})	0.04 %/°C
Temp. Coeff. of V_{oc} (TK V_{oc})	-0.34 %/°C
Temp. Coeff. of P_{max} (TK P_{max})	-0.44 %/°C

3.2.2 Junction box

The function of an electrical junction box is to enclosure electrical connections, protect them and have a safety barrier. The junction box has the role of connecting the PV panels to the inverter. Moreover, it measures the current and voltage of each string and then the data is sent to the logger.

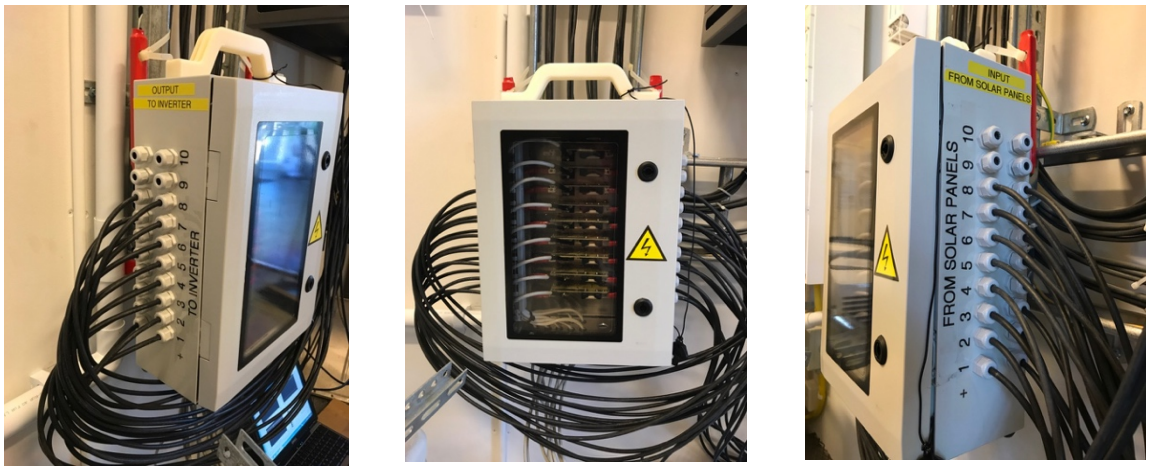

Figure 24. Junction box: on the left, output to the inverter and on the right, input from the 8 solar panels

3.2.3 Inverter

A solar inverter is a component of the balance of system of a PV system. The main function of an inverter is to convert direct current (DC) to alternating current (AC). In the case of solar inverters, they have two more functions: maximum power point tracking (MPPT) and anti-islanding protection.

The inverter is connected to the junction box, which at the same time is connected to the solar panels. As it has been explained in the theoretical background, the PV modules convert the energy from the sun to direct current. So, the inverter needs to transform the direct current to alternating current for matching the phase and voltage of the grid.

The inverter used in this installation is from SUNGROW and the model is SG30KTL-M. The maximum efficiency and the maximum input power are 98.3% and 30 800 W respectively [31].

It has eight connections, one for each string, separated into two maximum power points tracking. So, four panels are connected to MPPT1 and the other four to MPPT2, as it is seen in Figure 25.

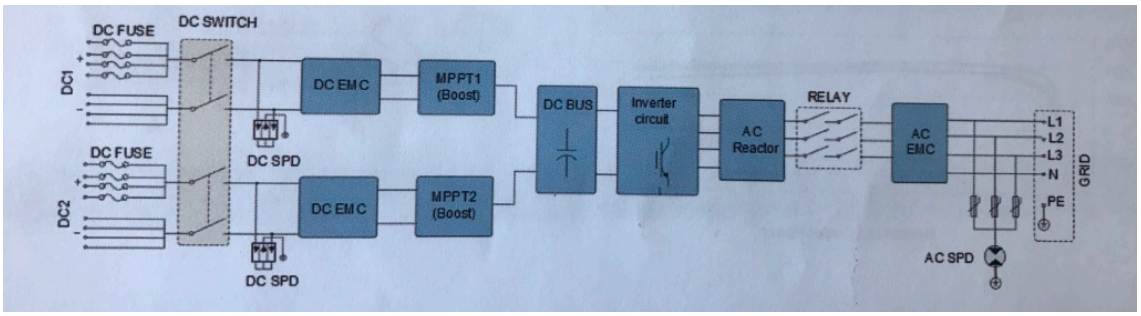

Figure 25. Circuit diagram of the string inverter SG30KTL-M [31]

Moreover, the inverter has a small screen which shows the current power P_{ac} [kW], the energy produced during the day E_{day} [kWh] and the total energy production E_{total} [kWh].

Figure 26. SUNGROW inverter

3.2.4 Monitoring system

Solar energy is intermittent and it is known that the output power of a PV system can vary drastically due to that. To study these changes, a monitoring system was installed. After doing a deep literature review research, it is noticeable that the most important parameters to consider are solar radiation, temperature and PV voltage and current [2]. The different devices to collect the data were installed in a wooden base, with the same orientation and position than the PV panels.

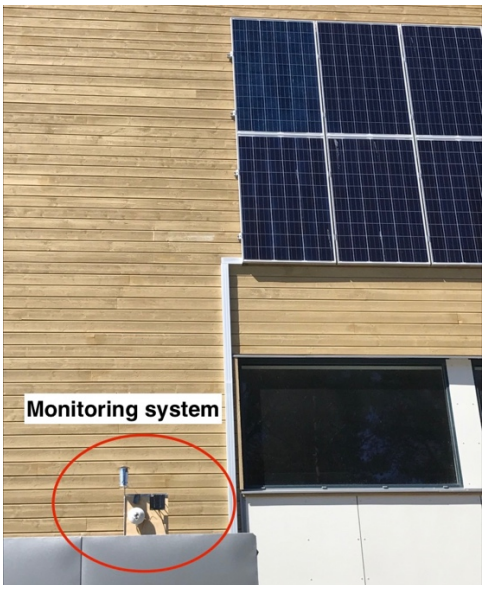

Figure 27. Location of the monitoring system

The monitoring system includes a pyranometer to measure the irradiance, a temperature sensor to evaluate the ambient temperature and a reference solar cell to quantify the short-circuit current I_{sc} and the open-circuit voltage V_{oc}. The three devices are connected to the logger, subsequently the data is obtained.

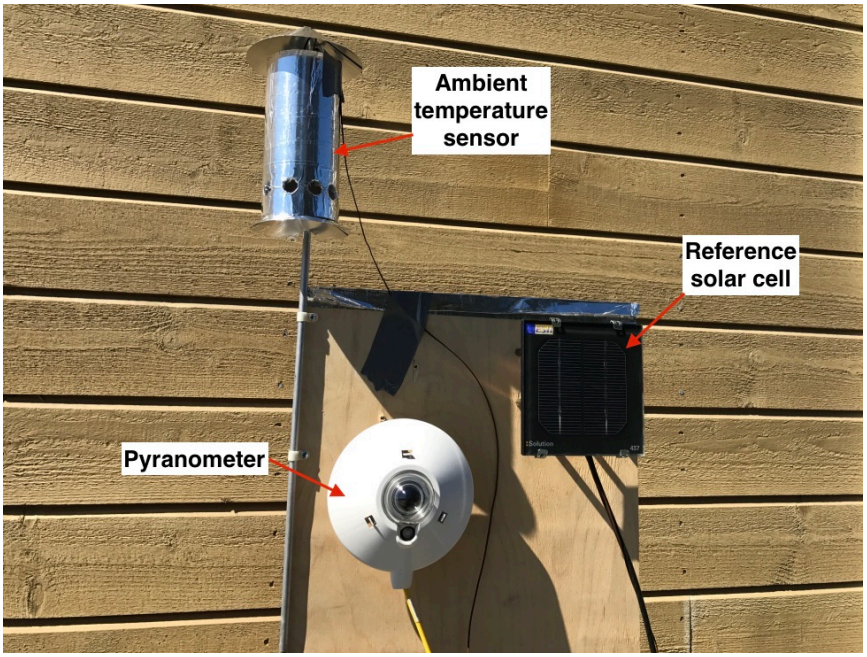

Figure 28. Monitoring system: ambient temperature sensor, pyranometer and reference solar cell

3.2.4.1 Ambient temperature sensor

Knowing the ambient temperature in each moment is important because it affects the temperature of the modules and consequently, the performance of the PV system. To achieve the best reliability the sensor was placed inside that casing with some holes to allow the airflow pass through it. In this way, despite being in the sun, the air temperature will be correct.

3.2.4.2 Pyranometer

A pyranometer is an instrument which measures global solar radiation on a flat surface. It is made of two hemispherical transparent glass covers and white disk, which restricts the acceptance angle to 180° [2]. As it was explained before, the irradiance is the factor that influences the most the operation of a PV module. With the installation of a pyranometer it will be possible to understand the changes in the output power due to the variation of the irradiance.

The sensor of the pyranometer measures the difference of voltage [mV] on it. The relation between the voltage and the irradiance can be expressed as: 13.11 mV when the irradiance is 1 000 W/m^2.

3.2.4.3 Reference solar cell

The reference solar cell is an ESTI-sensor, which is based on a monocrystalline silicon solar cell. The cell is divided into two: one half is connected to a shunt and delivers the I_{sc} proportional to the irradiance; the other half remains on open circuit and monitors the temperature [32].

It will be useful to display the IV curve because the I_{sc} and the V_{oc} will be obtained. Once the V_{oc} is known, it is possible to determine the temperature of the cell which will be estimated as the temperature of the modules. Table 3 shows the electrical characteristics of the reference solar cell.

Table 3. Electrical specifications of the ESTI-Sensor Nr.: ES1437 [32]

I_{sc} signal	28.7 mV@1 000 W/m^2
Alfa (α)	0.007 mV/°C
V_{oc} signal	586.7 mV@1 000 W/m^2
Beta (β)	-2.17 mV/°C
D	33.11 mV

3.2.5 Logger

A data logger is an electronic gadget that records data over time with instruments and sensors connected to it. Usually, their base is a digital processor. Its main function is to handle the output data of the sensors [2].

The model of the logger used is Agilent 3497A (Figure 29). It consists of a three-slot mainframe with a built-in 6 ½ digit digital multimeter. It has 20 channels which can be configured independently to measure one of 11 different functions [33]. In this study, all the channels were used: 16 connected to the solar panels and 4 to the monitoring system.

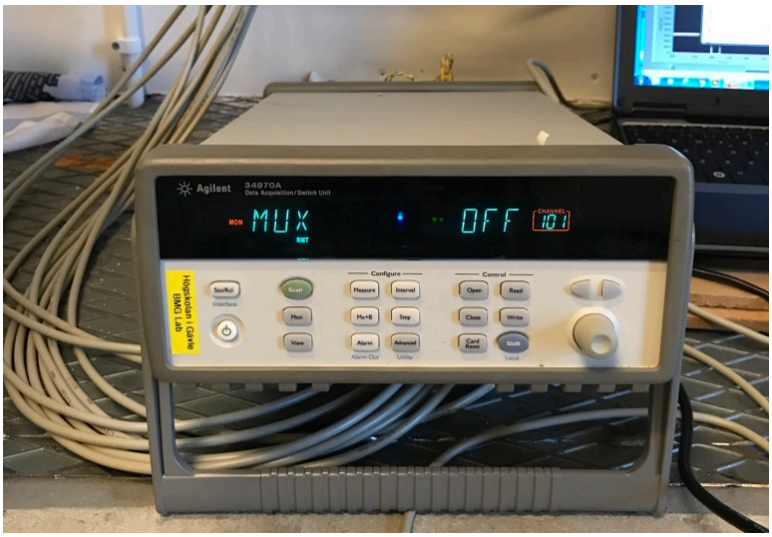

Figure 29. Data logger 34970A

The logger is connected to the junction box and the monitoring system. Therefore, the results of the performance of the PV panels and the meteorological parameters will be sent to the computer.

3.3 Data acquisition

The data is obtained from the logger which is connected to a computer. The program used to acquire the data is LabVIEW (Laboratory Virtual Instrument Engineering Workbench) from National Instruments. It is a platform and development environment for designing systems, with a graphical visual programming language. It is recommended for hardware and software systems tests and design, since it supports data acquisition and automatic and manual control of the parameters of the system [34].

As has been explained before, the logger has 20 channels and all of them were used. The connection with the PV system uses 16 channels, since there are 8 panels and the current and the voltage of each panel are obtained. The other 4 channels connect the logger to the monitoring system and then, the short-circuit current, the open circuit voltage, the ambient temperature and the voltage of the pyranometer are acquired.

The logger is configured to send data every minute. It takes 3 seconds to get the 20 measurements and it keeps doing it the whole minute. Then, it calculates the mean value of each parameter during that minute. So, finally, the data of each minute of the day is obtained.

The measuring system was installed the 24th of May. So, the study has been done with the data obtained since then, from the 25th until the 30th of May (6 full days). During those days, the system was evaluated under different weather conditions.

3.4 Obtaining of results

Once the data was acquired, some calculations using Microsoft Excel have been done to evaluate the performance of the system. Mainly, the analysis is based on the comparison between the real power produced by the system and the theoretical power calculated using the data obtained with the measurement system.

3.4.1 Real power

The real power is the output power produced by the PV system and used to supply electricity to the building or sell it to the grid. Each panel works independently and produces its amount of power. Then, the sum of the power of all the panels provides the total power of the system.

The information obtained from the panels is the current (I) and the voltage (V) of each string at every minute. So, as it is explained in the subsection *2.3.3 IV curve*, to calculate the power of each string the equation 19 was used.

$$P\ (W) = I \cdot V \tag{19}$$

Once the power of the 8 strings is calculated, it is possible to know which string produces more power and the evolution during the day depending on the weather conditions.

3.4.2 Theoretical power

The theoretical power is the power calculated experimentally and expected to be delivered by the system. The equation 20 explained in the subsection *2.3.2 Output of a PV module* was used.

$$P_{theoretical}(T,\theta) = P_{peak}(25{,}0) \cdot \frac{[K_b(\theta) \cdot G_b + K_d \cdot I_d] \cdot [1 + (T_m - 25) \cdot \alpha]}{1000} \tag{20}$$

In the following subsections, it is explained how the parameters of the equation were obtained or calculated.

3.4.2.1 Peak power

The peak power of the modules is given by the manufacturer in the electrical specifications (Table 1). So, the peak power used is P_{peak} = 250 W_p. As there are 18 modules per each panel, to calculate the theoretical power of each string, the peak power was multiplied by 18, except for the first string which has 17 modules.

3.4.2.2 Irradiance

There are two ways to calculate the irradiance: with the pyranometer or with the reference solar cell installed. In the equation 20, the irradiance is divided into direct (beam) radiation and diffuse radiation. In this case, the devices provide the global radiation which for the calculations is all considered beam radiation. So, the diffuse radiation is considered 0.

On the one hand, the sensor connected to the pyranometer provides the difference of voltage [mV] on it. Knowing the relation between the voltage and the irradiance (13.11 mV, 1 000 W/m^2), the irradiance at every minute can be calculated as:

$$Irradiance_{pyr}\left(\frac{W}{m^2}\right) = \frac{V_{pyr} \cdot 1000}{13.11} \quad (21)$$

On the other hand, as the short-circuit current of the reference solar cell is measured and the equivalence with the irradiance is also known (Table 3), the irradiance can also be calculated as:

$$Irradiance_{refcell}\left(\frac{W}{m^2}\right) = \frac{I_{sc} \cdot 1000}{28.7} \quad (22)$$

In this case, a calibration of the solar cell towards the pyranometer with a factor of 1.02 was applied.

3.4.2.3 Angle of incidence correction factor

The angle of incidence varies during the day due to the position of the Sun. When using the irradiance measured with the pyranometer, a correction factor needs to be applied. In the case of the irradiance obtained from the solar cell, it is not necessary because the reference solar cell is oriented in the same way as the modules.

In the subsection *2.1.1 Angle of incidence*, it is explained how to calculate the angle of incidence. In this case, an Excel file with some equations was used. So, inserting the location and orientation of the system together with the day of the year, the angle of incidence each minute was acquired.

Once the angle of incidence was known, it was possible to calculate the correction factor using the equation 23.

$$K_b = 1 - b_0 \cdot \left(\frac{1}{\cos\theta} - 1\right) \quad (23)$$

There is a problem using this equation when the angle of incidence is around 90°. Because cos (90°) = 0 and it implies a division by 0 which causes an incorrect amount of power. To solve this, the data of the moments of the day when the angle of incidence is around 90° was not considered.

3.4.2.4 Temperature of the module

The temperature of the module affects the performance of the PV system, as was explained in the subsection *2.4 Effect of irradiance and temperature*. The module temperature can be calculated in two ways: by convective heat transfer using the temperature of the air or with the reference solar cell. Firstly, it was calculated by convective heat transfer:

$$T_{module} = T_{ambient} + \frac{G}{h} \quad (24)$$

Where:

- T_{module}: Temperature of the modules [°C]
- $T_{ambient}$: Temperature of the air [°C]
- G: Irradiance [W/m^2]
- h: Convective heat transfer coefficient [W/m^{2}K]

The convective heat transfer coefficient can very between 20 and 30 W/m^{2}K. So, the temperature of the module was calculated with three different convective heat

transfer coefficients (20, 25 and 30 W/m^{2}K) to adjust the module temperature to the one given by the reference solar cell.

Then, to calculate the module temperature with the reference solar cell, the open-circuit voltage measured was used. Table 3 gives the open-circuit voltage at 25°C, which is 586.7 mV. Knowing this and the parameter β = -2.17 mV/°C, which means that V_{oc} decreases 2.17 mV per each degree, the module temperature is obtained:

$$T_{module} = \frac{V_{oc} - V_{oc}(25°C)}{\beta} + T_{STC} = \frac{586.7 - V_{oc}}{2.17} + 25 \quad (25)$$

After some calculations, it was seen that to obtain a similar module temperature with both methods, the convective heat transfer coefficient should be 25 W/m^{2}K.

Another thing to consider is the temperature coefficient. It is given by the manufacturer of the modules (Table 2), α = -0.44 %/°C.

3.4.2.5 Efficiency

Finally, to adjust better the theoretical and the real power, an efficiency coefficient (η) was applied. After some research, an efficiency of 95% was considered correct. So, the amount of theoretical power of each string was calculated as:

$$P_{theoretical}(T, \theta) = \eta \cdot N_m \cdot P_{peak} \cdot \frac{[K_b(\theta) \cdot G] \cdot [1 + (T_m - 25) \cdot \alpha]}{1000} \quad (26)$$

3.4.3 Reliability of the monitoring system

To assure that the measures done with the monitoring system were correct, different charts were created. The calculations were done using both, the irradiance obtained from the pyranometer and the one from the reference solar cell.

First, the peak power of the strings was calculated for the whole day. It was used the output power of the string 8 because it is the closest one to the monitoring system.

$$P_{peak} = \frac{P_{string}}{Irradiance} \quad (27)$$

Moreover, it was also represented the relation between the real power and the irradiance. It is supposed to be a straight line, since the output power is directly proportional to the irradiance.

3.4.4 Expected power

Knowing that the PV array contains 143 modules and the peak power of each module is 250 W_p, the promised power of the system is 35.75 kW. Considering just one string of 18 modules, the output power when the irradiance is 1 000 W/m^2 should be 4 500 W.

To know if the system is providing the expected amount of power, the power at nominal conditions was estimated for both cases (pyranometer and reference solar cell). The nominal power was calculated using as reference the equation 20.

Equation 28 and 29 show how to calculate the nominal power in the case of the pyranometer and the reference solar cell respectively. They consider the temperature correction factor and in the first case, the angle of incidence correction factor as well.

$$P_{nominal\ string}(Pyr) = \frac{I \cdot V}{K_b(\theta) \cdot [1 + (T_m - 25) \cdot \alpha]} \quad (28)$$

$$P_{nominal\ string}(RefCell) = \frac{I \cdot V}{[1 + (T_m - 25) \cdot \alpha]} \quad (29)$$

4 Results

This section explains the performance of the PV system during some days under different weather conditions and the results obtained after the calculations. The 27th of May 2017 was taken as reference because it was a sunny day. The results and charts of the rest of the days are represented in the appendixes.

Moreover, all the calculations and comparisons regarding to just one string were done with the string 8, since it is the closest one to the monitoring system.

4.1 Reliability of the monitoring system

Figure 30 and Figure 31 show the peak power of the string 8 during the 27th of May of 2017. Evaluating it with the output power of the other strings, the same shape is obtained.

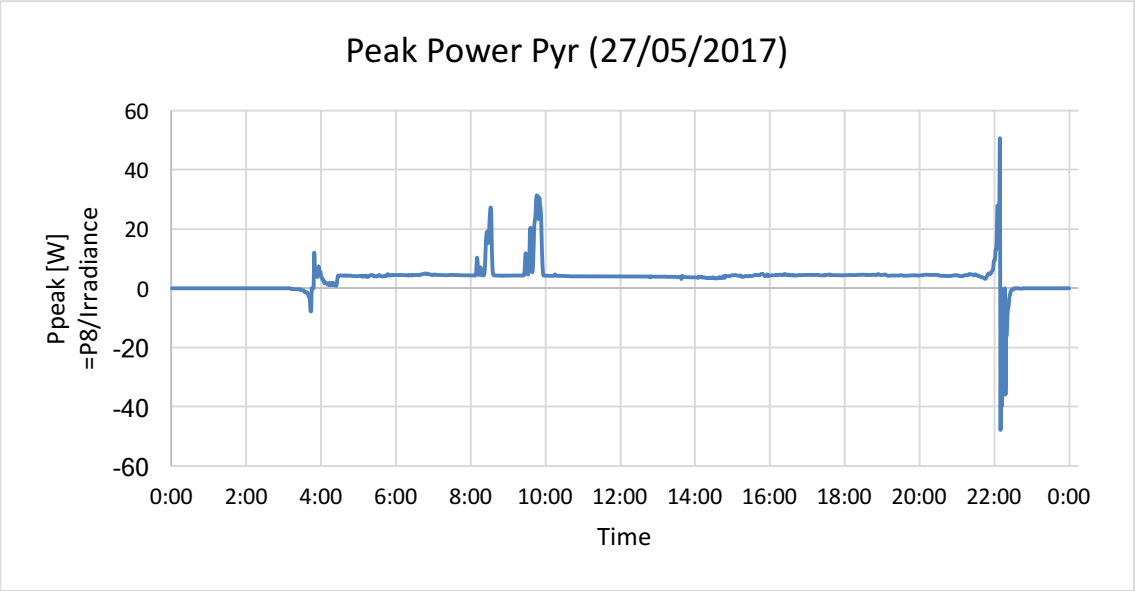

Figure 30. Peak power of the string 8 calculated with the irradiance from the pyranometer

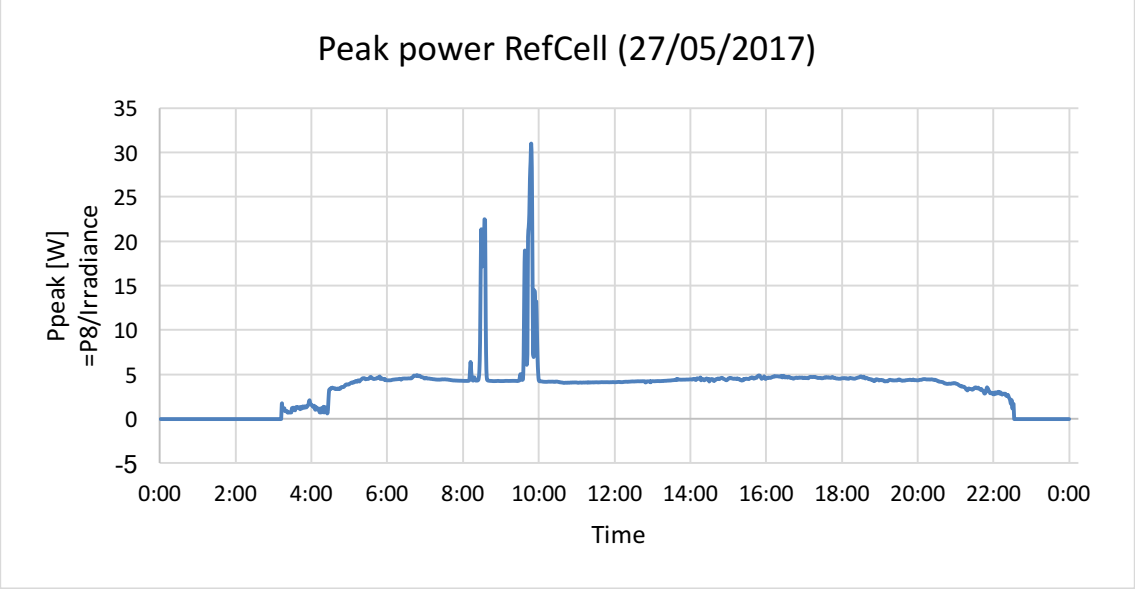

Figure 31. Peak power of the string 8 calculated with the irradiance from the reference solar cell

In Figure 32 and Figure 33, the relation between the output power of the string 8 and the irradiance is represented.

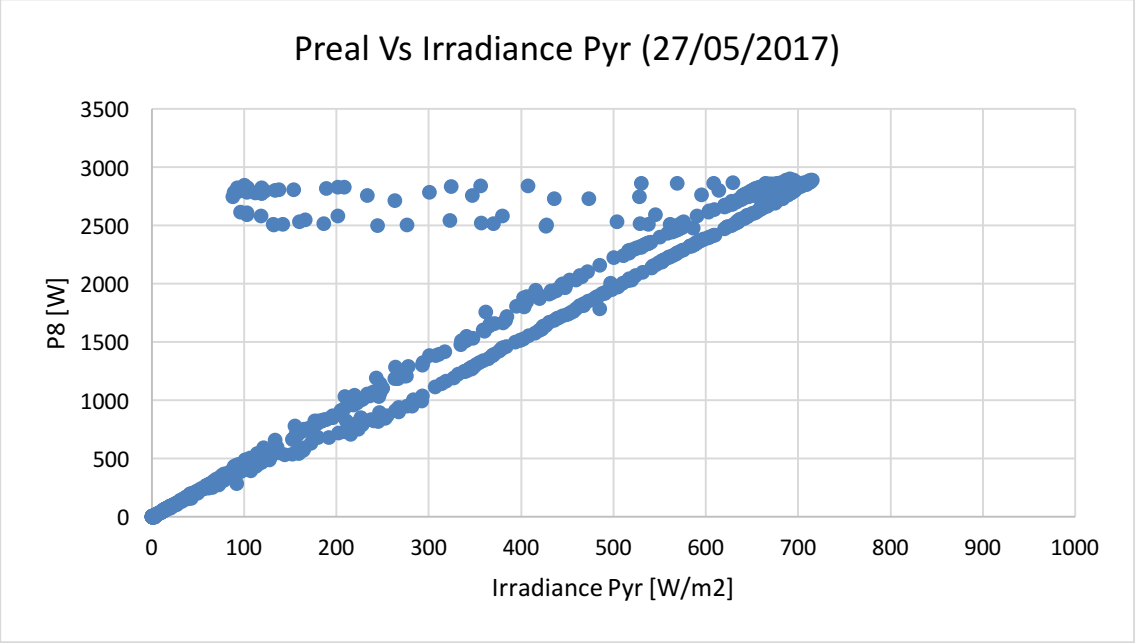

Figure 32. Relation between the output power of string 8 and the irradiance from the pyranometer

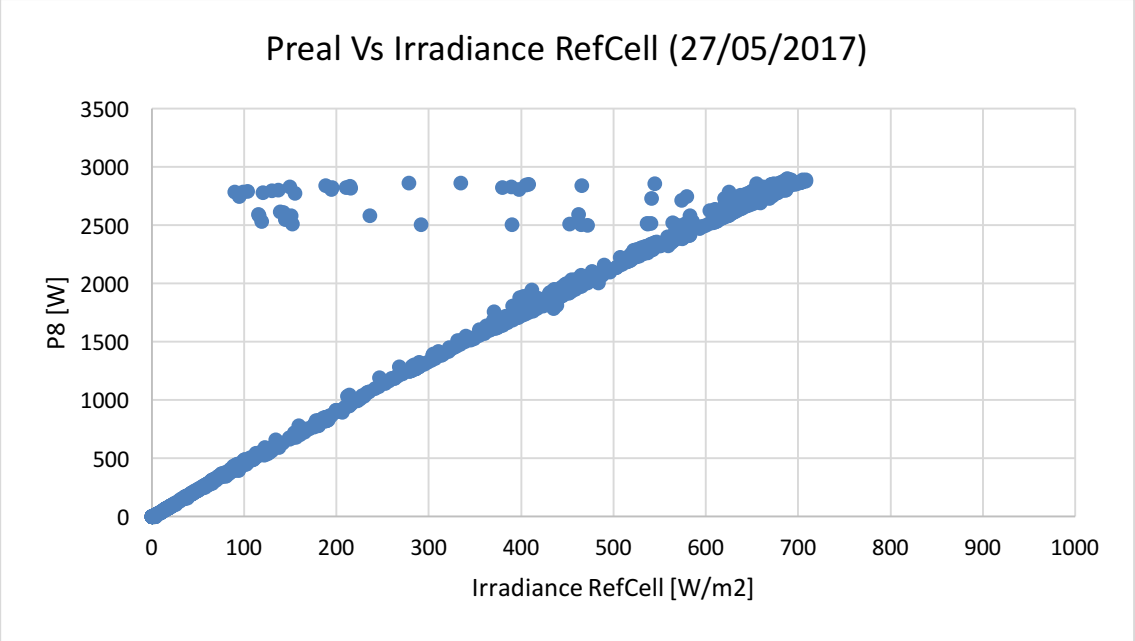

Figure 33. Relation between the output power of string 8 and the irradiance from the reference solar cell

After seeing some irregularities in the charts, some data was not considered to check the reliability of the measurement system. So, Figure 34 and Figure 35 show again the relation between the output power and the irradiance, just taking into account the data between 04:30 and 21:00, without considering the data between 08:00 and 10:00.

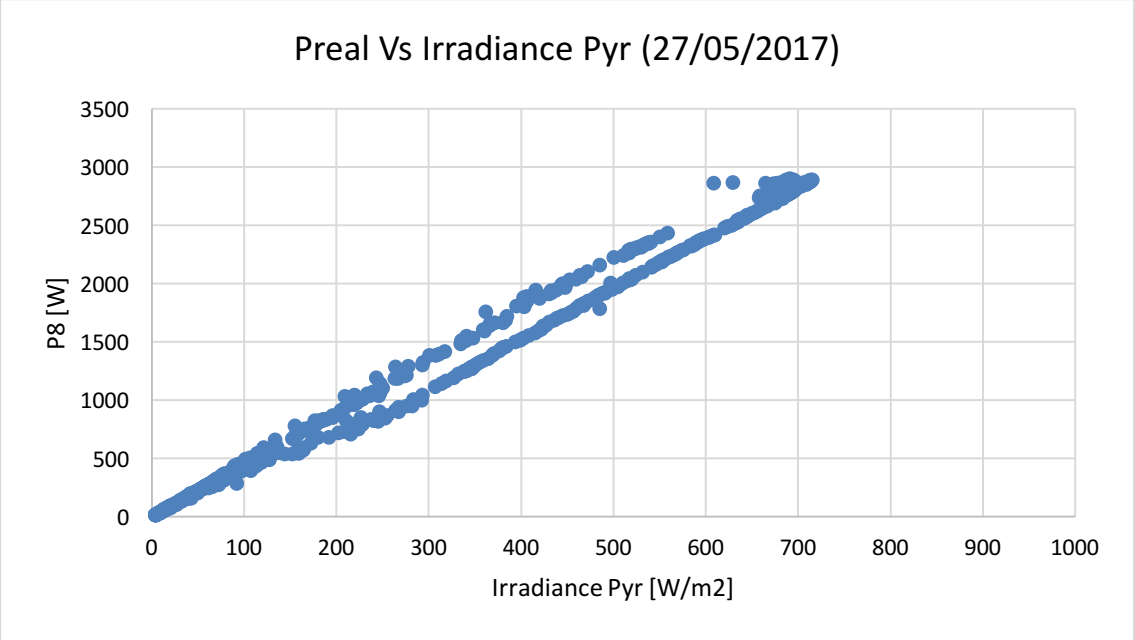

Figure 34. Relation between the output power of string 8 and the irradiance from the pyranometer, once some data was not considered

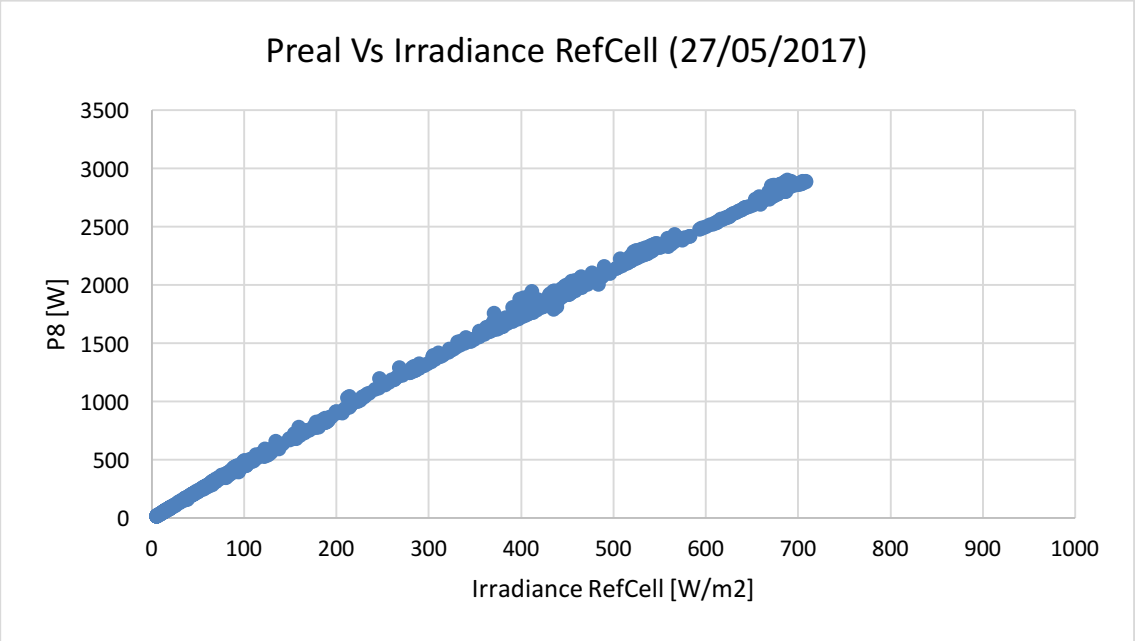

Figure 35. Relation between the output power of string 8 and the irradiance from the reference solar cell, once some data was not considered

4.2 Angle of incidence

The angle of incidence was calculated for all the days. Figure 36 illustrates the angle of incidence on the surface of the modules the 27th of May of 2017 (day number 147 of the year). As the evaluation was done during one week, the angle of incidence between the different days is almost the same.

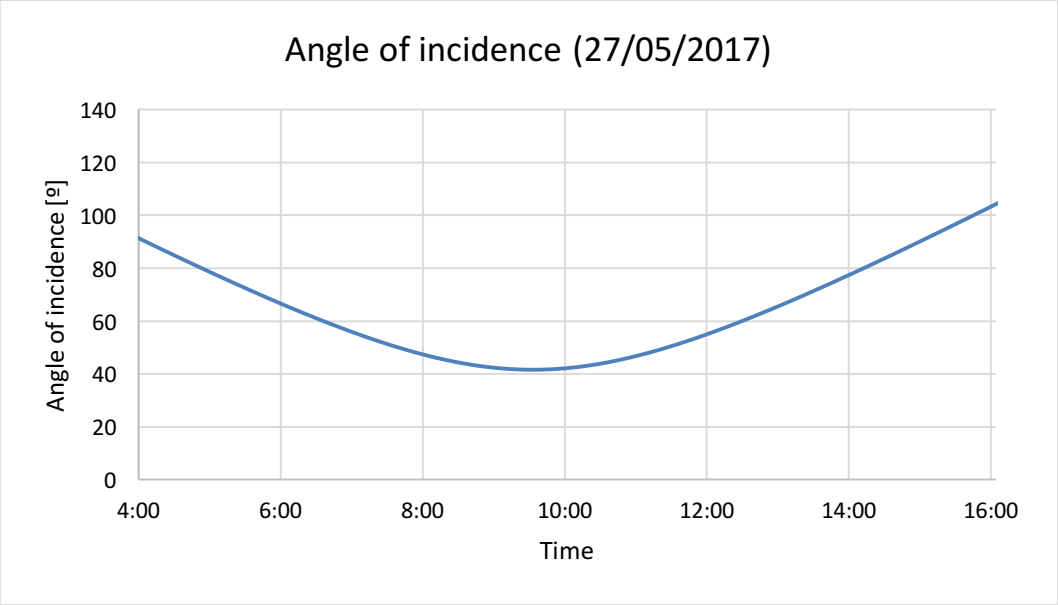

Figure 36. Angle of incidence on the surface of the modules

4.3 Real and theoretical power

The theoretical power was calculated by two methods:

1. Irradiance from the pyranometer and the temperature of the module obtained through heat transfer.
2. Irradiance and temperature of the module from the reference solar cell.

Figure 37 shows the relation between the theoretical power and the real output power of one string.

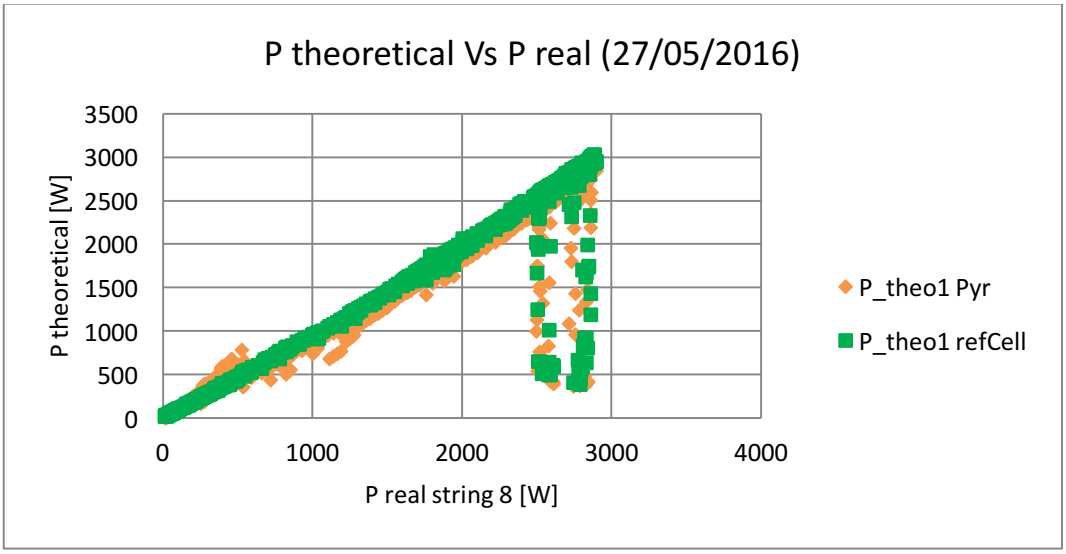

Figure 37. Relation between the theoretical power and the real output power (string 8)

Considering the data between 04:30 and 21:00, Figure 38 illustrates the evolution of the output power during the day and it is possible to compare the real with the theoretical power. In the case of the theoretical power obtained with the measurements done with the pyranometer, the data between 14:15 and 15:15 is not considered because at this time the angle of incidence is around 90° and in consequence an asymptote appears. So, there is a small gap in the chart.

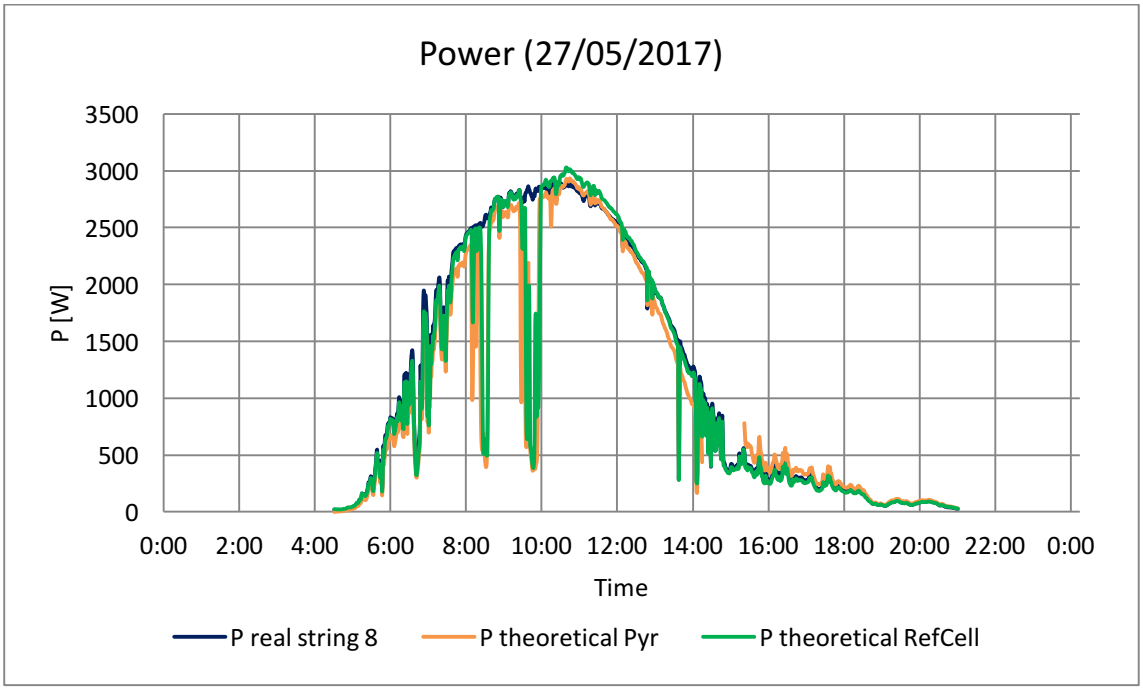

Figure 38. Evolution of real and theoretical power during the 27th of May 2017

4.4 Performance of the PV system

The performance of the eight strings and the whole PV system is shown below. Different days are represented, so it is possible to see how the weather, the temperature and the irradiance influence in the operation of the PV system (Table 4, Figure 39 and Figure 40).

Table 4. Weather conditions of each day and maximum power of the PV system

Day	Weather	Mean ambient temperature	Maximum irradiance measured	Maximum power of the PV system
25/05/2017	Sun and clouds	16.5 °C	796.7 W/m^2	27.81 kW
26/05/2017	Sun and clouds	14.2 °C	853.3 W/m^2	29.66 kW
27/05/2017	Sun	21 °C	711.9 W/m^2	23.35 kW
28/05/2017	Sun	20.3 °C	730.5 W/m^2	24.16 kW
29/05/2017	Clouds and sun	10.6 °C	861.8 W/m^2	33.02 kW
30/05/2017	Rain	9.6 °C	57.7 W/m^2	2.51 kW

The PV system reaches the maximum power of the day between 10:00 and 10:30, if it is a clear day.

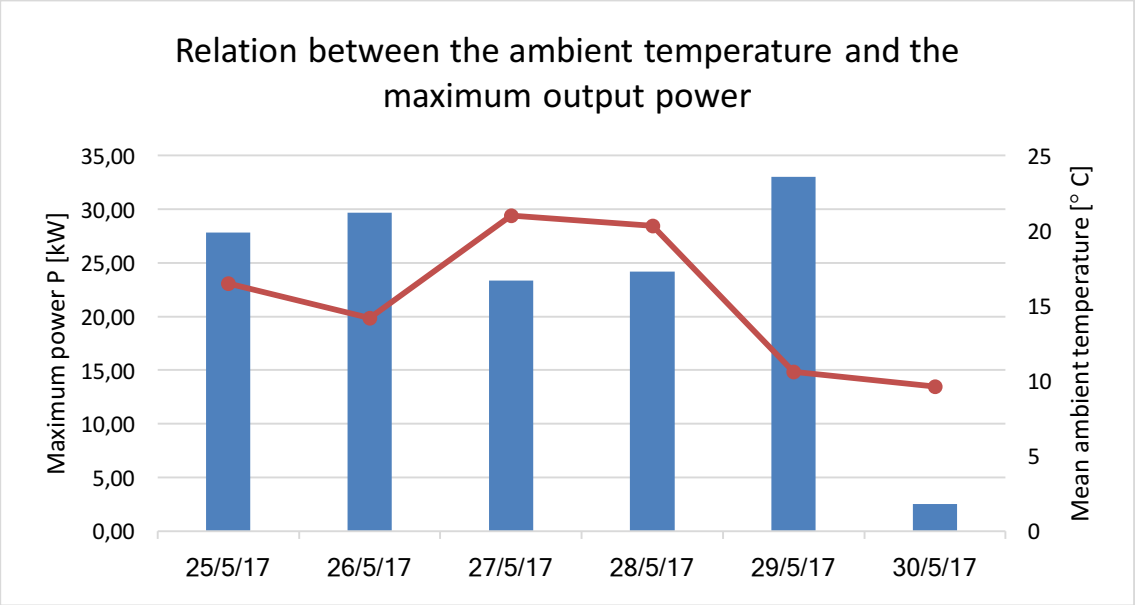

Figure 39. Relation between the ambient temperature and the maximum output power of the PV system

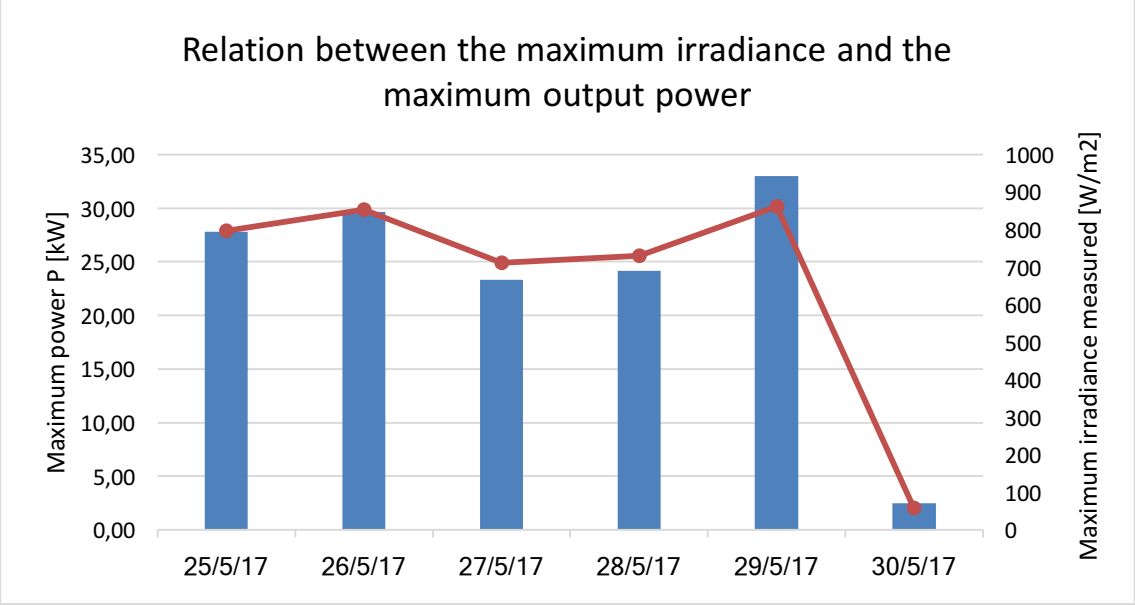

Figure 40. Relation between the maximum irradiance measured and the maximum output power of the PV system

Figure 41 shows the total power that each string produces during a sunny day. It is possible to observe the differences between the strings. The variation between the strings of 18 modules is less than 2.7% and with the panel of 17 modules is around 6%.

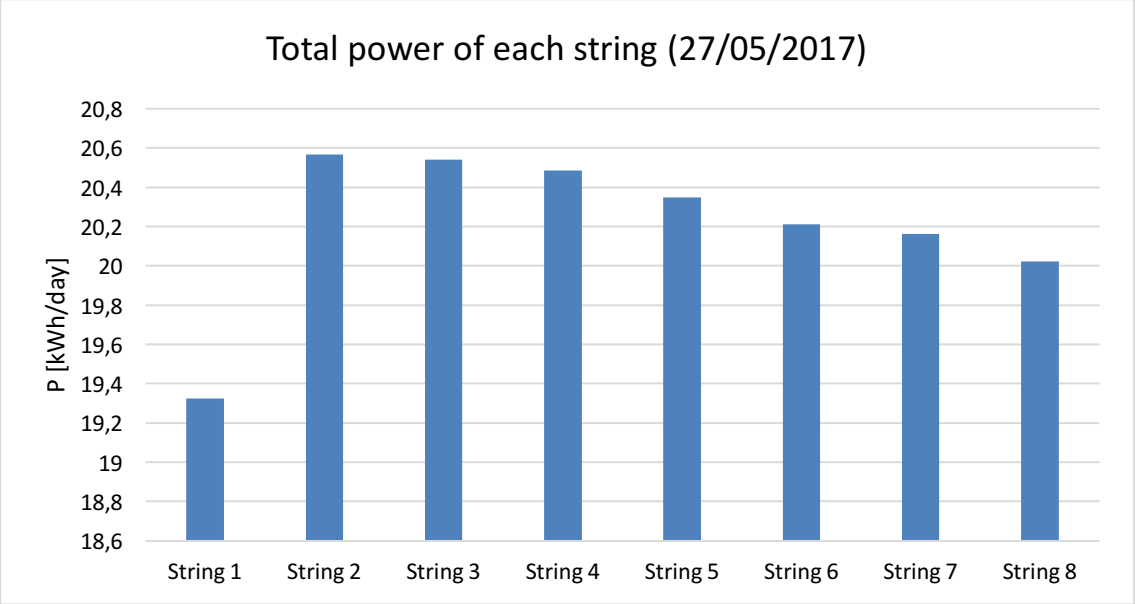

Figure 41. Total power of each string the 27th of May 2017

In the following subsections, the performance of the eight strings during the 27th, 29th and 30th of May is shown (Figure 42, Figure 44 and Figure 46 respectively). In Figure 43, Figure 45 and Figure 47 is represented the output power of the whole PV system.

4.4.1 Sunny day

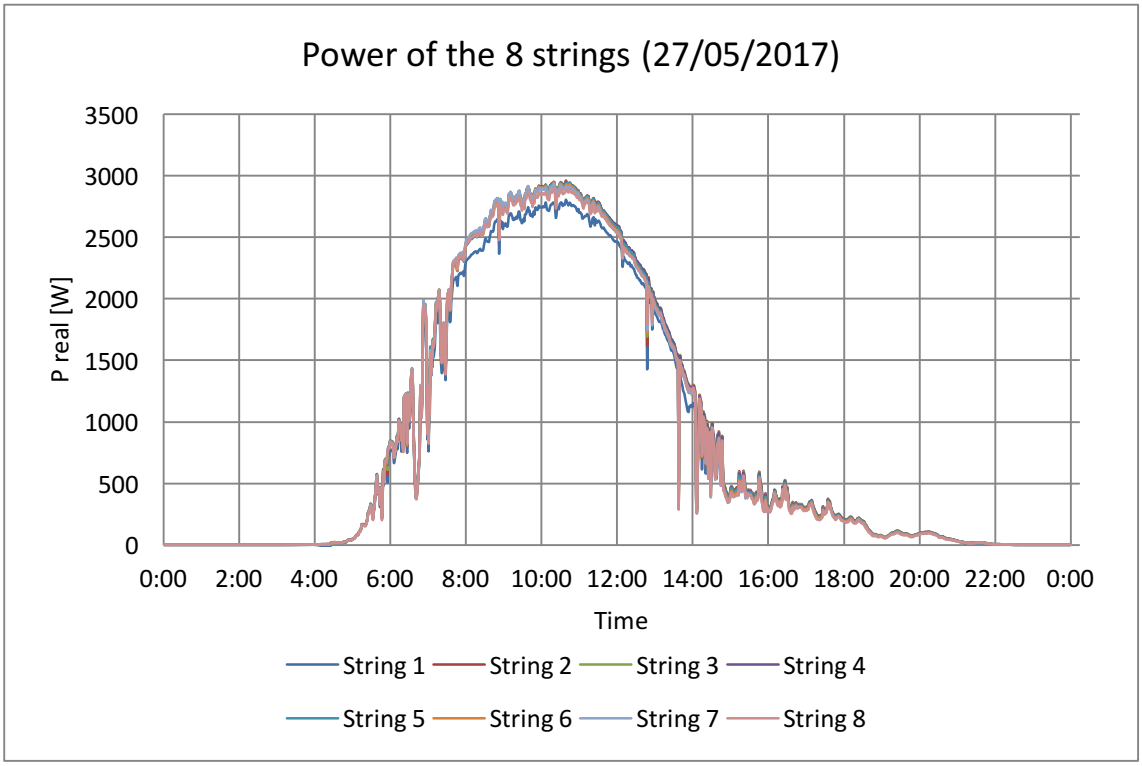

Figure 42. Performance of the eight strings the 27th of May 2017

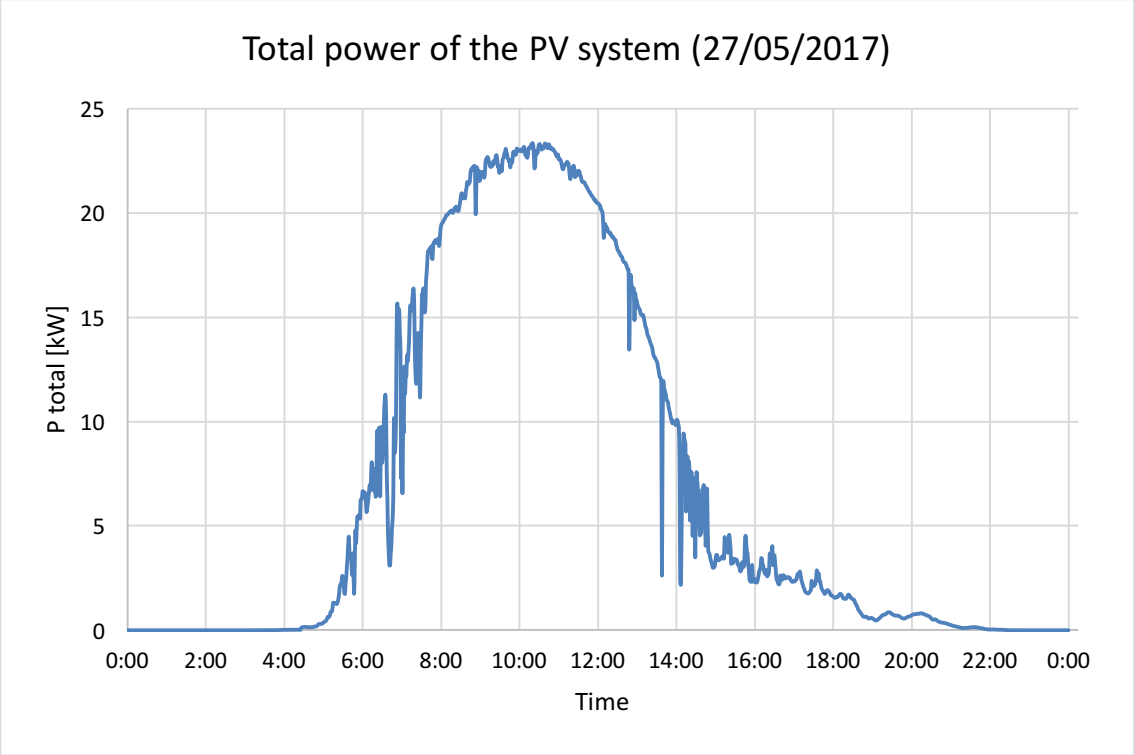

Figure 43. Performance of the PV system the 27th of May 2017

4.4.2 Partially sunny day

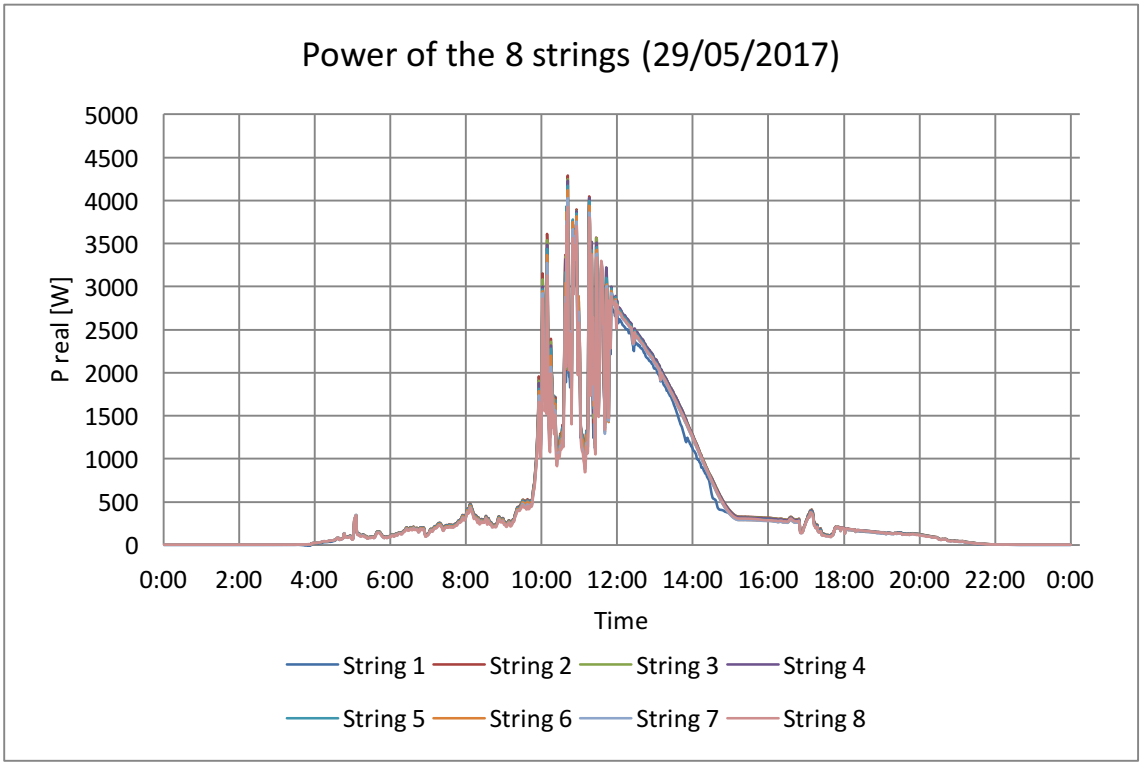

Figure 44. Performance of the eight strings the 29th of May 2017

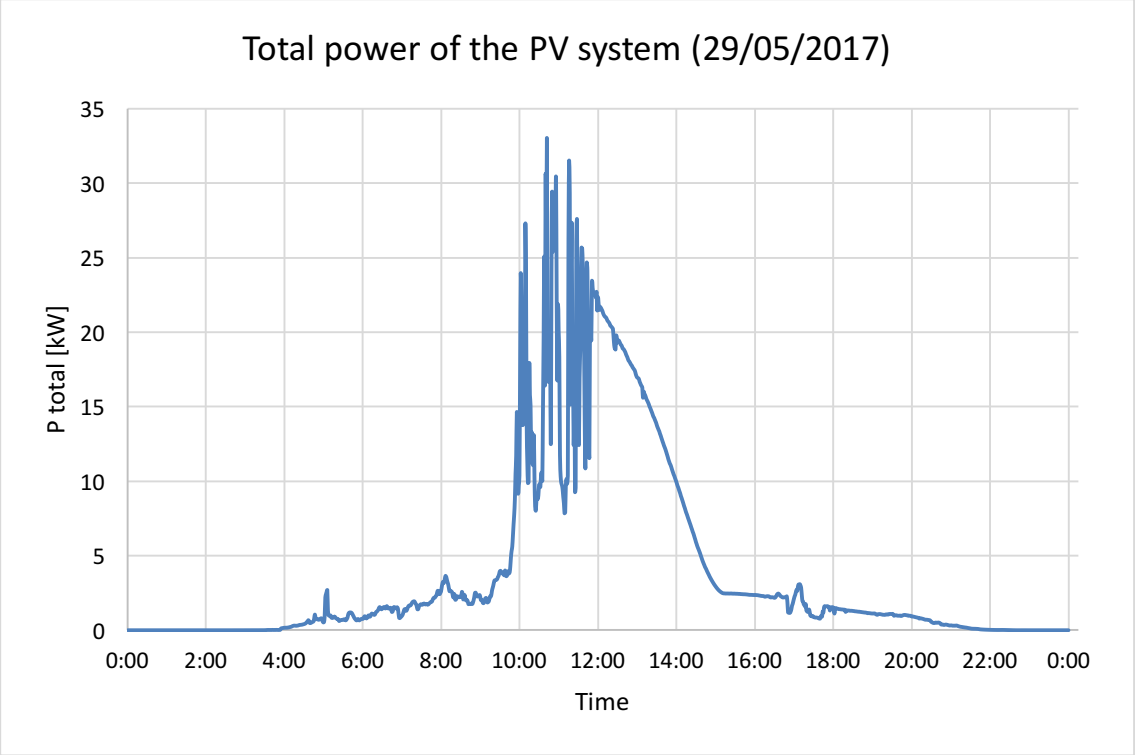

Figure 45. Performance of the PV system the 29th of May 2017

4.4.3 Rainy day

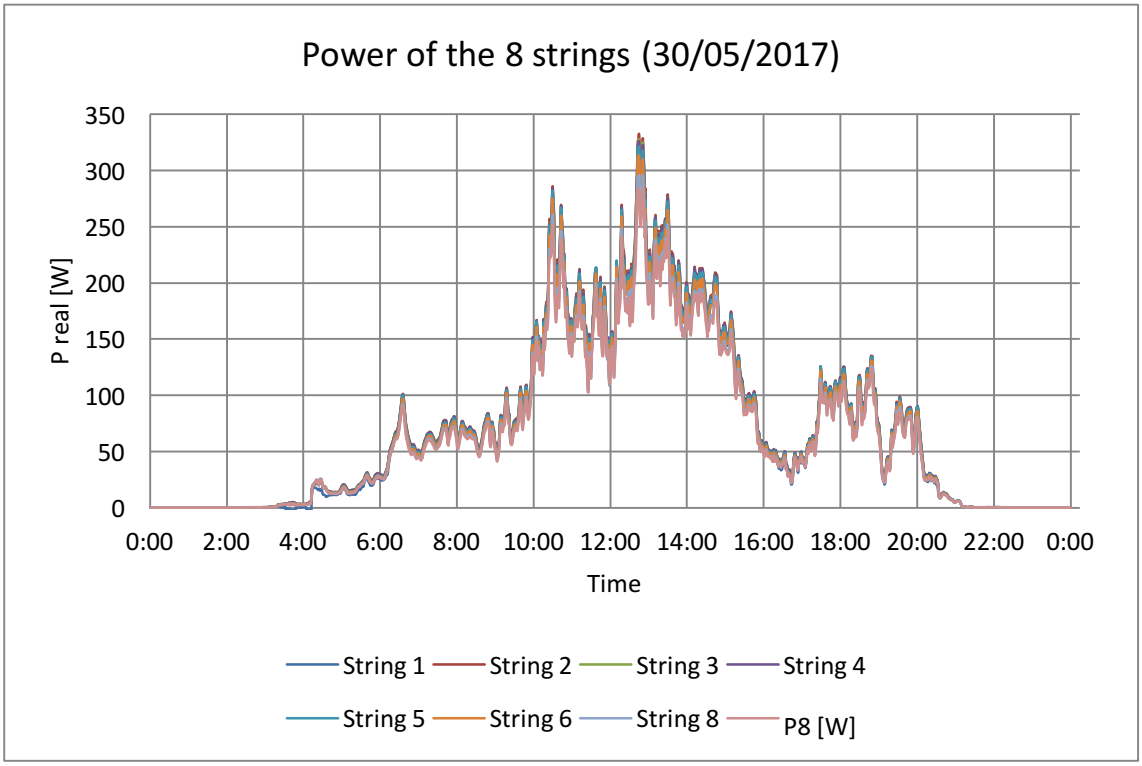

Figure 46. Performance of the eight strings the 30th of May 2017

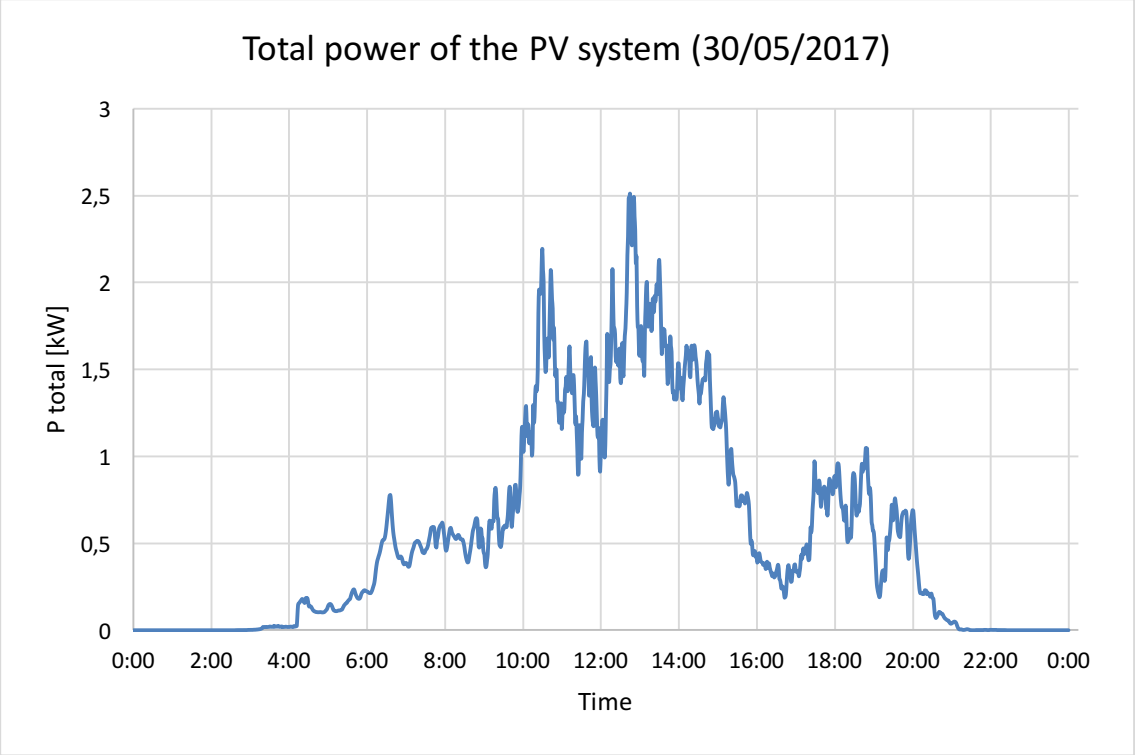

Figure 47. Performance of the PV system the 30th of May 2017

4.5 Expected power

Next figures represent theoretically the expected power at nominal conditions of the string 8. Blue points are the power obtained at that irradiance and the red line the expected power at higher irradiances. In both cases the output power would reach 4 500 W (nominal power).

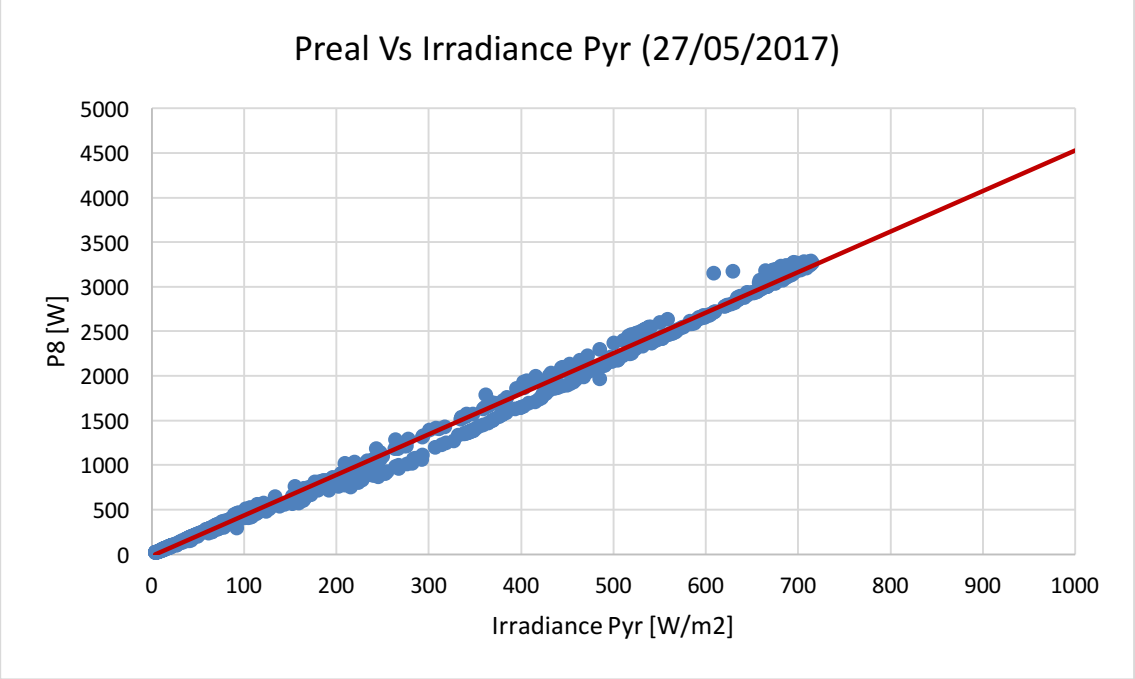

Figure 48. Expected output power in relation with the irradiance measured with the pyranometer

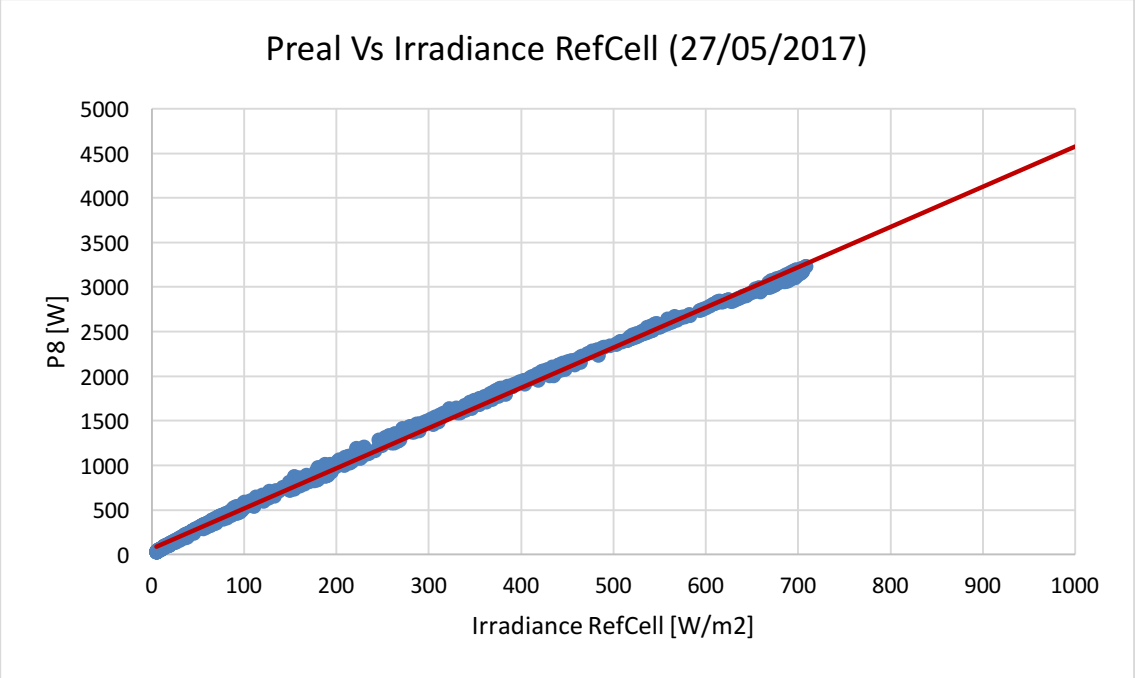

Figure 49. Expected output power in relation with the irradiance measured with the reference solar cell

5 Discussion

5.1 Reliability of the monitoring system

First of all, it was necessary to know if the monitoring system was working properly. So, the peak power of the strings was represented for the whole day for both irradiances. Theoretically, the peak power should be constant during the time of power production and otherwise, zero.

On the one hand, for the irradiance calculated with the pyranometer, in Figure 30, it is possible to observe that there are some irregularities at the beginning and at the end of the day and between 08:00 and 10:00. On the other hand, for the irradiance measured with the reference solar cell, in Figure 31, the same irregularities between 08:00 and 10:00 appear, but the other ones do not.

In the case of the peaks at the beginning and at the end, it happens because the difference of voltage in the pyranometer at some time is zero and subsequently the irradiance is zero as well. So, calculating the peak power appears an asymptote. To avoid this, the study will be focused between 04:30 and 21:00. Apart from that, the system does not produce power before and after these hours.

The other irregularities, between 08:00 and 10:00, appear as a result of the shadow of the trees in front of the arena on the monitoring system (Figure 50).

Figure 50. Shadows of the trees on the monitoring system

During these two hours, the shadow reaches the monitoring system two times. First, between 08:00 and 08:30 (Figure 50) and later, between 09:00 and 10:00 (the shadow on the left moves to the right due to the Sun). When it is cloudy, this does not happen, since the PV system is shadowed just like the monitoring system. Then, the peak power curve is correct. See Figure 57, Figure 58, Figure 59 and Figure 60, Appendix I.

During this time of the year, as the sun is high, it has been verified that the trees do not shadow the PV modules. If the monitoring system was placed at the same height as the PV modules, the theoretical results would be more precise.

Regarding the relation between the output power and the irradiance, it should be a straight line. In Figure 32 and Figure 33, there are some points out of the line. These points correspond to the data between 08:00 and 10:00. So, to assure the reliability of the system, these points were removed, together with the beginning and the end of the day. Then, Figure 34 and Figure 35 were obtained. The relation is correct, because when the irradiance increases also does the output power. In Figure 34, two different lines appear. One correspond to the morning and the other to the afternoon, this occurs because the pyranometer is not perfectly aligned.

5.2 Angle of incidence

At the end of May, the Sun is quite high. As the PV modules are placed vertically, the angle of incidence on the surface during the day is higher than in winter, when the sun is lower.

The modules are oriented towards south-east, so the lowest angle of incidence takes place in the morning. The lower the angle of incidence, the greater the irradiance reaching the surface and higher the output power produced.

5.3 Real and theoretical power

It is important to compare the theoretical power calculated and the real power obtained. In Figure 37, the relation between the two theoretical powers and the real power is represented. There are some points on the right that do not follow the line. These are the points between 08:00 and 10:00 (shadows), which have not been removed to compare the results with the real power. In the case of the pyranometer, there are some points that do not match completely. This is because of the start and the end of the asymptote explained before (*4.3 Real and theoretical power*).

In Figure 38, the evolution of the three powers during the day is shown. All of them have the same curve, except for the drop of the theoretical powers between 08:00 and 10:00 because of the shadows, and not considering the irregularities due to the asymptotic behaviour in the case of the pyranometer.

Regarding the amount of power, the theoretical power from the reference solar cell matches almost perfectly with the real power and in this case, it is a bit higher. On the other hand, the theoretical power from the pyranometer also matches but there are some small differences.

So, in this case, using a reference solar cell to extract the measurements to simulate the theoretical performance of the system is more accurate than employing a pyranometer. Even though, there is the possibility that the pyranometer is not perfectly calibrated.

5.4 Performance of the PV system

An important part of the study was to evaluate the performance of the PV system and see the differences between the panels.

As it is seen in Table 4, during the six days of measurements, the weather, the ambient temperature and the irradiance were different. In this way, it is possible to observe the variation of the power due to these factors (Figure 39 and Figure 40).

The factor that influences the most the performance of the system is the irradiance. It is directly related to the weather, when the sky is covered the power is lower. The first two days, the sky was partially covered, so there were a lot of ups and downs in the output power (Figure 87 and Figure 88, Appendix III). The 27th (Figure 43) and 28th (Figure 90, Appendix III) of May were completely clear days, so the power curve is almost perfect. In the case of the 29th (Figure 45), during the morning the sky was covered, but then it cleared up. Finally, the last day (Figure 47), it was raining all day and therefore the power obtained is so low.

Regarding the effect of the temperature, as it can be seen in Figure 39 graphically, although the 27th and the 28th were the sunniest days, they do not have the highest maximum output power because the temperature was elevated. In contrast, the 29th, when the sky was clear the power of the PV system was much higher because the ambient temperature was low. The first two days are in between.

In Figure 41 is shown the total output power of each string during a sunny day. String 1 produces less power than the others, since it has one module less. Although the other strings have the same number of modules, there are some differences due to dust and dirt accumulation. Figure 42, Figure 44 and Figure 46 show the performance of each string during different days. The curve of all the strings follow the same form, so all of them work simultaneously and correctly.

It would be interesting to study the PV system when the sun is lower in the sky, because then, the trees will shadow the PV panels and the performance of each string would be different. Moreover, a different connection of the strings to the inverter, that is to the MPPTs, could improve the total output power of the system.

5.5 Expected power

The promised amount of power before the installation of the system was 35.75 kW at nominal conditions. As it is unlikely that a PV system works at STC, the maximum power registered these days was 33.02 kW, but it is not far from the expected one. It must be said that is possible that it was a spike with a very high irradiance when the maximum power of 33 kW was reached. This can happen during a short time when the sun is unshaded but the sky is cloudy. So, solar radiation is reflected in the clouds.

Figure 48 and Figure 49 show an estimation of which would be the output power of one string at nominal conditions, calculated with the pyranometer and the reference solar cell respectively. In both cases, the expected power for one string is reached (4 500 W). So, the PV system is working properly because the power that the system is providing corresponds to the promised one.

6 Conclusion

After doing a thorough analysis of the data obtained, some conclusions can be extracted.

Firstly, the measurement system installed is reliable, since the behavior of the system is the one expected. Even though, it would be better to install the monitoring system in the same height as the PV modules to achieve more accurate results and avoid irregularities.

Secondly, it can be concluded that the model used to calculate the nominal power is correct. The main goal of the thesis was to know if the PV system is providing the power promised. There were some doubts but it has been proved that the system works at nominal power.

Moreover, as it was observed, the model used to calculate the theoretical powers is also precise. The theoretical power curves match almost perfectly with the real power one. Additionally, with the comparison between both methods to obtain the theoretical power, it has been seen that, in this case, using a reference solar cell to extract the measurements to simulate the theoretical performance of the system is more precise than employing a pyranometer. This is because a reference solar cell is easier to align and it has the same angular behaviour as a PV module. Even though, there is the possibility that the pyranometer was not perfectly oriented and this can cause some errors.

Another question was to know if all the strings worked simultaneously and if all of them provide the same power. It has been verified that the eight panels operate as expected and deliver a similar amount of power.

Regarding the effect of the temperature and the solar radiation, it has been proved that photovoltaics systems work better when the ambient temperature is lower and consequently, the module temperature is not very high. In this way, the losses in the system due to temperature are smaller. As it was expected, the higher the irradiance reaching the modules the bigger the amount of power produced.

For further studies, it would be interesting to monitor the system the whole year, being able to evaluate the shadows of the trees that affect the performance of the system when the Sun is lower. In this way, it would be possible to know which panels are more shadowed and an optimal connection to the inverter could be done.

References

[1] W. B. Group, "The World Bank," 2014. [Online]. Available: http://data.worldbank.org/indicator/EG.USE.COMM.FO.ZS. [Accessed 20 October 2016].

[2] S. R. Madeti and S. N. Singh, "Monitoring system for photovoltaic plants: A review," *Renewable Sustainable Energy Reviews,* vol. 67, pp. 1180-1207, 2017.

[3] A. Mohammedi, N. Mezzai, D. Rekioua and T. Rekioua, "Impact of shadow on the performances of a domestic photovoltaic pumping system incorporating an MPPT control: A case study in Bejaia, North Algeria," *Energy Conversion and Management,* vol. 84, pp. 20-29, 2014.

[4] Y. Kim, W. Lee, M. Pedram and N. Chang, "Dual-mode power regulator for photovoltaic module emulation," *Applied Energy,* vol. 101, pp. 730-739, 2013.

[5] I. Yahyaoui and M. E. V. Segatto, "A practical technique for on-line monitoring of a photovoltaic plant connected to a single-phase grid," *Energy Conversion and Management,* vol. 132, pp. 198-206, 2017.

[6] P. G. V. Sampaio and M. O. A. González, "Photovoltaic solar energy: Conceptual framework," *Renewable and Sustainable Energy Reviews,* vol. 74, pp. 590-601, 2017.

[7] F. M. Vanek and D. L. Albright, Energy Systems Engineering: Evaluation and Implementation, McGraw-Hill, 2008, pp. 225-278.

[8] M. Súri, T. A. Huld, E. D. Dunlop and H. A. Ossenbrink, "Pontential of solar electricity generation in the European Union member states and candidate countries," *Solar Energy,* vol. 81, pp. 1295-1305, 2007.

[9] J. A. Duffie and W. A. Beckman, Solar Engineering of Thermal Processes, 4th ed., New Jersey: John Wiley & Sons, 2013.

[10] K. A. Lemke, "Renewable Energy Concepts," [Online]. Available: http://www.renewable-energy-concepts.com/solarenergy/solar-basics/diffuse-beam-global-radiation.html. [Accessed 2 05 2017].

[11] "Itacanet," [Online]. Available: http://www.itacanet.org/the-sun-as-a-source-of-energy/part-3-calculating-solar-angles/. [Accessed 23 05 2017].

[12] B. Parida, S. Iniyan and R. Goic, "A review of solar photovoltaic technologies," *Renewable and Sustainable Energy Reviews,* vol. 15, pp. 1625-1636, 2011.

[13] M. Vilathgamuwa, D. Nayanasiri and S. G, Power Electronics for Photovoltaic Power Systems, Morgan & Claypool Publishers, 2015.

[14] "Canada Mortgage and Housing Corporation," 2010. [Online]. Available: https://www.cmhc-schl.gc.ca/en/co/grho/grho_009.cfm. [Accessed 9 5 2017].

[15] M. A. Green, "Photovoltaic principles," *Physica E,* vol. 14, pp. 11-17, 2002.

[16] "Seaward Group USA," [Online]. Available: http://www.seaward-groupusa.com/userfiles/curve-tracing.php. [Accessed 15 05 2017].

[17] S. R. Wenham, M. A. Green, M. E. Watt and R. Corkish, Applied photovoltaics, Earthscan, 2007.

[18] C. Honsberg and S. Bowden, "PV education," [Online]. Available: http://www.pveducation.org/pvcdrom/iv-curve. [Accessed 15 5 2017].

[19] "National Instruments," 10 05 2012. [Online]. Available: http://www.ni.com/white-paper/7230/en/. [Accessed 15 05 2017].

[20] A. El-Shaer, M. T. Y. Tadros and M. A. Khalifa, "Effect of Light intensity and Temperature on Crystalline Silicon Solar Modules Parameters," *International Journal of Emerging Technology and Advanced Engineering,* vol. 4, no. 8, pp. 311-318, 2014.

[21] "Ingelibre," 9 11 2014. [Online]. Available: https://ingelibreblog.wordpress.com/2014/11/09/influencia-de-la-irradiacion-y-temperatura-sobre-una-placa-fotovoltaica/. [Accessed 15 5 2017].

[22] S. Dubey, J. N. Sarvaiya and B. Seshadri, "Temperature Dependent Photovoltaic (PV) Efficiency and Its Effect on PV Production in the World - A Review," *Energy Procedia,* vol. 33, pp. 311-321, 2013.

[23] F. Zaoui, A. Titaouine, M. Becherif, M. Emziane and A. Aboubou, "A combined experimental and simulation study on the effects of irradiance and temperature on photovoltaic modules.," *Energy Procedia,* vol. 75, pp. 373-380, 2015.

[24] A. E. Ghitas and M. Sabry, "A study of the effect of shadowing location and area on the Si solar cell electrical parameters," *Vacuum,* vol. 81, pp. 475-478, 2006.

[25] R. E. Hanitsch, D. Schulz and U. Siegfried, "Shadinf Effects on Output Power of Grid Connected Photovoltaic Generator Systems," *Power Engineering,* pp. 93-99, 2001.

[26] S. Silvestre and A. Chouder, "Effects of Shadowing on Photovoltaic Module Performance," *Progress in Photovoltaics: Research and Applications,* vol. 16, pp. 141-149, 2008.

[27] D. Sera and Y. Baghzouz, “On the Impact of Partial Shading on PV Output Power,” *Renewable Energy Sources,* pp. 229-234, 2008.

[28] F. Spertino, J. Ahmad, P. Di Leo and A. Ciocia, “A method for obtaining the I-V curve of photovoltaic arrays from module voltages and its applications for MPP tracking,” *Solar Energy,* vol. 139, pp. 489-505, 2016.

[29] “Date and time,” [Online]. Available: http://dateandtime.info/citycoordinates.php?id=2712414. [Accessed 23 05 2017].

[30] “ET Solar,” [Online]. Available: http://www.etsolar.com/PV_components-product-portfolio.asp. [Accessed 23 05 2017].

[31] “SUNGROW Green and effective,” [Online]. Available: http://en.sungrowpower.com/product/string-inverter/SG50KTL_M_SG60KTL_M_110.html. [Accessed 23 05 2017].

[32] M. Lundqvist, C. Helmke and H. A. Ossenbrink, “ESTI-LOG PV plant monitoring system,” *Solar Energy Materials and Solar Cells,* vol. 45, pp. 289-294, 1997.

[33] “Keysight technologies,” [Online]. Available: http://www.keysight.com/en/pd-1000001313%3Aepsg%3Apro-pn-34970A/data-acquisition-data-logger-switch-unit?nid=-33261.536881544&cc=US&lc=eng. [Accessed 24 05 2017].

[34] “National Instruments,” [Online]. Available: http://www.ni.com/sv-se/shop/labview.html. [Accessed 26 05 2017].

Appendix I: Reliability of the monitoring system

A. Peak power

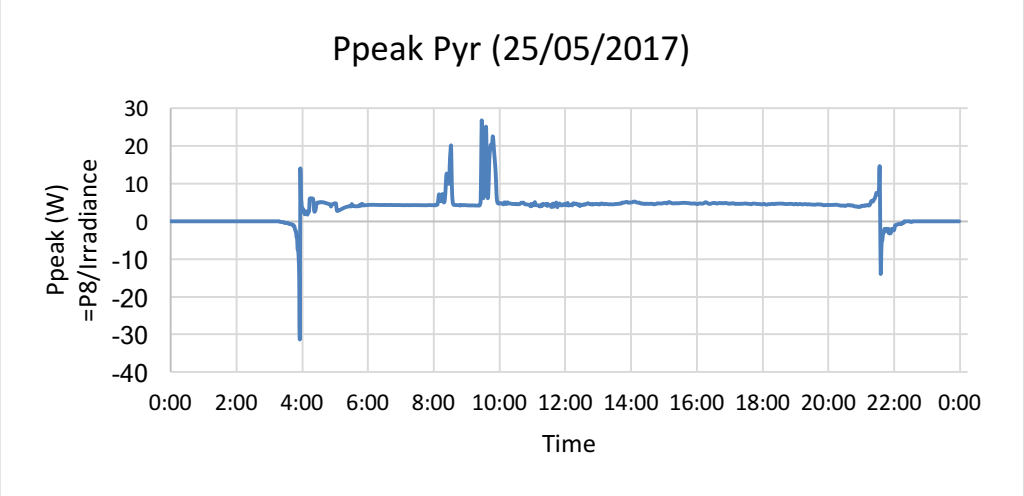

Figure 51. Peak power of the string 8 calculated with the irradiance from the pyranometer

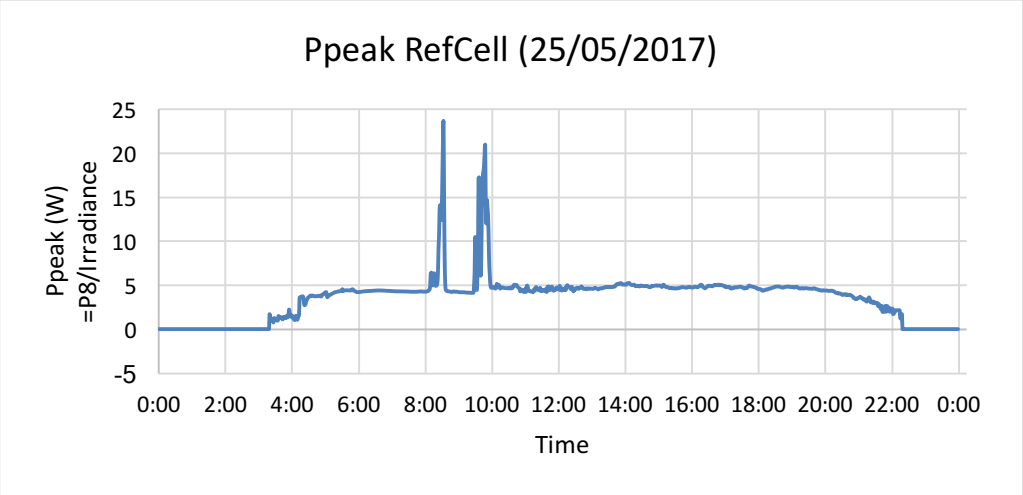

Figure 52. Peak power of the string 8 calculated with the irradiance from the reference solar cell

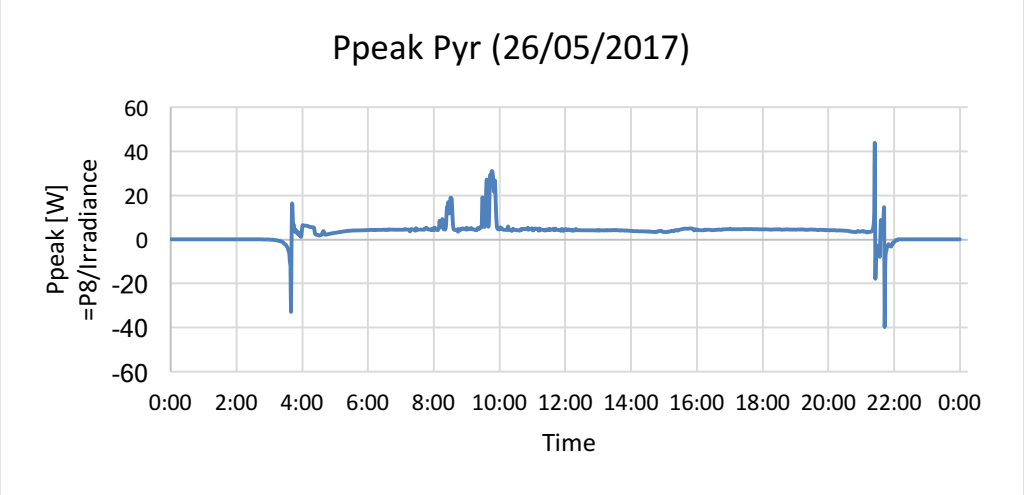

Figure 53. Peak power of the string 8 calculated with the irradiance from the pyranometer

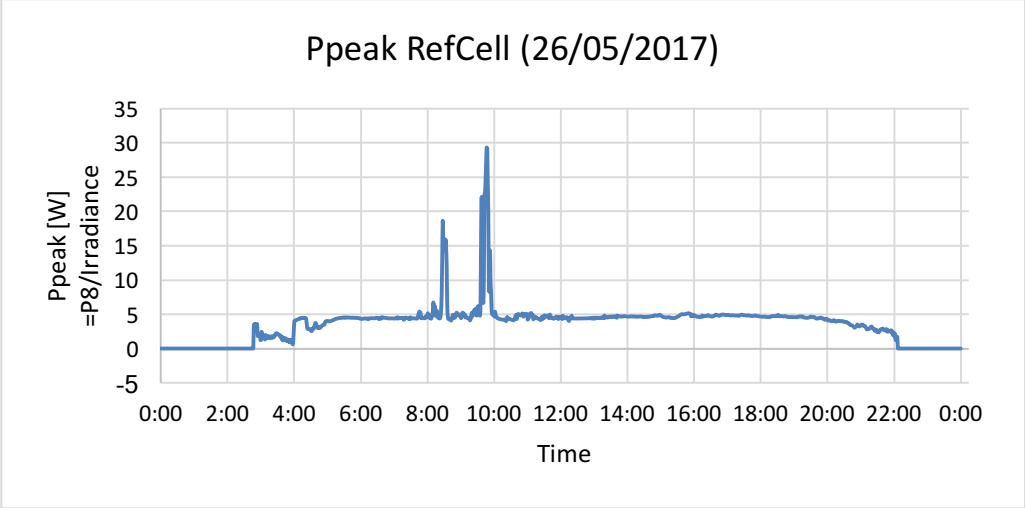

Figure 54. Peak power of the string 8 calculated with the irradiance from the reference solar cell

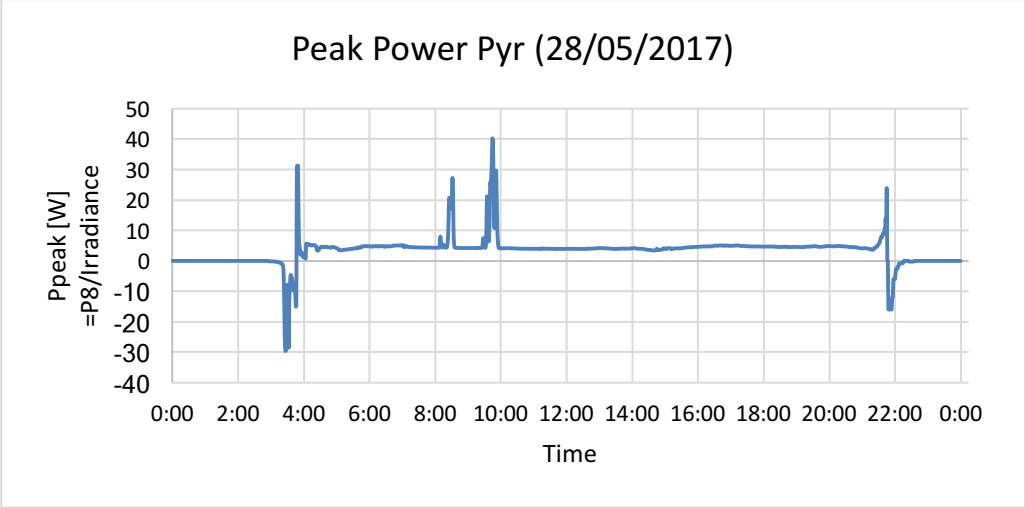

Figure 55. Peak power of the string 8 calculated with the irradiance from the pyranometer

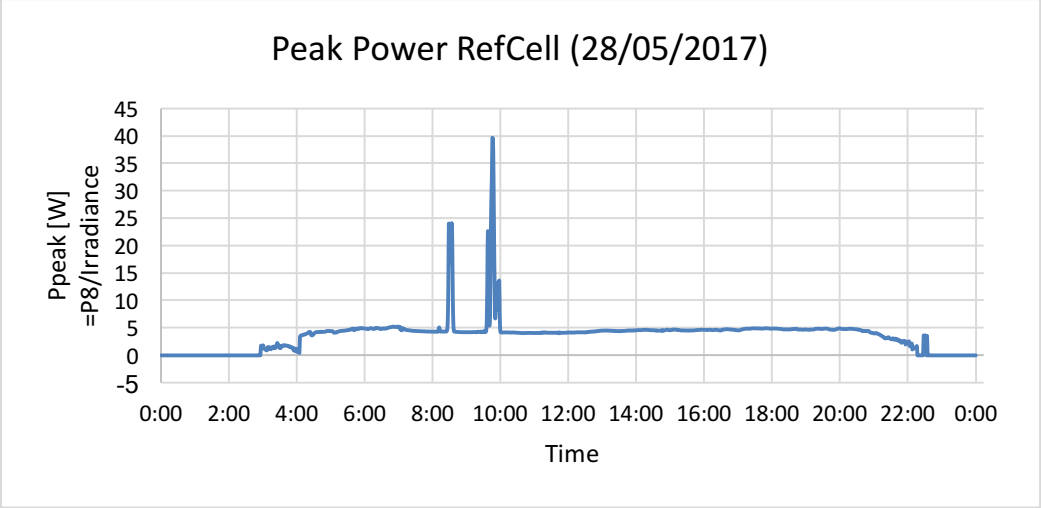

Figure 56. Peak power of the string 8 calculated with the irradiance from the reference solar cell

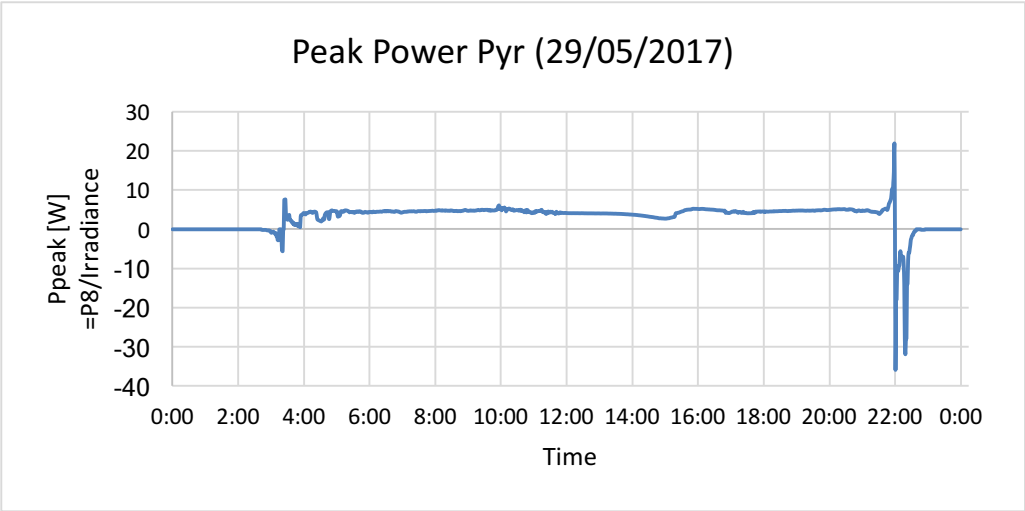

Figure 57. Peak power of the string 8 calculated with the irradiance from the pyranometer

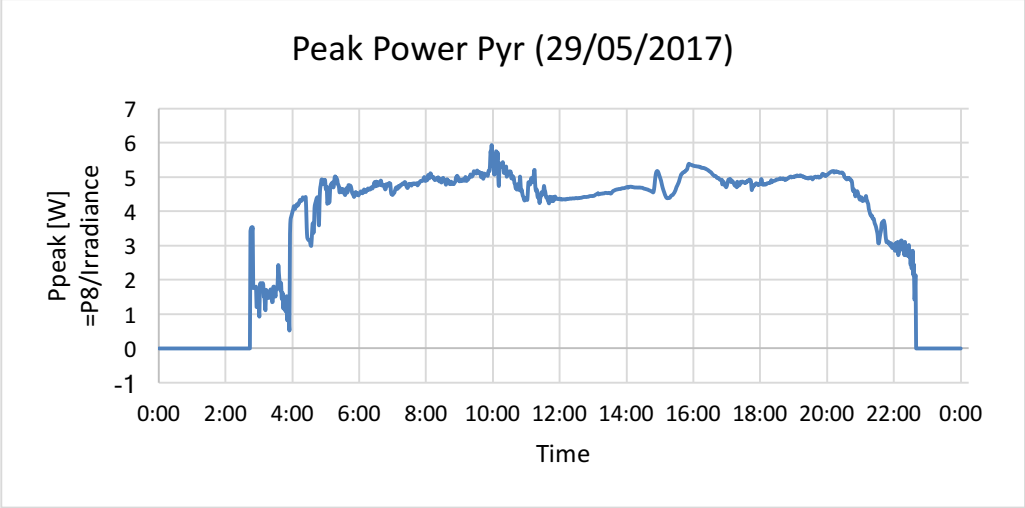

Figure 58. Peak power of the string 8 calculated with the irradiance from the reference solar cell

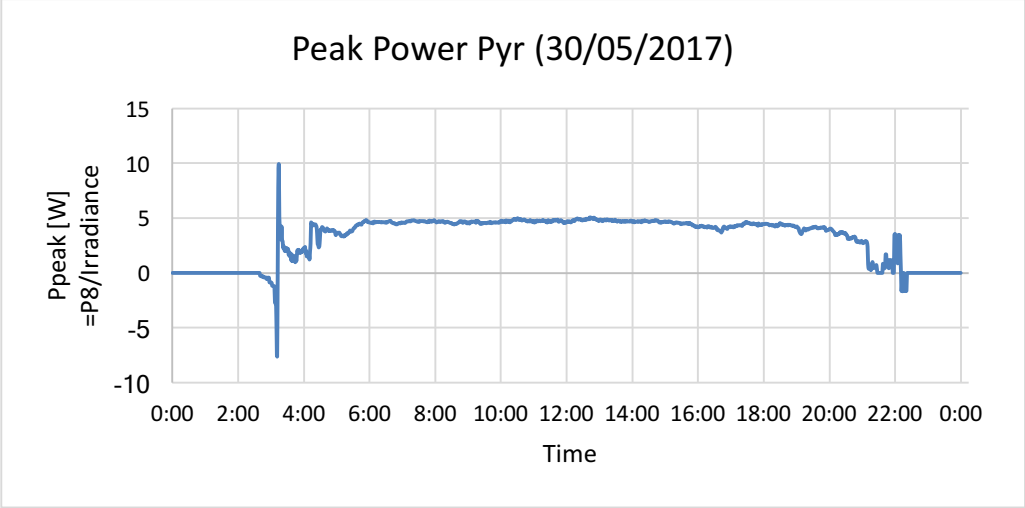

Figure 59. Peak power of the string 8 calculated with the irradiance from the pyranometer

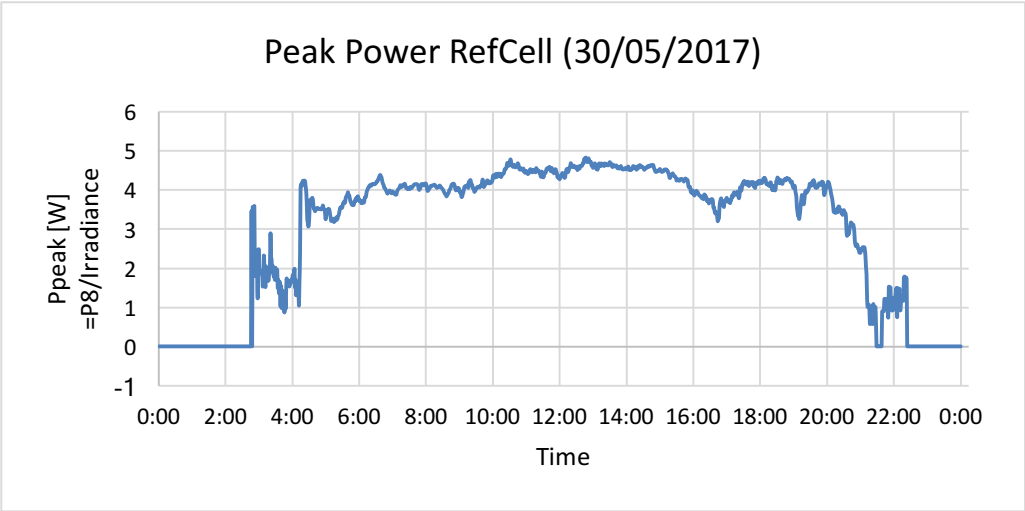

Figure 60. Peak power of the string 8 calculated with the irradiance from the reference solar cell

B. Real power and Irradiance

With all the data

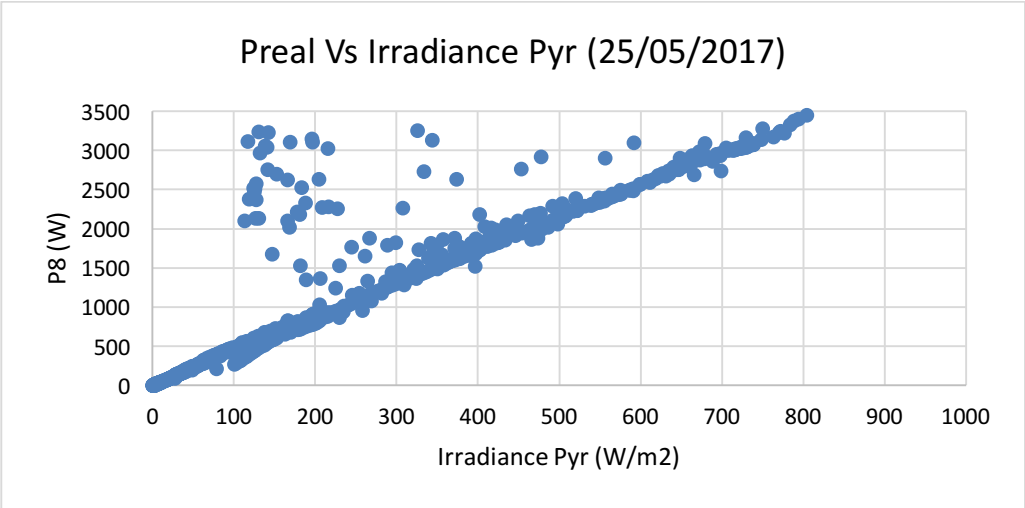

Figure 61. Relation between the output power of string 8 and the irradiance from the pyranometer

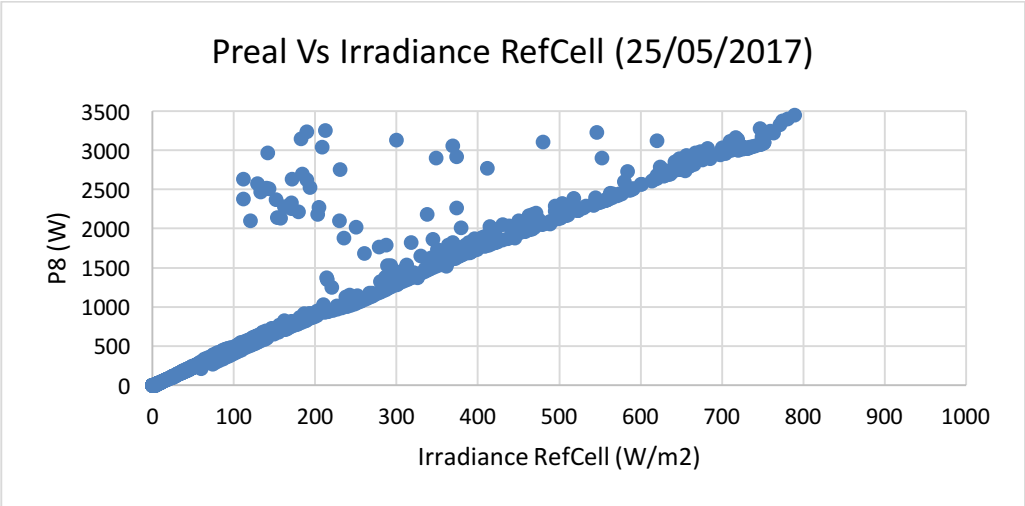

Figure 62. Relation between the output power of string 8 and the irradiance from the reference solar cell

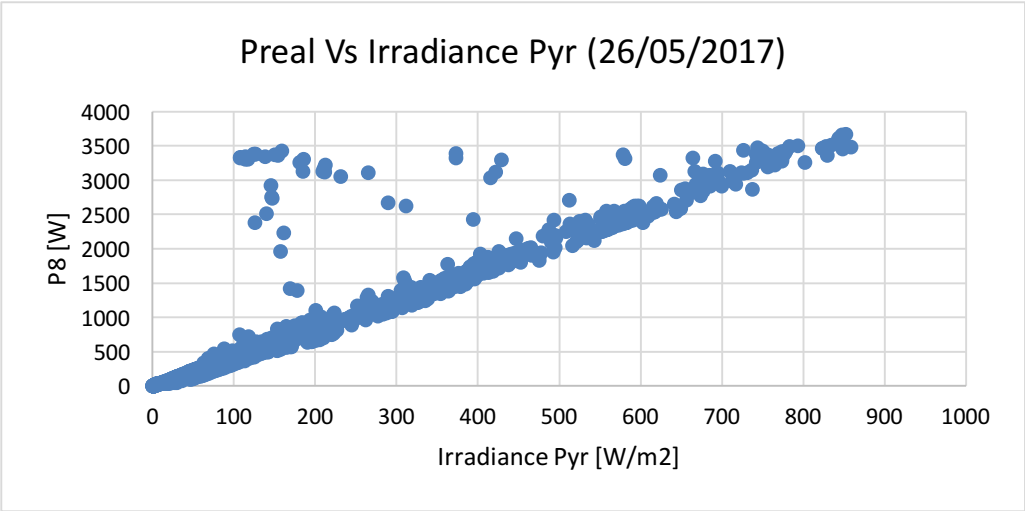

Figure 63. Relation between the output power of string 8 and the irradiance from the pyranometer

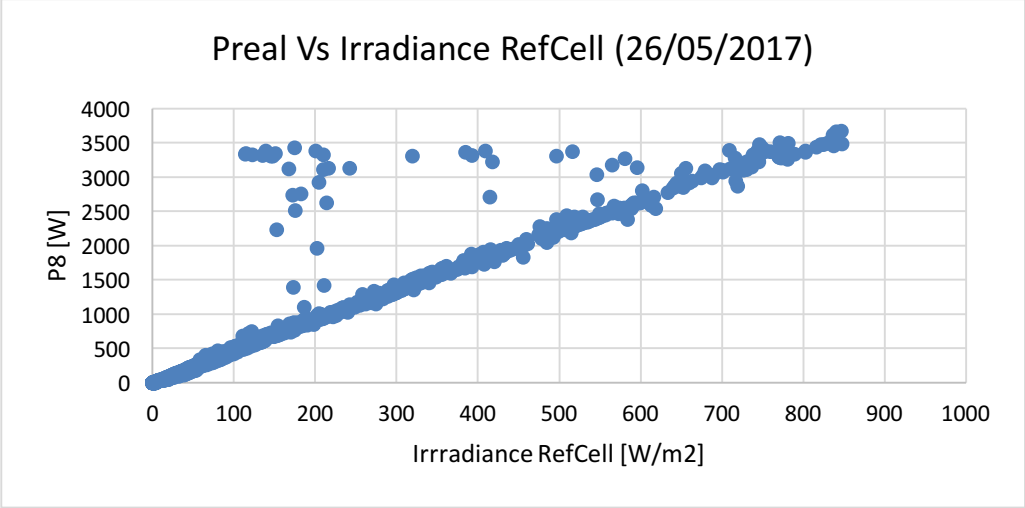

Figure 64. Relation between the output power of string 8 and the irradiance from the reference solar cell

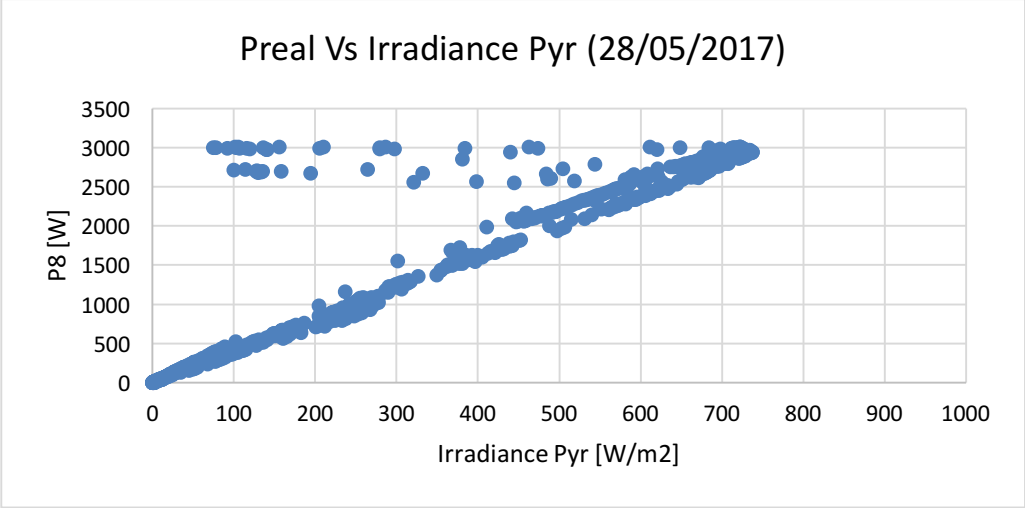

Figure 65. Relation between the output power of string 8 and the irradiance from the pyranometer

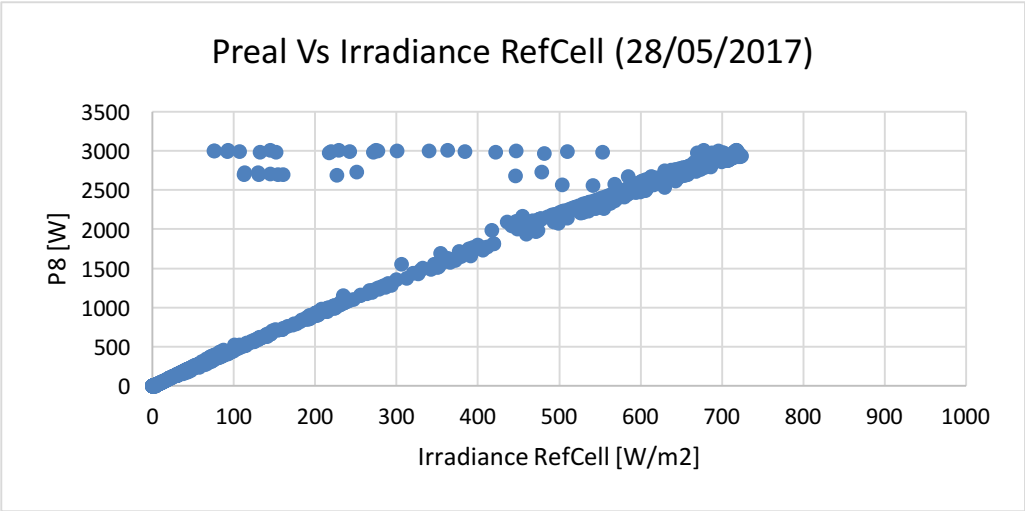

Figure 66. Relation between the output power of string 8 and the irradiance from the reference solar cell

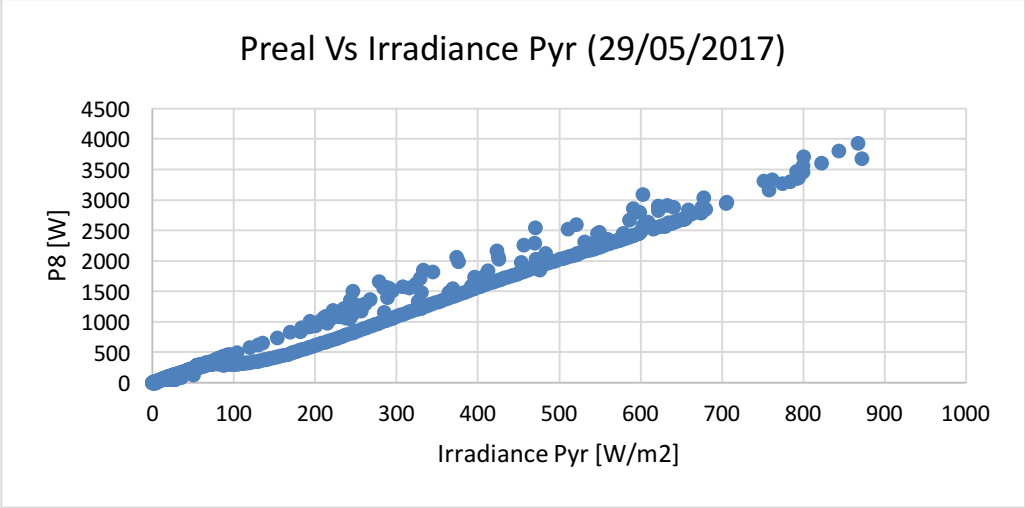

Figure 67. Relation between the output power of string 8 and the irradiance from the pyranometer

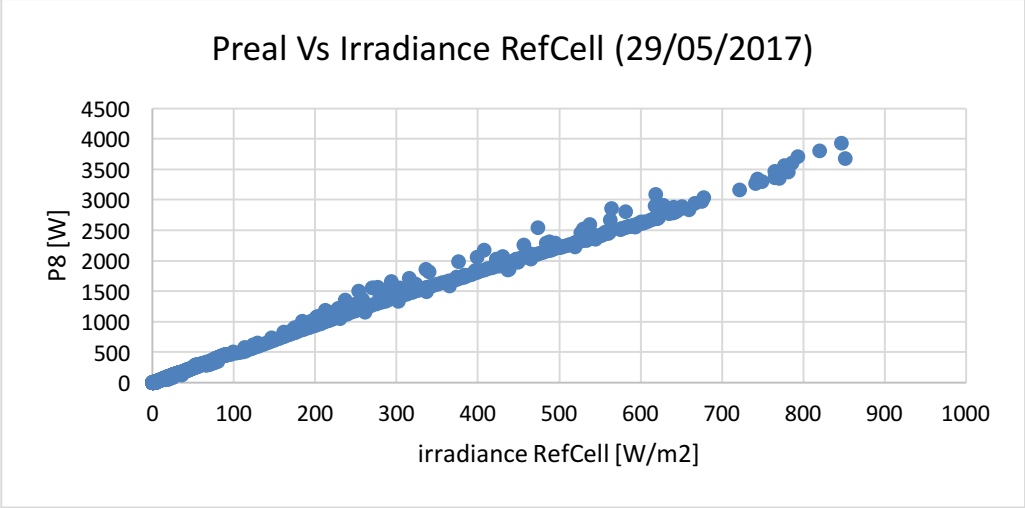

Figure 68. Relation between the output power of string 8 and the irradiance from the reference solar cell

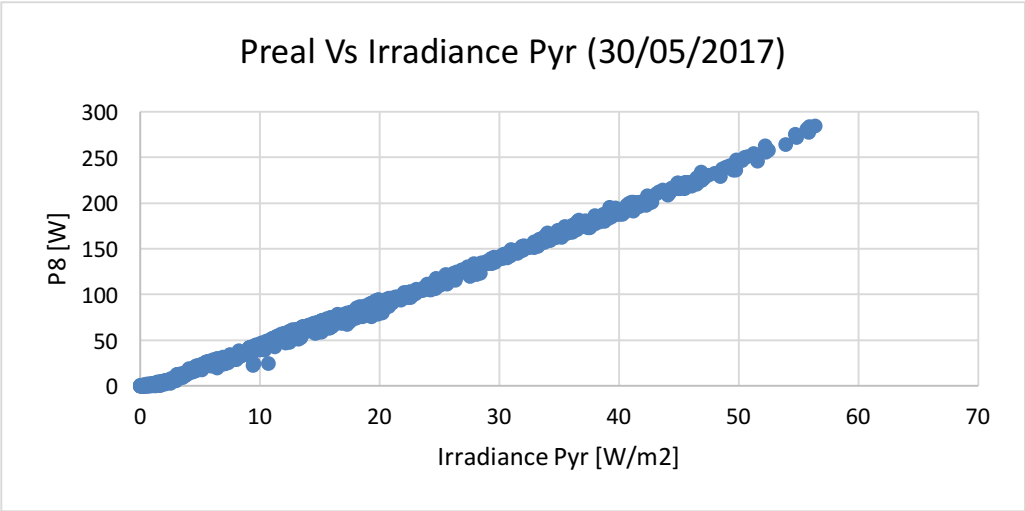

Figure 69. Relation between the output power of string 8 and the irradiance from the pyranometer

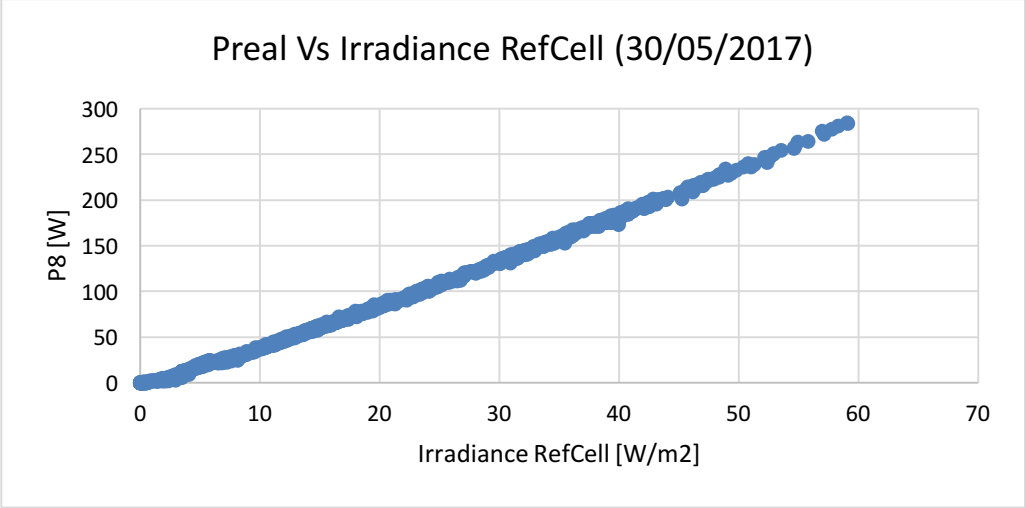

Figure 70. Relation between the output power of string 8 and the irradiance from the reference solar cell

Without the deleted data

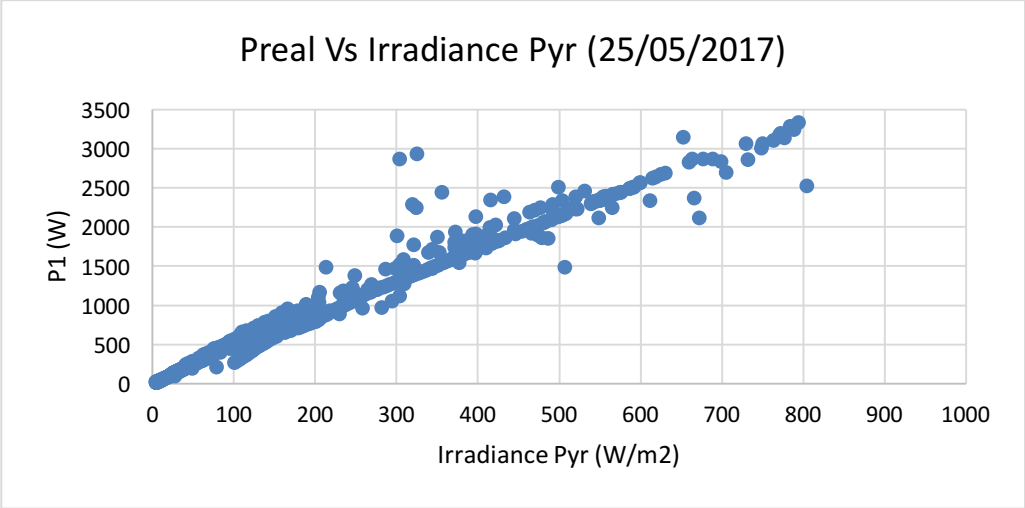

Figure 71. Relation between the output power of string 8 and the irradiance from the pyranometer, once some data was not considered

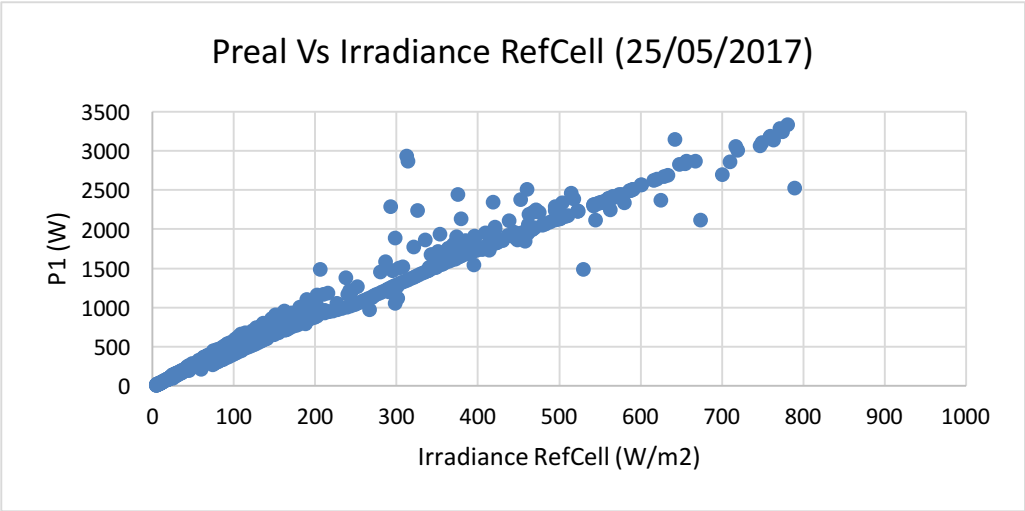

Figure 72. Relation between the output power of string 8 and the irradiance from the reference solar cell, once some data was not considered

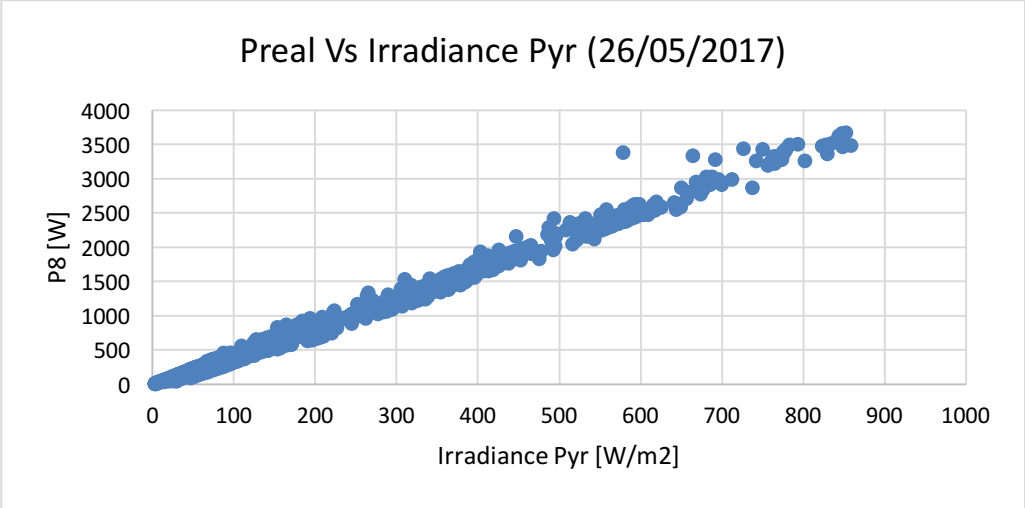

Figure 73. Relation between the output power of string 8 and the irradiance from the pyranometer, once some data was not considered

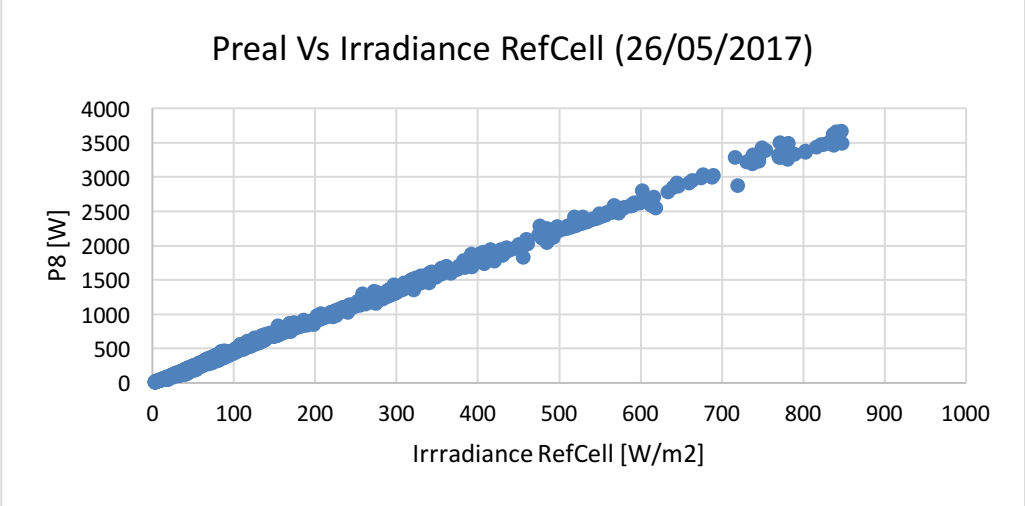

Figure 74. Relation between the output power of string 8 and the irradiance from the reference solar cell, once some data was not considered

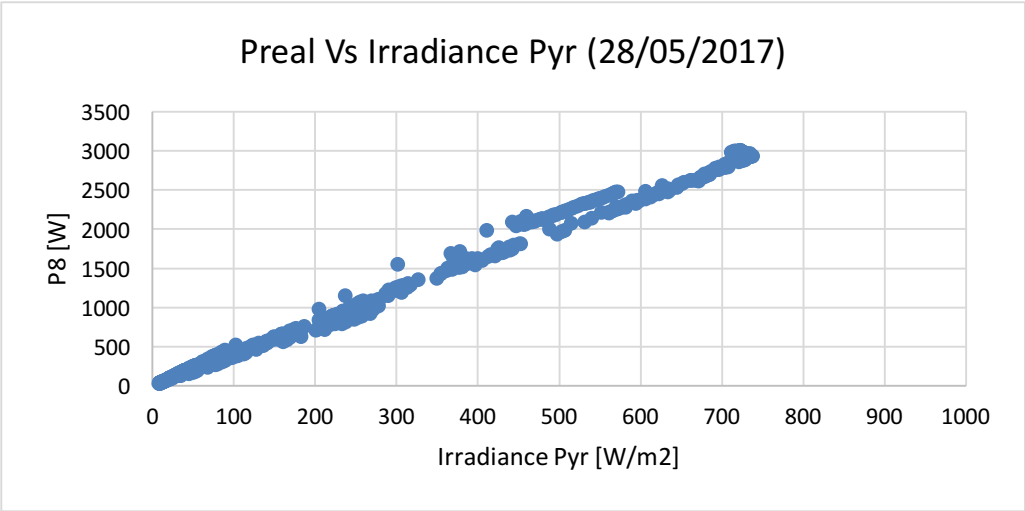

Figure 75. Relation between the output power of string 8 and the irradiance from the pyranometer, once some data was not considered

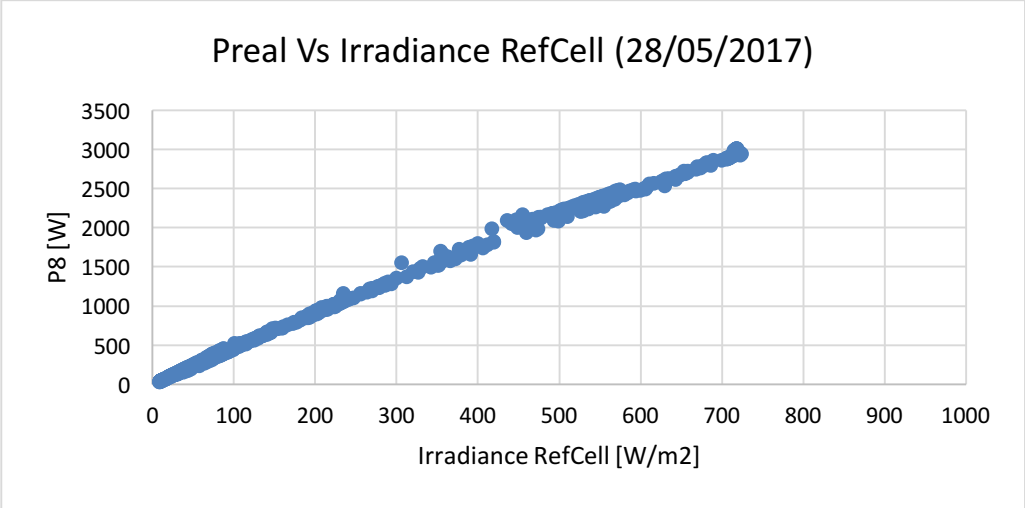

Figure 76. Relation between the output power of string 8 and the irradiance from the reference solar cell, once some data was not considered

Appendix II: Real and theoretical power

A. Theoretical power Vs Real power

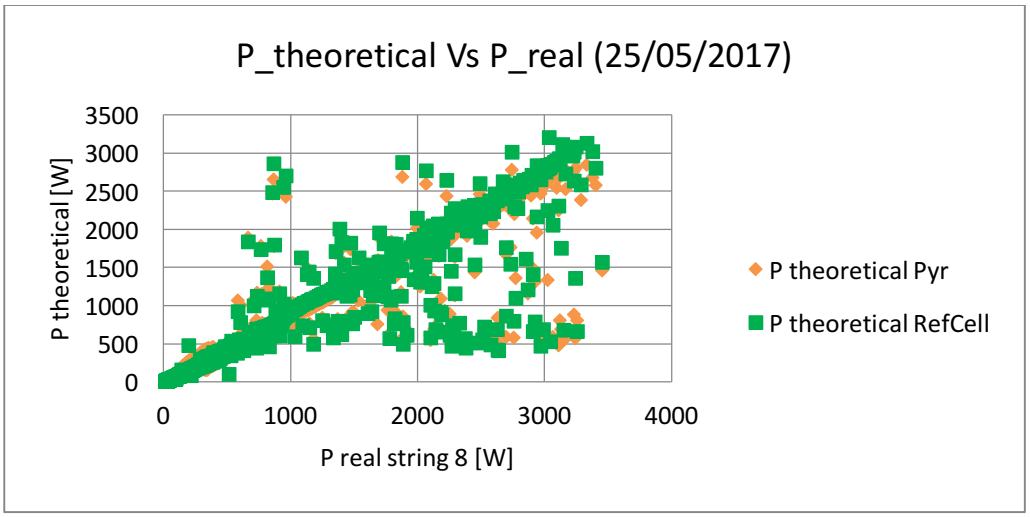

Figure 77. Relation between the theoretical power and the real output power (string 8)

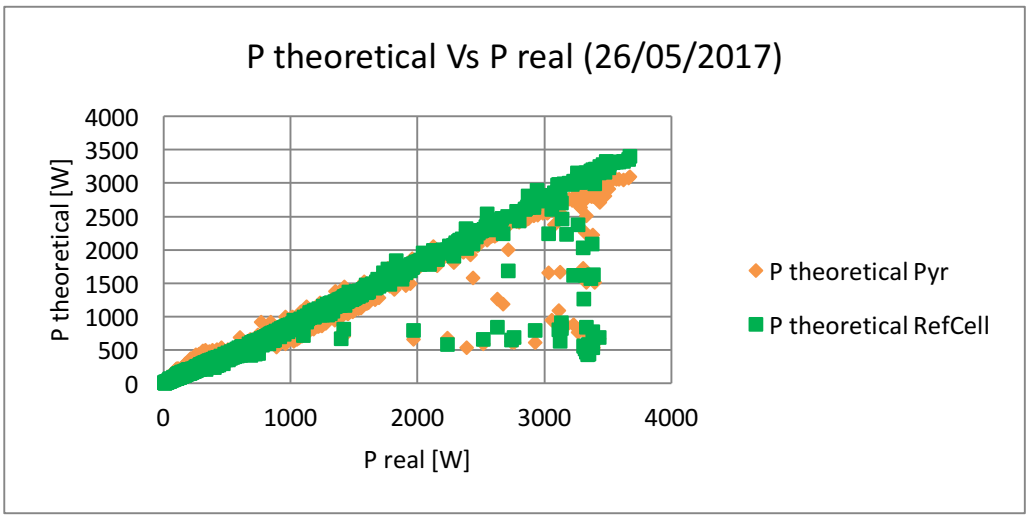

Figure 78. Relation between the theoretical power and the real output power (string 8)

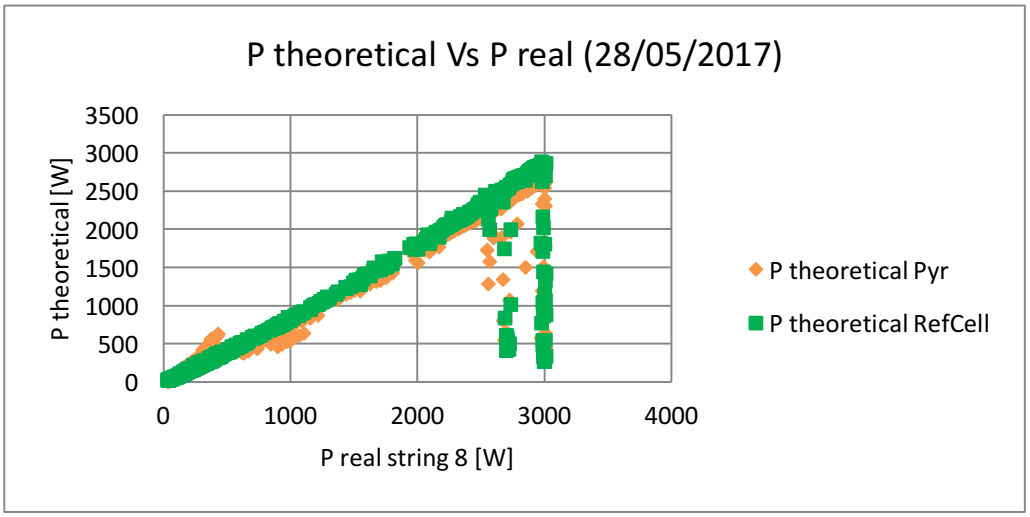

Figure 79. Relation between the theoretical power and the real output power (string 8)

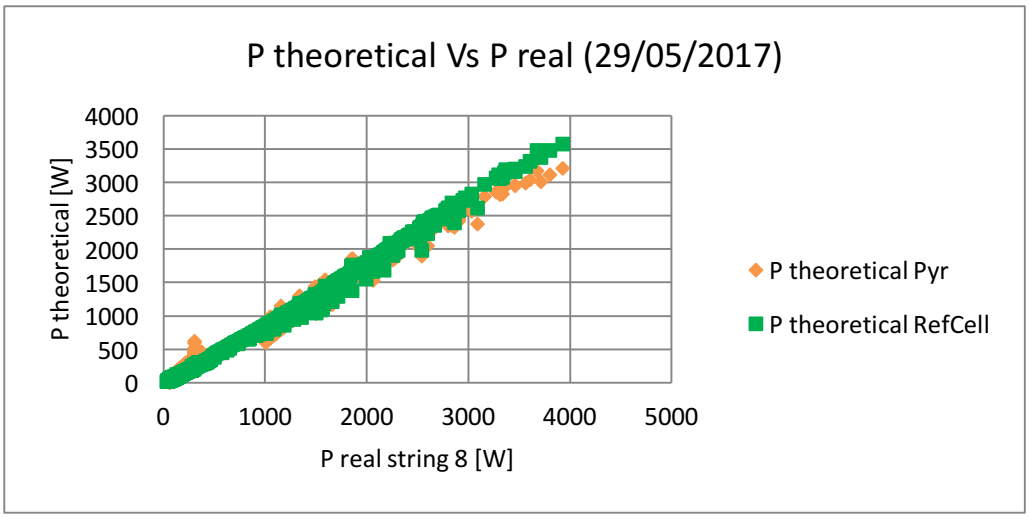

Figure 80. Relation between the theoretical power and the real output power (string 8)

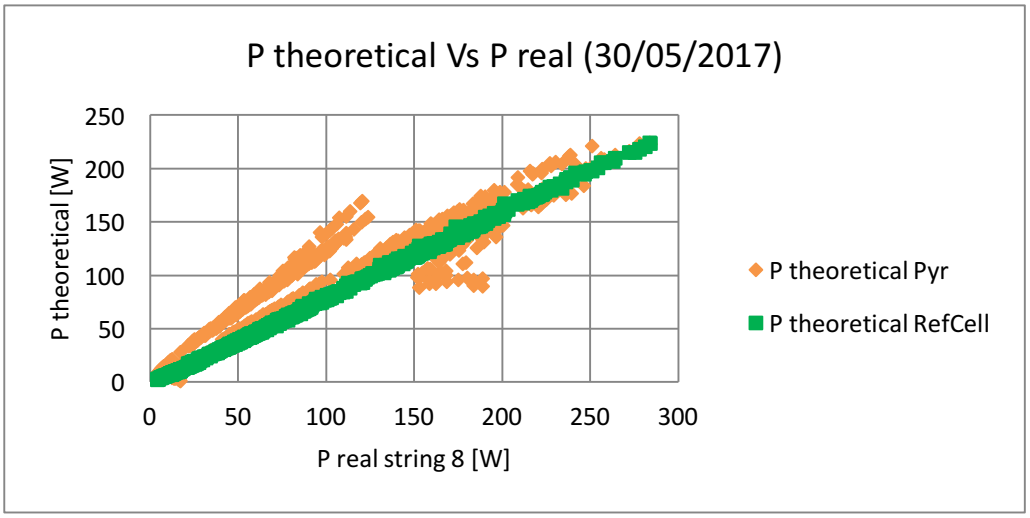

Figure 81. Relation between the theoretical power and the real output power (string 8)

B. Evolution of the power during a day

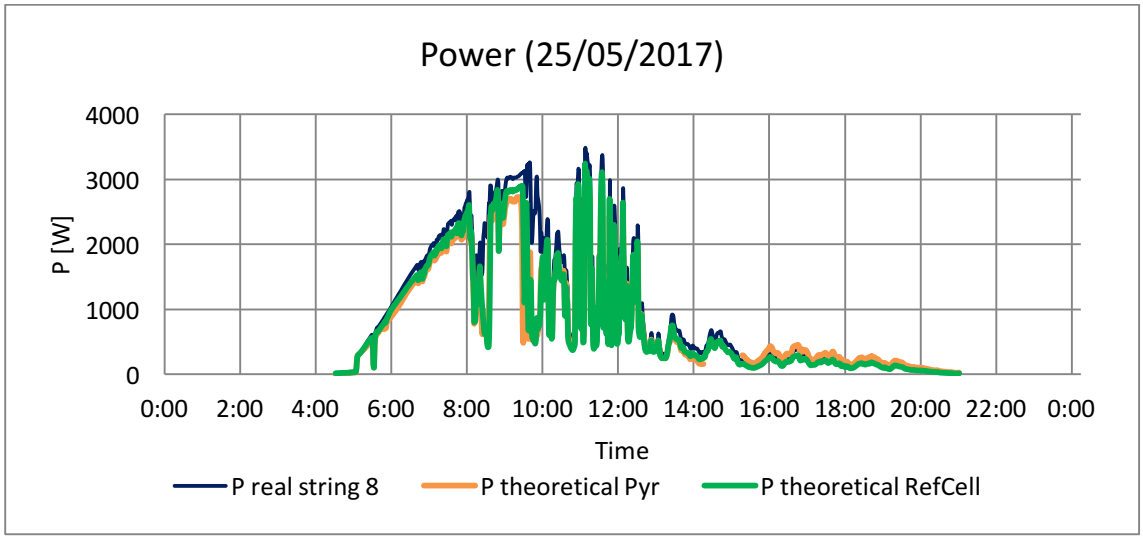

Figure 82. Evolution of the real and theoretical power during the 25th of May 2017

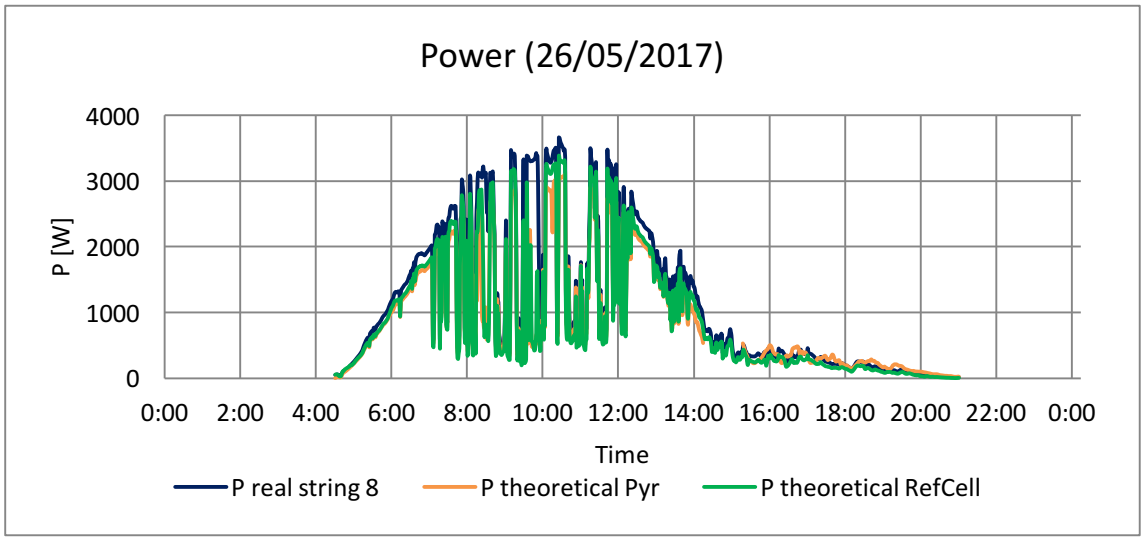

Figure 83. Evolution of the real and theoretical power during the 26th of May 2017

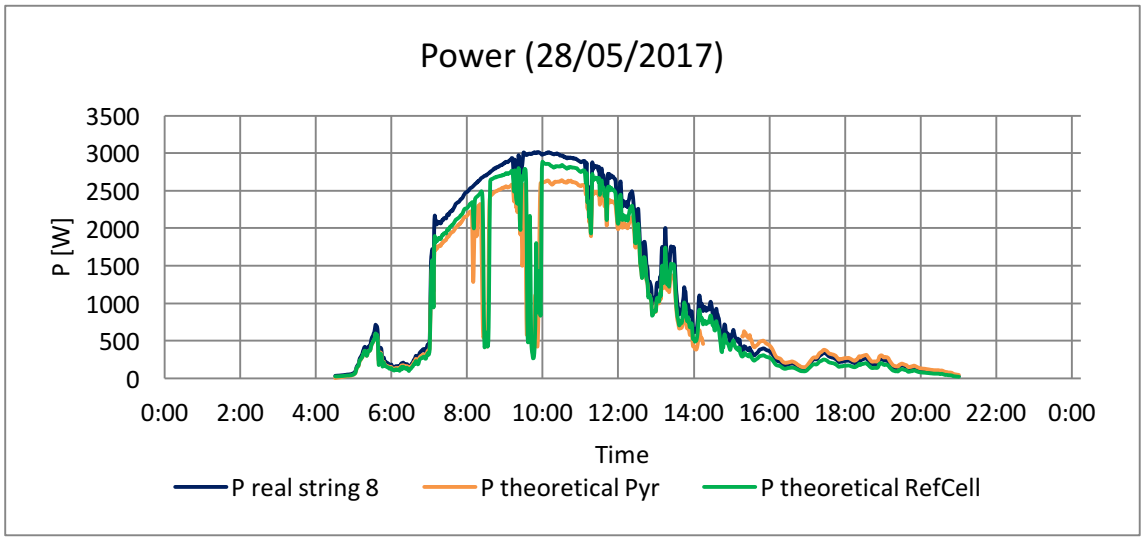

Figure 84. Evolution of the real and theoretical power during the 28th of May 2017

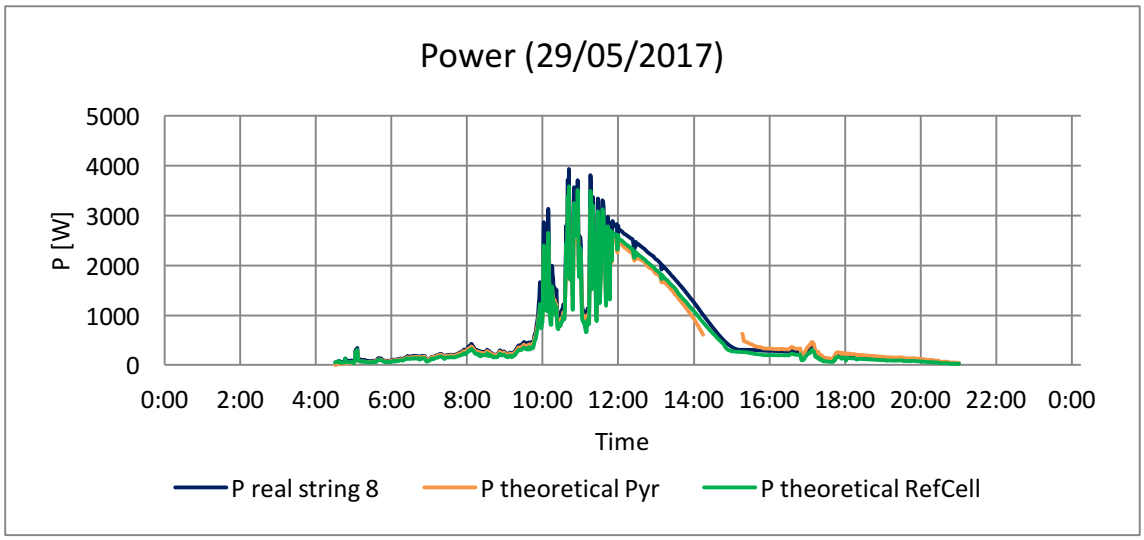

Figure 85. Evolution of the real and theoretical power during the 29th of May 2017

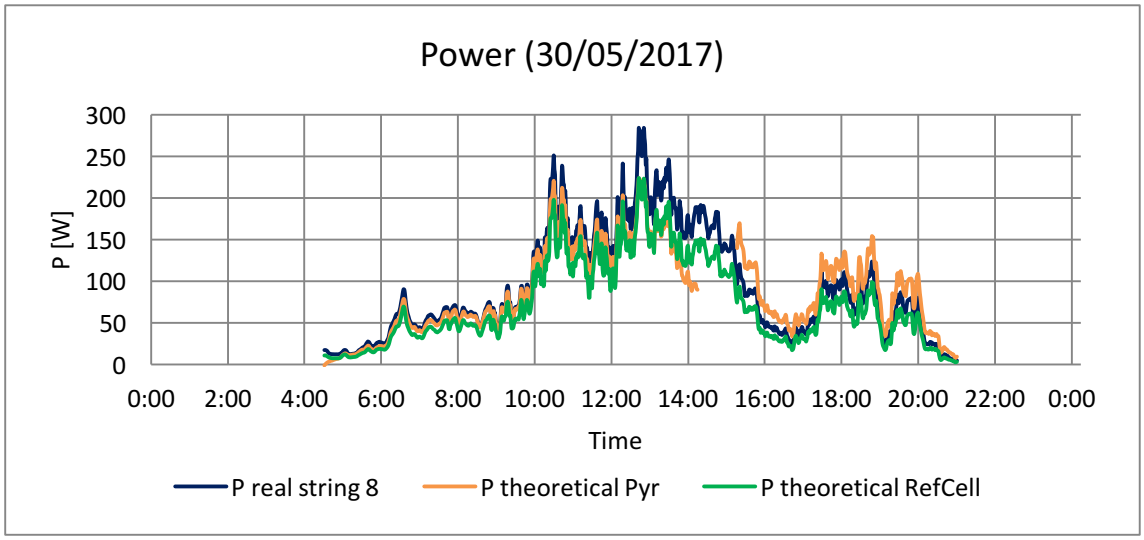

Figure 86. Evolution of the real and theoretical power during the 30th of May 2017

Appendix III: Performance of the system

A. Performance of the power of the eight strings

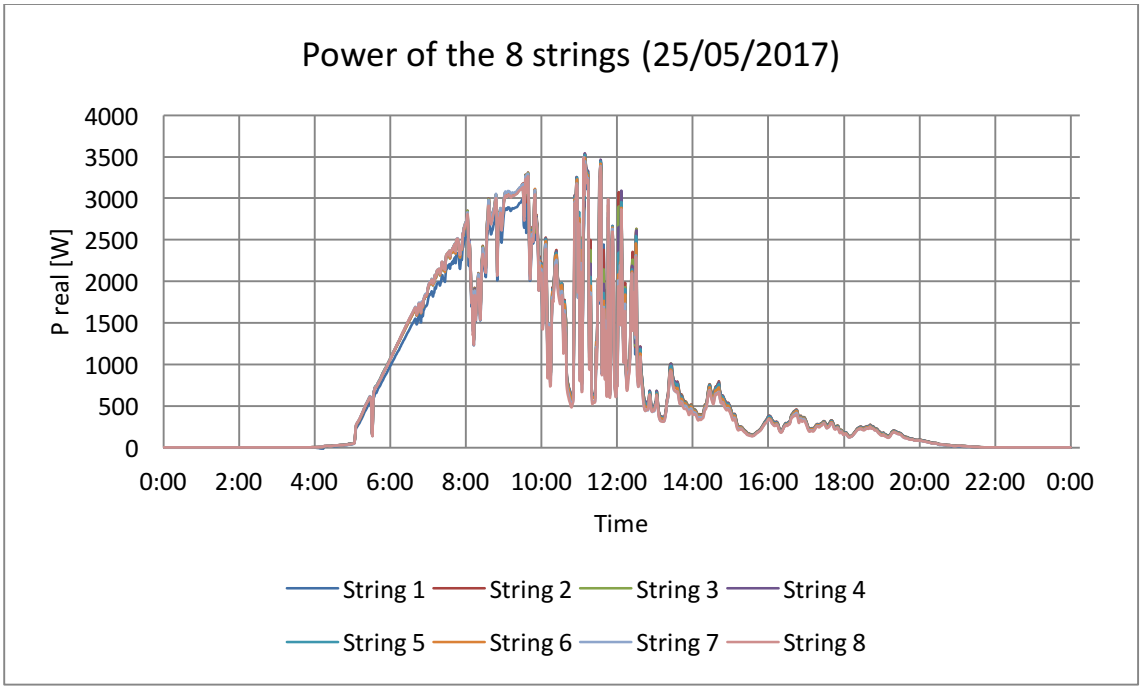

Figure 87. Performance of the eight strings the 25th of May 2017

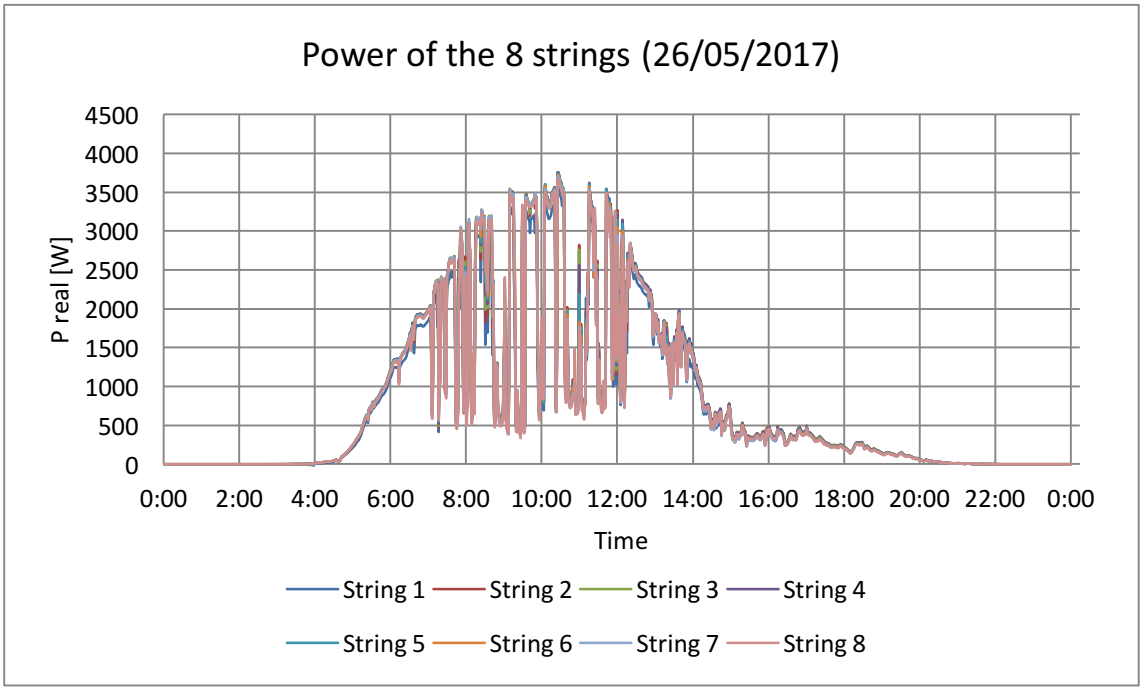

Figure 88. Performance of the eight strings the 26th of May 2017

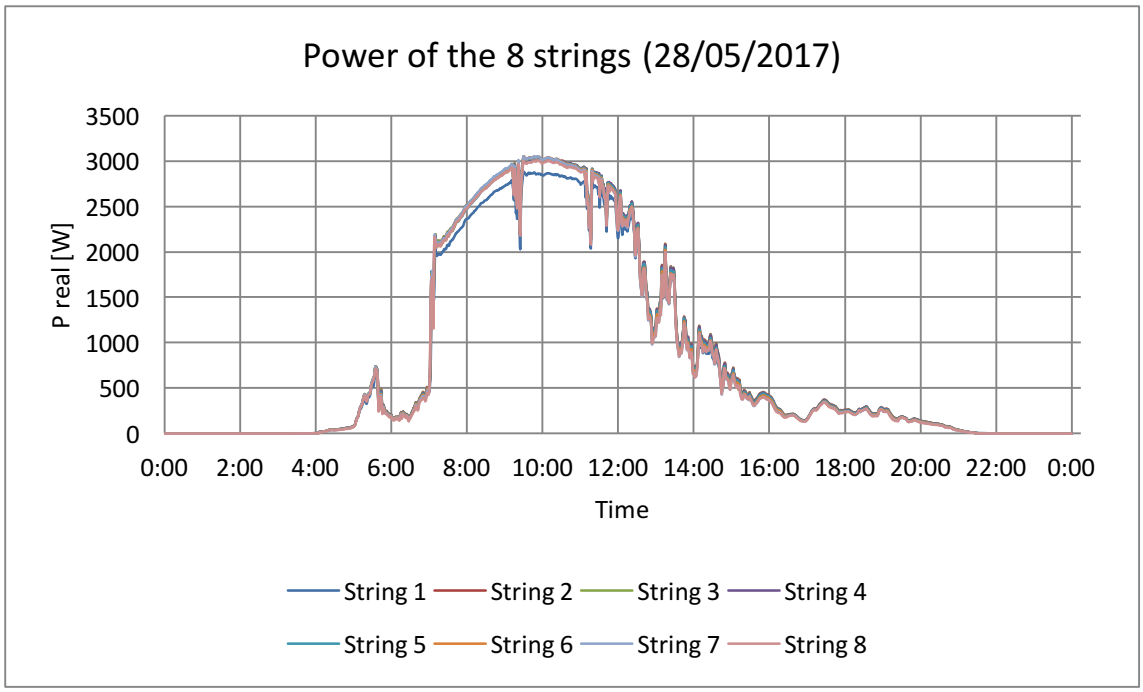

Figure 89. Performance of the eight strings the 28th of May 2017

B. Evolution of the power of the PV system

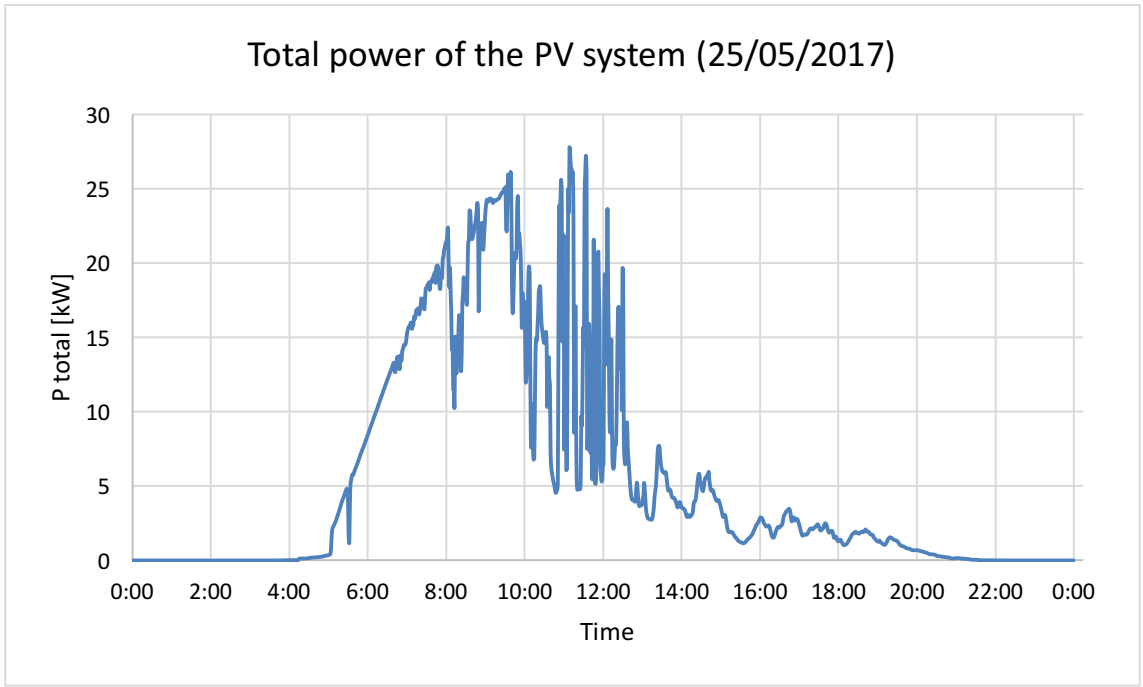

Figure 90. Performance of the PV system the 25th of May 2017

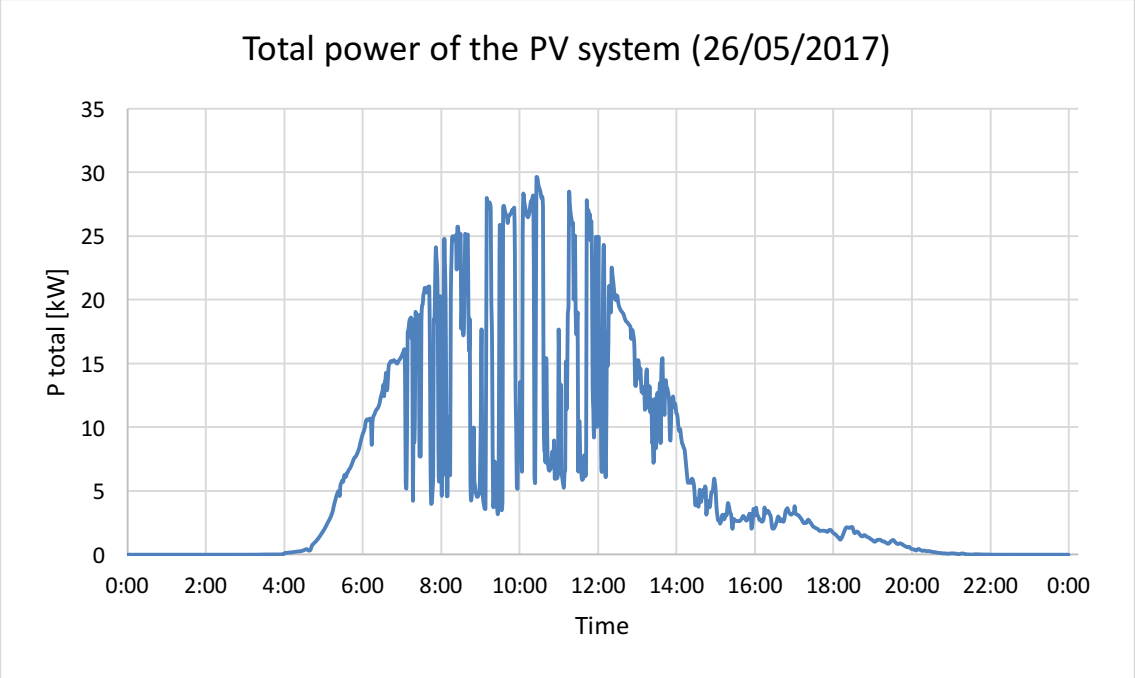

Figure 91. Performance of the PV system the 26th of May 2017

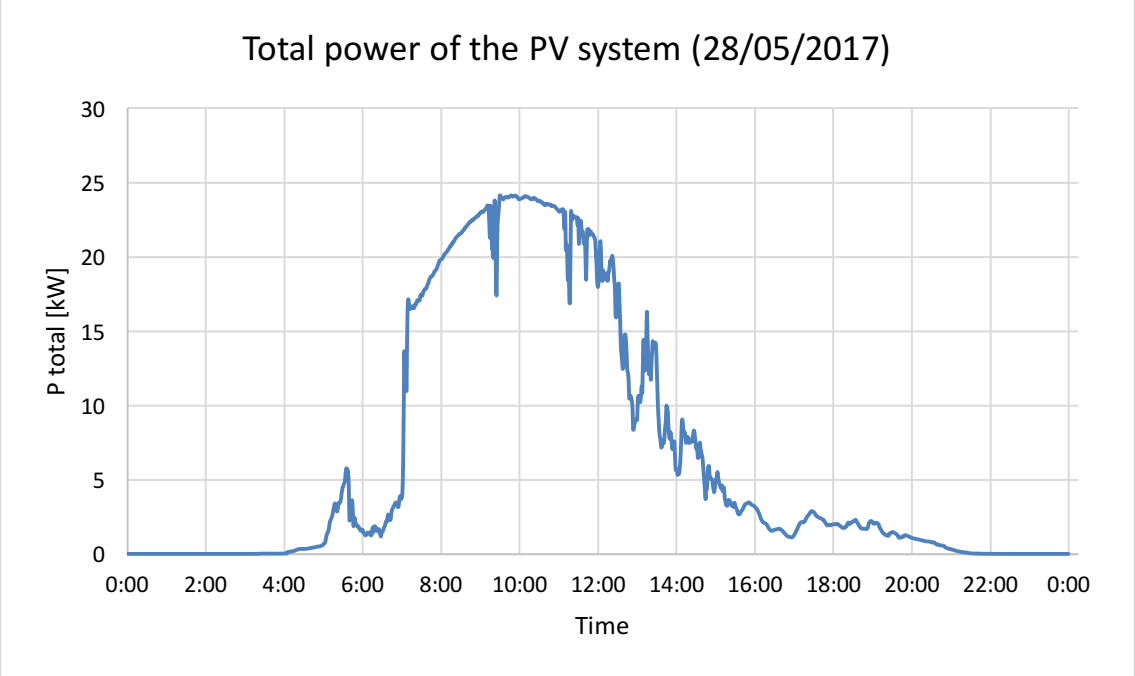

Figure 92. Performance of the PV system the 28th of May 2017

C. Total output power of each string

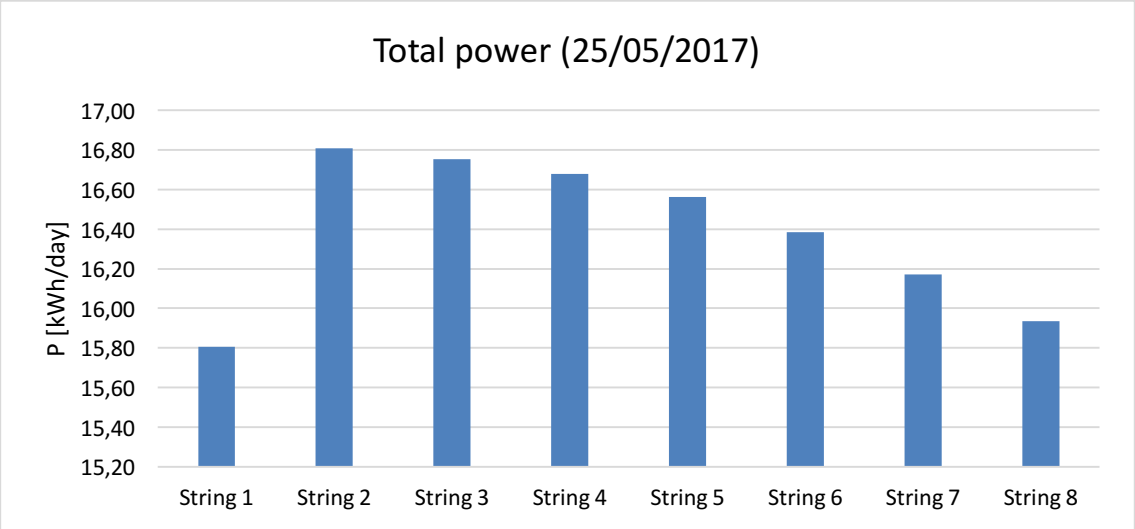

Figure 93. Total output power of each string the 25th of May 2017

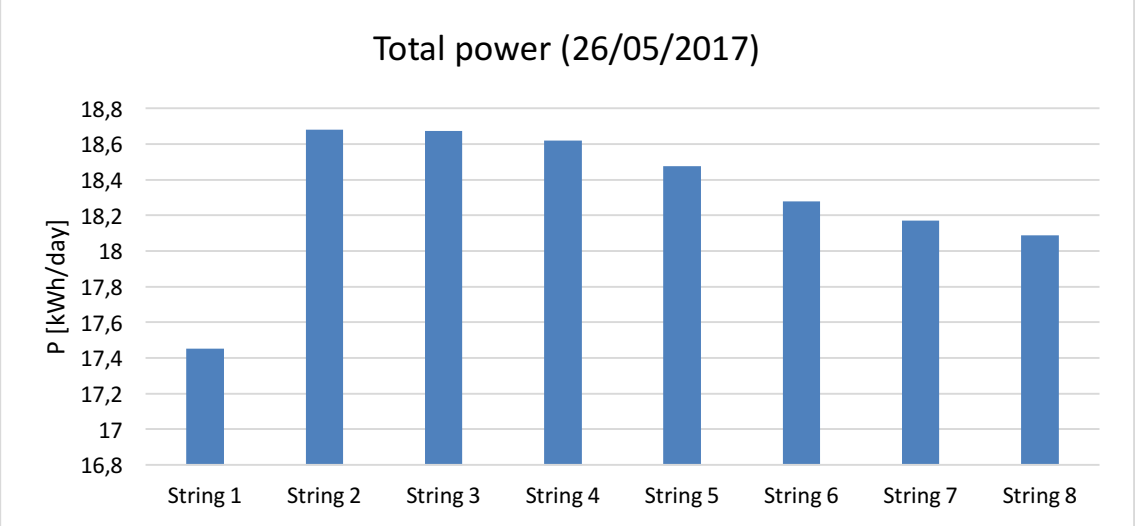

Figure 94. Total output power of each string the 26th of May 2017

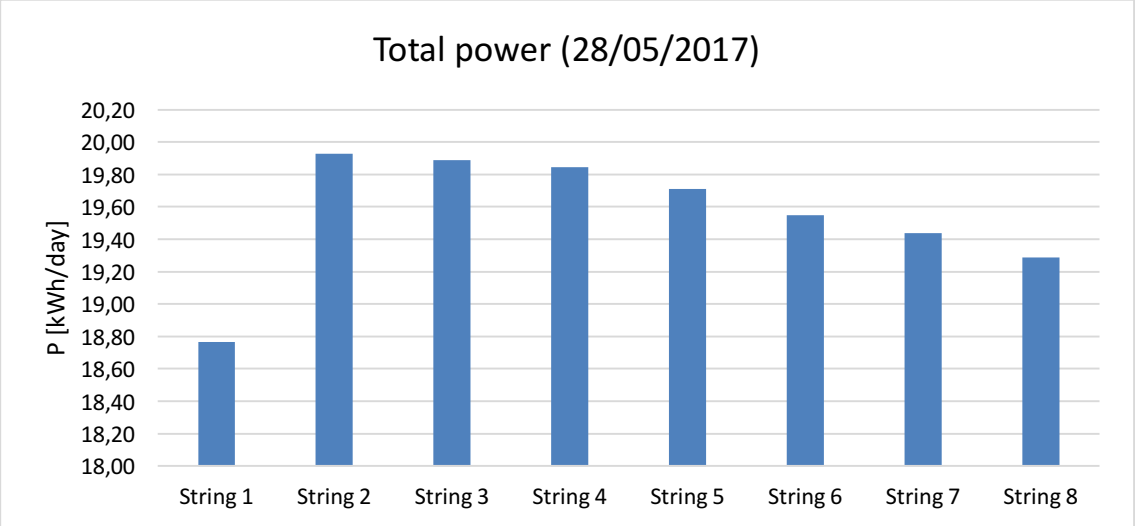

Figure 95. Total output power of each string the 28th of May 2017

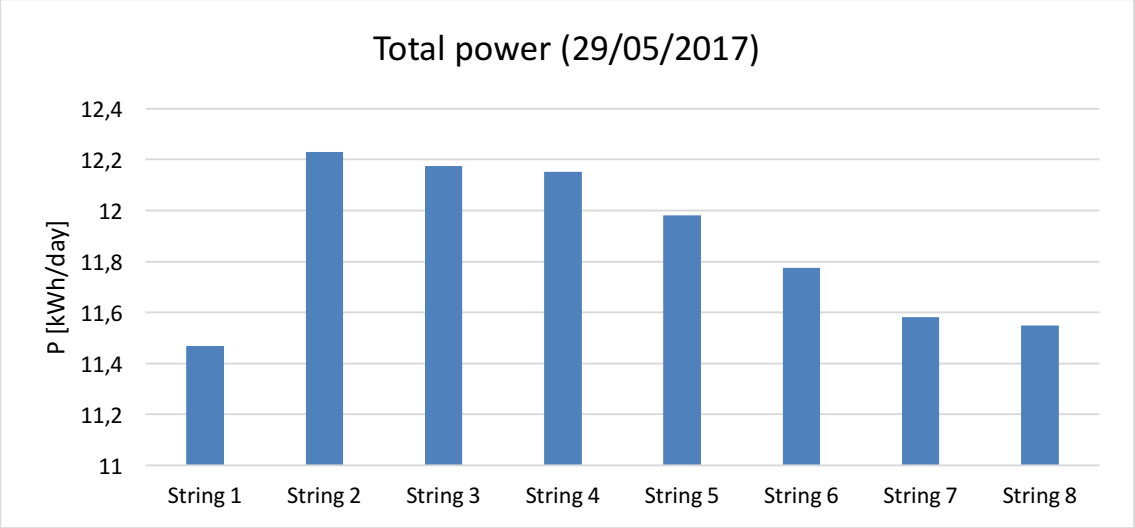

Figure 96. Total output power of each string the 29th of May 2017

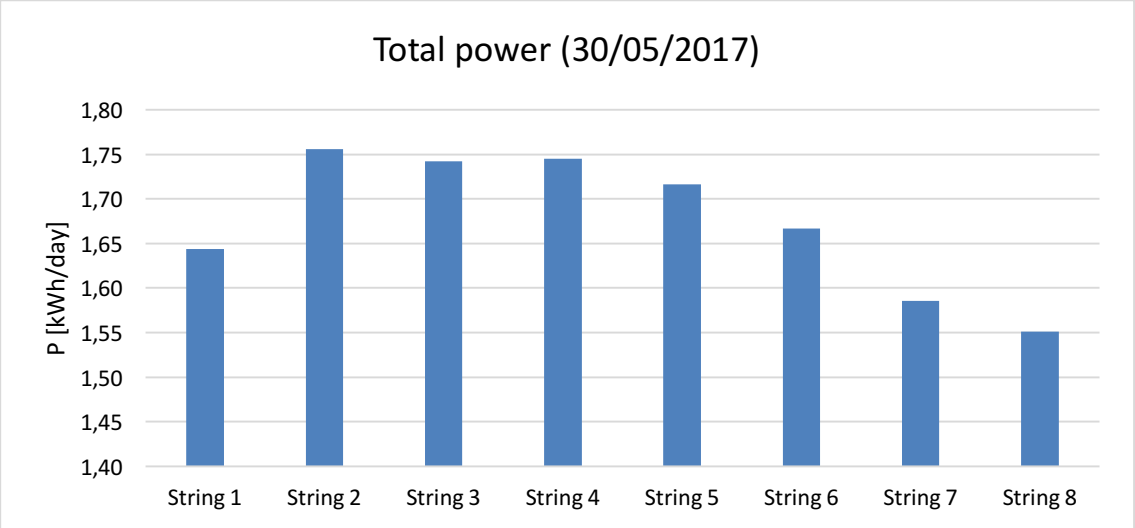

Figure 97. Total output power of each string the 30th of May 2017